This is to certify that the

thesis entitled

A NUMERICAL PREDICTION MODEL FOR FOOD
FREEZING USING FINITE ELEMENT METHODS

presented by

Hadi Karia Purwadaria

has been accepted towards fulfillment
of the requirements for

Ph.D. degree in Agricultural
Engineering

D.R. Heldman
Major professor

Date Dec. 28, 1979

A NUMERICAL PREDICTION MODEL FOR FOOD FREEZING USING FINITE ELEMENT METHODS

By

Hadi Karia Purwadaria

A DISSERTATION

Submitted to
Michigan State University
in partial fulfillment of the requirements
for the degree of

DOCTOR OF PHILOSOPHY

Department of Agricultural Engineering

1980

ABSTRACT

A NUMERICAL PREDICTION MODEL FOR FOOD FREEZING USING FINITE ELEMENT METHODS

By

Hadi Karia Purwadaria

The rate of freezing is one of the most important factors in designing an efficient freezing process for foods in order to achieve good product quality and to avoid excessive energy consumption. Significant improvements have been achieved in the area of freezing process simulation, however, the phenomena of phase-change, the influence of product thermal properties, the importance of product geometry and the effect of freezing environment on the freezing rate are not fully understood.

The objective of this investigation was to develop a numerical simulation model using the finite element method to predict freezing rate in anomalous food product geometries while accounting for the non-linear temperature dependent product properties and various boundary conditions. To verify the model, experimental tests were conducted for elliptical and trapezoidal product shapes using ground beef as the food product. The experiments

were conducted in a wind tunnel placed in a low temperature room and temperature measurement was recorded for 24 node locations within the critical cross-section of the product during the freezing process.

The finite element computer simulation used to predict the food product freezing rate of anomalous shape has been developed and verified by experimental data. The results illustrate the capability of the simulation model to incorporate various boundary conditions and various product geometries. Closer approximation to the experimental data was obtained by using the prediction incorporating a boundary condition with the surface heat transfer coefficient varying as a function of location. More efficient freezing times are predicted by utilizing an approach based on area average enthalpy as compared to the conventional method based on the slowest freezing point location. Time steps in the range from one to three minutes do not influence the stability of the finite element scheme. While geometric size has significant influence on the rate of freezing, the influence on initial product temperature in the range from 14.0 to 22.0°C interval is negligible.

Approved D.R. Heldman
Major Professor

Approved B.A. Stout
Department Chairman

ACKNOWLEDGMENTS

The author is deeply indebted to Dr. Dennis R. Heldman, Professor of the Agricultural Engineering Department and Department of Food Science and Nutrition, for suggestion of the research topic and his continuous support, interest, and patient guidance throughout the course of this study.

Sincere appreciation is extended to the guidance committee members: Dr. Larry J. Segerlind, Agricultural Engineering Department; Dr. K. Jayaraman, Chemical Engineering Department; and Dr. Lawrence E. Dawson, Department of Food Science and Nutrition; and to the external examiner, Dr. James F. Steffe, Agricultural Engineering Department. Their review and suggestions to the manuscript have been the most helpful. Special thanks go to Dr. Haruhiko Murase, Research Associate in Agricultural Engineering Department, for his helpful suggestions in the laboratory experiments.

The author also wishes to express his gratitude to Dr. Andi Hakim Nasoetion, President of Bogor Agricultural University, for his encouraging support and to the Government of Indonesia which provided the opportunity for the author to continue his study.

The contribution from Dr. Merle L. Esmay in laboratory equipment and the supportive cooperation of all fellow students, especially Rong-ching Hsieh and Fred W. Hall are fully appreciated.

TABLE OF CONTENTS

Page

LIST OF TABLES

LIST OF FIGURES

Figure		Page

Figure Page

Figure | Page

LIST OF APPENDICES

LIST OF SYMBOLS

A	Area of a triangular finite element, m^2
a(T)	Coefficient of temperature balance at temperature T, m^2/h
a, b, c	Parameters defined in equation (3.34), a in m^2 and b & c in m
[B]	Gradient matrix defined in equation (3.39)
[C]	Capacitance matrix defined in equation (3.41)
C	Volumetric specific heat capacity, J/m^3 K
CPA	Apparent specific heat of product, J/kg K
CPI	Specific heat of ice, J/kg K
CPS	Specific heat of solid, J/kg K
CPW	Specific heat of water, J/kg K
c_p	Specific heat of product, J/kg K
[D]	Matrix defined in equation (3.28)
DI	Density of ice, kg/m^3
DS	Density of solid, kg/m^3
DW	Density of water, kg/m^3
EMS	Effective mass of solids, kg solids/kg product
EMW	Effective mass of water, kg water/kg product
{F}	Force vector defined in equation (3.41)
{g}	Matrix defined in equation (3.27)

H	Enthalpy, J/kg
h	Local surface heat transfer coefficient, $W/m^2\ K$
$\overline{h}$	Average surface heat transfer coefficient, $W/m^2\ K$
I	Specific enthalpy, J/m^3
IK	Initial thermal conductivity, W/m K
ICP	Initial specific heat of product, J/kg K
IWC	Initial water content, kg water/kg product
[K]	Stiffness matrix defined in equation (3.41)
KPI	Thermal conductivity of ice, W/m K
KPS	Thermal conductivity of solids, W/m K
KPW	Thermal conductivity of water, W/m K
k	Thermal conductivity of product, W/m K
$k(T)$	Thermal conductivity of product at temperature T, W/m K
k_c	Thermal conductivity of continuous phase, W/m K
k_d	Thermal conductivity of discontinuous phase, W/m K
k_{xx}	Thermal conductivity in x direction, W/m K
k_{yy}	Thermal conductivity in y direction, W/m K
k_{zz}	Thermal conductivity in z direction, W/m K
L	Area coordinates of a triangular element defined in equation (3.36)
L_A	Latent heat of fusion of solvent A, J/kg
LW	Latent heat of fusion of water, J/kg

L_1	Latent heat of fusion of product, J/kg
M_A	Molecular weight of solvent A, kg/kg-mole
M_B	Molecular weight of solvent B, kg/kg-mole
MS	Molecular weight of solids, kg/kg-mole
MW	Molecular weight of water, kg/kg-mole
M^3	Volume fraction of discontinuous phase, dimensionless
m_A	Effective mass of solvent A, kg/kg product
m_B	Effective mass of solvent B, kg/kg product
mc	Mass fraction of water in the product, kg water/kg product
N	Shape function defined in equation (3.33)
$\hat{n}$	Number of nodal volume
PD	Product density, kg/m^3
Q	Parameter defined in equation (3.9)
Q'	Heat generation inside the body
R_1	Gas constant, 8314 J/kg-mole K
R, Z	Coordinates of triangular nodes for axisymmetric element, m
s	Surface area, m^2
T	Temperature, °C
T_{DF}	Depressed freezing point, K
T_F	Freezing point temperature, K
T_{IF}	Initial freezing point, K
T_{IN}	Initial product temperature, K

T_s	Product surface temperature, °C
T_{se}	Temperature at the half thickness of the slab, °C
T_1	Temperature at the first nodal point from the product surface, °C
T_∞	Ambient temperature, °C
t	Time, second
Δt	Time step, second
UFWC	Unfreezable water content, kg water/kg product
V	Volume, m^3
VFD	Volume fraction of discontinuous phase, dimensionless
VFI	Volume fraction of ice, dimensionless
VFS	Volume fraction of solids, dimensionless
VFW	Volume fraction of water, dimensionless
v	Air speed, m/s
$\bar{v}$	Specific volume, m^3/kg
WC	Unfrozen water content, kg water/kg product
X_A	Mole fraction of solvent A, dimensionless
X_W	Mole fraction of water, dimensionless
x, y	Coordinates of triangular nodes for two-dimensional element, m
Δx	Space increment in finite difference scheme, m
ρ	Density, kg/m^3
λ	Latent heat effect, J/m^3

λ_w Heat fraction of water, J/m^3

χ Chi function

Subscripts

f Condition after freezing

i, j, k Nodes of a triangular finite element

p Condition before freezing

u Define nodal point in finite difference scheme,

$x = u \Delta x$

Superscripts

m Define time level in finite difference scheme

e A triangular finite element

1. INTRODUCTION

Frozen food is one of the most important food products in the United States. The total pack and sales value of frozen foods in the United States reported by product category in 1966 was 6,284 million kilograms and 6,244 million dollars (Tressler et al., 1968) respectively. The design of food freezing processes is based primarily on refrigeration requirements for freezing and rate of product freezing. Appropriate methods to estimate the rate of freezing is important to achieve optimum design which results in good product quality and in an efficient process to avoid excessive energy consumption. Even though there have been significant improvements in the prediction of food freezing rates, the phenomena of phase-change, the influence of product thermal properties, the importance of product geometry and the effect of freezing environment on the freezing rate are not fully understood.

The most recognized exact solutions to predict the freezing time in the food freezing process are Plank's equation and Newmann's solution (Bakal and Hayakawa, 1973) or the solution recently developed by Golovkin et al. (1973). All of these are limited to special boundary conditions, constant product thermal properties and to geometrically regular shapes, i.e., infinite slab, infinite cylinder, and sphere. Numerical solutions utilizing finite differences methods for temperature dependent thermal properties and regular geometric shapes have been discussed by Bonacina et al. (1973), Charm et al. (1972), Cleland and Earle (1977), Fleming (1973), Joshi and Tao (1974), Heldman (1974b), Heldman and Gorby (1974b), Hsieh et al. (1977), Lescano and Heldman (1973), and Tarnawski (1976). The finite difference approximations are acceptable, but the simulation method lacks flexibility to incorporate more complex geometry of food products and boundary conditions.

Comini and Bonacina (1974), De Baerdemaeker et al. (1977), Rebellato et al. (1978) and Singh and Segerlind (1974) suggested the implementation of finite element methods for estimating freezing time of food to reduce complex geometry and boundary condition problems. While the finite element analysis has proved excellent in accommodating linear and non-linear heat conduction in the freezing process, no investigations have verified the simulation results experimentally. It should be emphasized that previous investigations have assumed that the product thermal properties are constant or a linear function of temperature. Numerical techniques utilized by

Heldman and Gorby (1974b), Hsieh et al. (1977) and Lescano and Heldman (1973) to account for variation of product thermal properties during freezing have provided accurate predictions of freezing time.

During the freezing process when air is used as refrigerant, convective surface heat transfer coefficients become an important factor in prediction of freezing rate. Most of the investigations conducted have assumed constant surface heat transfer coefficient as the boundary condition for a given food product. Katinas et al. (1976) and Zdanavichyus et al. (1977) published an experimental result suggesting that the convective heat transfer coefficient varies sinusoidally along surface of a cylinder.

The primary objective of this research was to develop a numerical solution model using finite element methods to predict the rate of freezing of food products with anomalous shapes. Specific objectives were as follows:

1. To develop a computer program utilizing the finite element method to simulate the freezing process of elliptical and trapezoidal food products subjected to various boundary conditions.
2. To incorporate temperature dependent thermal properties during phase-change into the

computer algorithm for both two-dimensional and axisymmetric heat transfer problems.

3. To investigate the influence of various boundary conditions on the freezing time: constant surface heat transfer coefficient, heat transfer coefficient as a function of location on the surface of food product and variable surface temperature during freezing.
4. To incorporate a method to estimate an optimum freezing time based on area average enthalpy in the finite element analysis and to compare this estimate to a conventional method based on the slowest freezing point location.
5. To conduct experimental measurement of the freezing rate of elliptical and trapezoidal shape food product in the laboratory, using air-blast freezing method and ground beef for the freezing material, in order to verify the numerical solution.

2. LITERATURE REVIEW

2.1. Analytical Solution for Phase-Change Problems

Most analytical solutions used to estimate the freezing time in phase-change problems have been based on either solving heat balance equations (Plank's equation and Tanaka and Nishimoto's formula) or solving Fourier's equation of unsteady-state heat conduction (Newmann's solution, Tao's chart, and Tien's approach). All approaches have limitations of assuming constant product thermal properties and assuming regular geometrical shapes, i.e., infinite slab, infinite cylinder, and sphere (Bakal and Hayakawa, 1973; Carslaw and Jaeger, 1959). Bakal and Hayakawa (1973) indicated further that all the above methods used either a single temperature or a specified range of temperatures, during phase-change. Slavin (1964) pointed out the inaccuracy of Plank's formula for calculation of freezing times for food, and Charm and Slavin (1962) reported 40 to 80 percent differences between Newmann's equation and experimental data in freezing time for cod fillets.

Cho and Sunderland (1974) attempted to improve the exact solution by assuming thermal conductivity to vary linearly with temperature. The analysis applied to both melting and solidification of semi-infinite bodies but used the fusion temperature as a fixed temperature while phase-change occurred and did not account for the variability of product thermal properties other than thermal conductivity. Mikhailov (1976) developed an exact solution for freezing of a humid porous body, thus solving for moisture distribution as well as temperature distribution. The analytical method is applied to Stefan-like problems which consider the occurrence of phase-change at a single temperature. Riley and Duck (1977) used the heat-balance integral method for the Stefan problems in freezing of a three-dimensional cuboid with all thermal properties of the product assumed constant. The authors also mentioned the unresolved question of accuracy even though some criteria have been established for semi-infinite region by Langford (1973).

Golovkin et al. (1973) suggested mathematical models for freezing of meat in two-sided slab, cylinder, and sphere geometry. The Stefan assumptions on the phase interface in the integral form were applied to obtain more accurate solution than if the differential form was used.

Hayakawa and Bakal (1974) proposed formulas to predict transient temperatures in food during freezing and thawing. Phase changes are assumed to occur over a range of temperatures and the geometry of food is an infinite slab with insulation on one side. During freezing, the material is observed to move through an unfrozen state, partly frozen state and a frozen state. Freezing processes are divided into several periods: (a) precooling, (b) first phase-change, where a partly frozen zone moves along the direction of heat transfer, (c) intermediate phase-change, where a partly frozen zone exists throughout the body until the surface body temperature reaches the final freezing point, (d) second phase-change, where a frozen zone moves along the slab thickness, and (e) tempering when the body is completely frozen. The experiment conducted to verify the formula indicated that the mathematical model was in good agreement for all periods of the freezing process except intermediate phase-change. Difficulty was also encountered in determining the final freezing point during the intermediate phase-change.

2.2. Numerical Methods Using Finite Differences for Solving Phase-Change Problems

Many researchers have explored numerical techniques in order to get more accurate solutions for phase-change problems than obtained from analytical methods. Bonacina and Comini (1973a) developed a numerical solution using an implicit finite difference scheme suggested by Lees (1966) which involves three time levels.

$$- \frac{2}{3} \frac{(\Delta X)^2}{\Delta t} k^m_{i+\frac{1}{2}} \cdot T^{m+1}_{i+1} + [C^m_i + \frac{2}{3} \frac{(\Delta X)^2}{\Delta t}$$

$$(k^m_{i+\frac{1}{2}} + k^m_{i-\frac{1}{2}})] T^{m+1}_i - \frac{2}{3} \frac{(\Delta X)^2}{\Delta t} k^m_{i-\frac{1}{2}} \cdot T^{m+1}_{i-1}$$

$$= \frac{2}{3} \frac{(\Delta X)^2}{\Delta t} [k^m_{i+\frac{1}{2}} (T^m_{i+1} - T^m_i + T^{m-1}_{i+1} - T^{m-1}_i)$$

$$- k^m_{i-\frac{1}{2}} (T^m_i - T^m_{i-1} + T^{m-1}_i - T^{m-1}_{i-1})] + C^m_i T^{m-1}_i \quad (2.1)$$

The scheme was unconditionally stable and convergent and the applied boundary conditions were the first kind--prescribed surface temperature, and the fourth kind--variable surface temperature. Bonacina et al. (1973) checked the numerical method against the analytical solution for the one-dimensional freezing problem (Luikov, 1968) and found the agreement to be within 3 percent. Using the same method for two-dimensional heat transfer, Bonacina and Comini (1973b) investigated the second and third kind of boundary conditions which were constant heat flux and linear heat transfer at the surface, respectively. However, the analysis and the experiment to verify the method were conducted only for heating and cooling processes.

Cleland and Earle (1977b) discussed the above numerical solutions thoroughly and suggested the use of the third kind of boundary condition for food freezing.

$$h (T_\infty - T_s) = - k \left(\frac{dT}{dx}\right)_{x=0} \text{ for } t > 0 \quad (2.2)$$

Instead of using the finite difference boundary condition as proposed by Bonacina et al. (1973), the boundary condition was derived from a heat balance over the surface space increment which extended a distance of 0.5Δx from the surface.

$$\frac{k_{+\frac{1}{2}}}{\Delta x}(T_1 - T_s) = h(T_s - T_\infty) + C\,(T_s)\frac{dT_s}{dt} \qquad (2.3)$$

The numerical scheme for one-dimensional heat conduction was proved to be in good agreement with experimental data in freezing of mashed potato and minced lean beef.

Goodrich (1978) outlined a numerical procedure to solve one-dimensional phase-change problems with a defined moving boundary condition at a fixed temperature which was the product freezing point. The central difference scheme was utilized in the numerical technique and the thermal properties of product were considered to vary linearly with temperature.

Hashemi and Sliepcevich (1967) presented a numerical solution for one- and two-dimensional temperature distribution in an isotropic medium where phase-change occurred in finite temperature intervals. The procedure utilized predictor-corrector and implicit finite difference methods in solving Neumann's solution for one-dimensional heat transfer and incorporated the alternating direction method with the predictor-corrector formula for two-dimensional heat transfer.

Shamsundar and Sparrow (1975) employed an enthalpy model to analyze multidimensional conduction phase-change

$$\frac{d}{dt} \int_V \rho I \, dV = \int_A k \text{ grad } T \cdot \hat{n} \, dA \qquad (2.4)$$

The model was approximated by using the implicit finite difference method, but no experimental work was conducted to confirm the simulation.

Joshi and Tao (1974) utilized the finite difference method to solve the problem of axisymmetrical freezing of food products. The method implemented the first and third kind of boundary conditions and used forward-difference for the time derivative and central-difference for the space derivative. The product thermal properties varied with temperature and fraction of frozen water except for product density which was assumed constant. The verification of the numerical method in rectangular beef freezing experiments gave satisfactory results.

Tarnawski (1976) proposed a mathematical model to solve one-dimensional heat and mass transfer during food freezing using the third kind of boundary condition. The mathematical model took into account the discontinuity and nonlinearity of product thermal properties and was approximated by finite difference methods. The simulation results did not use the mass transfer potential as described in the model, and were not verified by experimental data.

Lescano and Heldman (1973) developed a mathematical model to predict the thermal properties of a food product based on variable composition of water and ice within the product as temperature changed during freezing. A numerical scheme was later outlined to solve the one-dimensional symmetric heat transfer problem with a boundary condition of the third kind using the Crank-Nicholson formula for finite difference analysis. The application of the computer simulation yielded good agreement with experimental data in freezing of slab codfish. Heldman and Gorby (1974a) improved the prediction model for variable product thermal properties by implementing the Kopelman equation (1966) to describe the relationship of thermal conductivity with product composition which was changing as temperature decreased during freezing. The improved mathematical model along with finite difference methods were utilized successfully to solve one-dimensional transient heat transfer in ice cream freezing. Numerical solutions, using finite difference method, to simulate the freezing process for spherical geometric food products, were developed incorporating the above prediction model for variable product thermal properties (Heldman and Gorby, 1975). The finite difference equations were derived by both forward and pure implicit methods and applied to IQF (Individual Quick Freezing) of cherries with acceptable results. Hsieh et al. (1977) modified the above computer simulation techniques to predict the freezing times and temperature history for different fruits and vegetables.

2.3. The Implementation of Finite Element Models to Phase-Change Problems

The application of finite element methods in solving heat conduction problems has been discussed by Zienkiewicz and Cheung (1965), Visser (1965), Wilson and Nickell (1966), and Richardson and Shum (1969). The analysis has included problems with steady and unsteady state heat transfer, linear and nonlinear boundary conditions and nonstationary temperature distribution. More examples of the finite element models applied to transient heat conduction can be found in references such as Zienkiewicz (1971), Desai and Abel (1972), and Segerlind (1976). Emery and Carson (1971), and Bruch and Zyvoloski (1974) discussed the accuracy and efficiency of the finite element method and illustrated acceptable comparison to exact solution and finite difference method for both linear and nonlinear two-dimensional heat conduction problems. Comini and Lewis (1976) developed a numerical solution using finite element methods for two-dimensional and axisymmetrical problems involving heat and mass transfer in porous media. The simulation was in agreement with analytical solution in drying of a geometrically slab material. Singh and Segerlind (1974) applied the finite element models to describe time-dependent axisymmetric problems in heating of a cylindrical food can containing homogeneous material and to simulate heating of a chicken leg composed of four different materials. De Baerdemaeker et al. (1977) discussed the application of finite element analysis to pear cooling and to rectangular beef steak frying.

Bonnerot and Jamet (1974) introduced the implementation of the finite element method for the one-dimensional Stefan problem to determine the position of the free boundary of phase-change. The quadrilateral elements were used and the temperatures were calculated for all element nodes as well as additional nodes along the moving boundary at each time step. The expanding grid used to track the free boundary is only useful for small boundary motions and for cases in which the temperatures on one side of the boundary are always zero (Wellford Jr. and Ayer, 1977). The latter authors proposed a fixed grid of standard space-time finite elements and discontinuous interpolation to define the finite element model on the special elements which were the quadrilateral elements crossed by the free boundary at any particular step in time. Krutz (1976) developed a finite element computer model for phase-change from solid to liquid in determining the time-temperature history of a welded joint. Thermal conductivity and specific heat were considered as a linear function of temperature and the model included radiation, convection and heat flux on the surface.

Comini et al. (1974) applied the finite element method to freezing analysis with nonlinear boundary conditions. The physical properties were considered to vary linearly with temperature in addition to a jump within a small temperature interval ($2\Delta T$) at the freezing point. The nonlinear boundary condition took into account imposed heat flux and rates of heat flow per unit area due to convection and radiation on the surface. Simple triangular elements were used and the three level scheme suggested by Lees (1966), as discussed previously in Section 2.1, was introduced for time-stepping instead of Crank-Nicholson algorithm. The freezing simulation program was used to predict the position of frozen boundary in slab form and for soil freezing.

Comini and Bonacina (1974) presented the application of the above method in food freezing to overcome the lack of flexibility of finite difference method in solving the irregular geometrically shape problems. The thermal properties were calculated based on the decreasing mass fraction of water during freezing but the method to detect the fraction of water during the freezing process was not given. The latter method will be discussed in the next section. Bonacina et al. (1974) compared results of the above finite element method with experimental data in freezing of Tylose samples which have been modeled after lean beef. The heat conduction problem was selected to be one-dimensional with boundary condition of the first kind. The error between measured and calculated temperature at the center and surface of the slab was found to be less than 2 percent. Rebellato et al. (1978) used this simulation program to solve the two-dimensional heat conduction problem utilizing a second-order quadrilateral element grid in estimating the freezing rate of lamb carcass and beef side. However, no experimental data has been reported so far to verify the results of this two-dimensional irregular geometry food freezing problem.

2.4. Factors Influencing the Rate of Food Freezing

The rate of food freezing is influenced by several factors including temperature of surrounding medium, size and shape of frozen product, thermal properties of the product and surface heat transfer coefficient. It has been widely known that the lower the surrounding temperature, the higher the rate of freezing. Tarnawski (1976) and Hsieh et al. (1977) showed that the relationship between freezing time and surrounding temperature was nonlinear. Size and shape have always been important factors to consider in the analysis of freezing as previously discussed for the analytical solution, the finite difference method and the finite element method. Hsieh et al. (1977) investigated the influence of product diameter on freezing time for various fruits and vegetables. The freezing time increased linearly as the product diameter became larger.

The determination of the transient temperature field and the rate of freezing for food products using the assumption that phase-change exists at a constant temperature is not accurate. Several investigators have proposed formulas to estimate product thermal properties as freezing occurs over a temperature range or during the whole process. Comini et al. (1974) suggested that phase-change could be assumed to occur at a temperature range from T_i (initial temperature) $\simeq -1°C$ until a certain value of T_f (final temperature) where there was T_p (peak temperature) $\simeq -3°C$ in between (Figure 2.1.). The

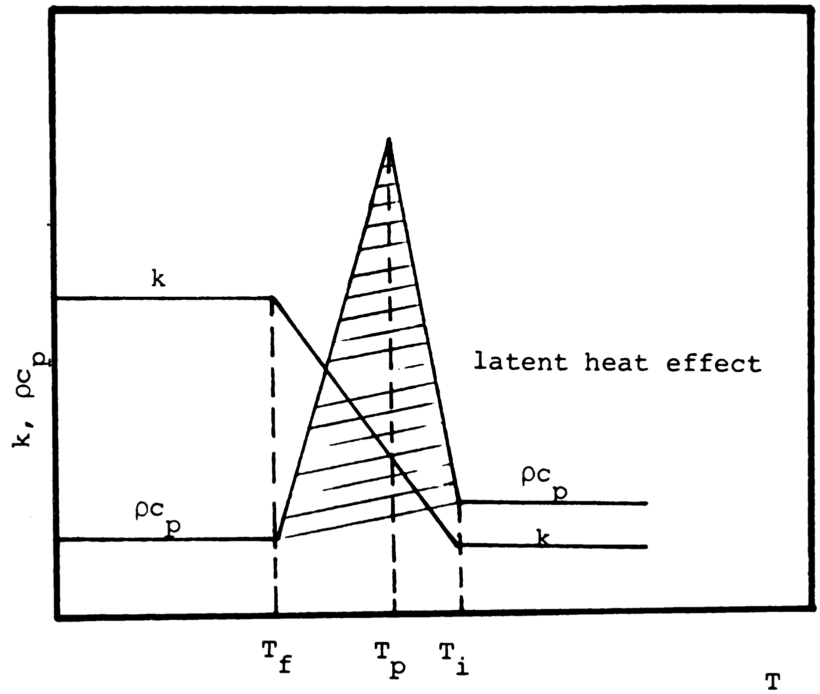

Figure 2.1. The relationship of thermal properties of food product and temperature during freezing according to Comini et al. (1974).

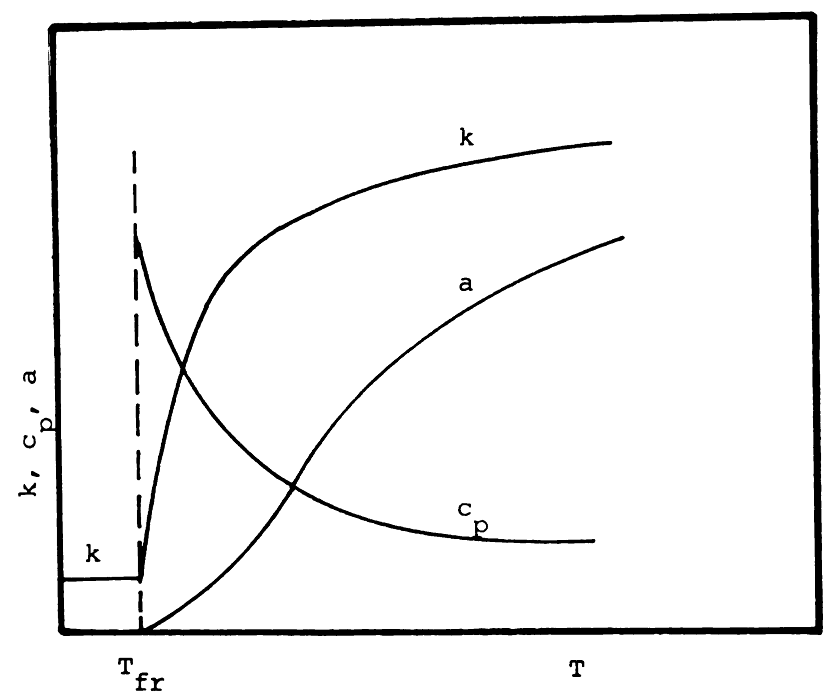

Figure 2.2. The relationship of thermal properties of food product and temperature during freezing according to Tarnawski (1976).

final temperature is estimated as the value that gives the best fit between calculated results and experimental data. The formulas to calculate thermal conductivity and specific heat capacity above and below freezing are given as follows

$$c_p = mc \cdot CPW + (1 - mc) \cdot CPS \qquad (2.5)$$

$$k_p = mc \cdot KW + (1 - mc) \cdot KS \qquad (2.6)$$

$$c_f = mc \cdot CPI + (1 - mc) \cdot CPS \qquad (2.7)$$

$$k_f = mc \cdot KI + (1 - mc) \cdot KS \qquad (2.8)$$

The value of heat capacity at T_p can be obtained from evaluating the latent heat effect which is the area of heat capacity versus temperature as T_i, T_p, and T_f are known

$$\lambda = mc \cdot \lambda_w \qquad (2.9)$$

The disadvantages of this method are that phase-change is assumed to occur only over a short temperature range, the final temperature has to be chosen arbitrarily if experimental data do not exist and the relationship between thermal properties and temperature is actually nonlinear.

Tarnawski (1976) presented nonlinear function to describe the relationship between physical parameters of a food product and temperature where the function was discontinuous and nondifferential at the freezing point (Figure 2.2). The model to compute thermal conductivity and specific heat is not published and the calculation for beef are given as follows

for $248\ K \leq T \leq T_F$

$$a(T) = [-11032.6509 - 261.42196\,(Z) - 18252.4705\,(Z)^2 - 26.133707\,(Z)^3 - 133.87762\,(Z)^4 - 7.31961337\,(Z)^5 - 0.11645322\,(Z)^6] \times 10^{-9}\ m^2/h \qquad (2.10)$$

$$k(T) = [-124634.1825 - 744465.0959\,(Z) - 160251.468\,(Z)^2 - 17695.612\,(Z)^3 - 102.877816\,(Z)^4 - 29.874884\,(Z)^5 - 0.343013138\,(Z)^6] \times 10^{-6}\ W/m\ K \qquad (2.11)$$

for $T_f \leq T \leq 303.16\ K$

$$a(T) = 0.00042 - 0.000001\,(Z) \qquad m^2/h \qquad (2.12)$$

$$k(T) = 0.476079324 - 0.0004026324\,(Z)\ W/m\ K \qquad (2.13)$$

where

$$Z = T - 273.16$$

Since changes in product thermal properties during freezing are due to continuous depression of freezing point and thus continuous changes in unfrozen water content, the best approach is the method proposed by Heldman (1974a), and Heldman and Gorby (1974b). The unfrozen water content can be detected at any given time assuming food product as a mixture consists of water (solvent A), and ice together with food solids (solute B)

$$m_A = \frac{M_A X_A m_B}{M_B (1 - X_A)} \tag{2.14}$$

where

$$X_A = \exp [(L_A \cdot M_A / R_1)(1/T_{IF} - 1/T_{DF})] \tag{2.15}$$

Thermal conductivity is obtained from the Kopelman equation (1967)

$$k = k_c (1 - Q)/[1 - Q (1 - M)] \tag{2.16}$$

$$Q = M^2 (1 - k_d/k_c) \tag{2.17}$$

Enthalpy and specific heat are computed from equations (Lescano and Heldman, 1973)

$$H = EMS \cdot CPS (T + 40) + WC \cdot L + WC \cdot CPW (T + 40) + MI \cdot CPI (T + 40) - UFWC \cdot L \tag{2.18}$$

$$c_p = \Delta H / \Delta T \tag{2.19}$$

The implementation of the above equations (2.14) - (2.19) are further discussed in the next chapter. Figure 2.3 illustrates the nonlinear relationship between thermal properties of food product with temperature as calculated using equations (2.14) - (2.19).

The influence of surface heat transfer coefficient on freezing time has been investigated by several researchers. Heldman (1974b) compared the surface heat transfer coefficient versus freezing time curves for lean beef obtained from various analysis, Charm (1971), Lescano and Heldman (1973), analysis graphical method, and modified Planck's equation (1958). The results indicated that the freezing time decreased significantly as the heat transfer coefficient increased to 25 W/m^2 K. The same result was confirmed by Tarnawski (1976) for beef freezing. Hsieh et al. (1977) found that the freezing time could be reduced significantly as the surface heat transfer increased to 40 W/m^2 K for freezing of various fruits and vegetables.

All the previous investigations were carried out for uniform surface heat transfer coefficient. The influence of variable local heat transfer coefficient on the surface of food product during freezing has not been published. Katinas et al. (1976) and Zdanavichyus et al. (1977) presented the local heat transfer coefficient as a

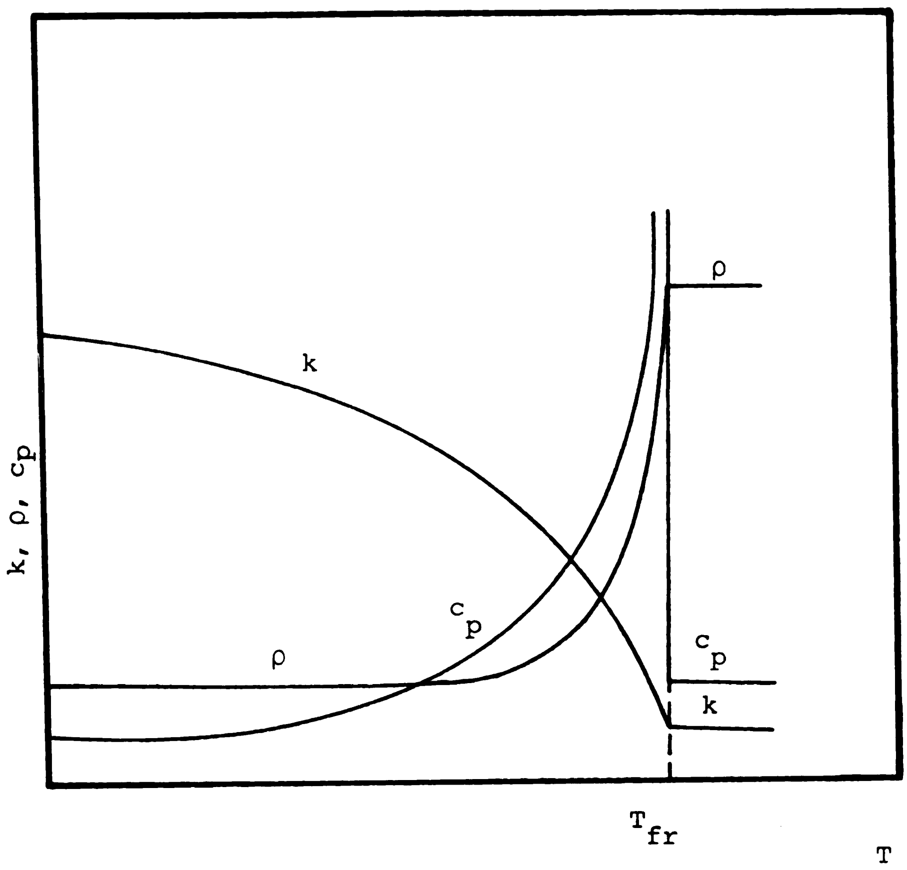

Figure 2.3. The relationship of thermal properties of food product and temperature during freezing according to Heldman and Gorby (1974).

function of location on the surface of a cylinder. The function behaved sinusoidally because the degree of turbulency of an inflowing air stream around the circular cylinder.

2.5. The Stability of the Finite Element Method in Comparison to the Analytical Solution and the Finite Difference Method

Emery and Carson (1971) evaluated the use of the finite element method in the computation of temperature for linear and nonlinear two-dimensional problems and compared it with the finite difference method. The finite element method applied was utilizing linear, quadratic, cubic and special cubic elements. For the finite difference method, three different kinds of time stepping schemes were analyzed, i.e., explicit, Crank-Nicholson, and Lex-Wendroff (1967). The authors concluded that the finite difference method required less core memory in the computer and gave faster execution time especially for variable thermal properties problems which needed computation at each time step. The finite element method had the advantages of solving heat conduction problems for arbitrary geometry and was more accurate. Furthermore, there were advantages associated with the ease of inputting the required data and the capability of altering the basic accuracy of the method.

Bruch and Zyvoloski (1974) discussed the implication of the finite element method to solve linear and nonlinear two-dimensional heat conduction problems. Rectangular prisms in a space-time domain were used as the finite elements and the implicit method was applied for the time-stepping scheme. The finite element solutions compared favorably with the results from analytical solutions and finite difference methods. It was found to be stable and convergent to the exact solution.

Yalamanchili and Chu (1973) analyzed the stability and oscillation characteristics of the finite difference method and the finite element method with and without use of Galerkin's method of weighted residuals. The stability criteria were established by utilizing the general stability, von Neumann formulas, and Dusinberre concepts (1961). For transient two-dimensional heat conduction in solids, the results showed that the region of favorable stability and oscillation characteristics were found to be significantly larger for the finite element method than for the finite difference method. The use of Galerkin method improved the degree of stability and reduced the oscillation.

3. THEORETICAL CONSIDERATIONS

3.1. Temperature Dependent Physical Properties

The change in thermal properties of a food product during freezing is due to continuous freezing point depression caused by a reduction in unfrozen water content. The development of mathematical equations to predict the thermal properties of food based on the freezing point depression has been described by Heldman (1974a) and Heldman and Gorby (1974a). This method has been successfully utilized to predict the thermal properties of food product during freezing (Heldman, 1974b; Heldman and Gorby, 1974b; Heldman and Gorby, 1975; Hsieh et al., 1977). Assumptions regarding the temperature dependent physical properties are as follows:

1. The food product is homogeneous and isotropic.
2. The thermal properties are constant above the initial freezing point.
3. The food product consists of solids, water, and ice during the freezing process. While the thermal properties of food product vary nonlinearly according to temperature, thermal properties of product solids remain constant.

4. Below the initial freezing point, the food product is assumed to be an ideal binary system with continuous and discontinuous phases. Since the frozen food consist of three phases, it is reduced to one binary system during the first step and to another system during the second step.

3.1.1. Unfrozen Water Content

The relationship between the mole fraction of solvent and the freezing point depression in a solution is described in equations (2.14) and (2.15). Heldman (1974a) proposed that the unfrozen water content at a given temperature during food freezing can be predicted using the above equations assuming the liquid water is the solvent and solids is the solute. The molecular weight of product solids above freezing point is calculated assuming product solids as the solute and water as solvent. Thus, equations (2.14) and (2.15) become

$$XW = \exp\left[(LW \cdot MW/R)(1/T_{IN} - 1/T_{IF})\right] \tag{3.1}$$

$$MS = \frac{EMS \cdot XW \cdot MW}{EMW\ (1 - XW)} \tag{3.2}$$

where

$$EMS = 1 - IWC \tag{3.3}$$

EMW in equation (3.2) is modified taking into account the small amount of unfreezable water content at low temperature. This approach has been thoroughly discussed by Lescano and Heldman (1973). The effective mass of water becomes

$$EMW = IWC - UFWC \tag{3.4}$$

The total unfrozen water content at any given temperature below the freezing point can be computed as follows

$$XW = \exp\left[(LW \cdot MW/R_1)(1/T_{IF} - 1/T_{DP})\right] \tag{3.5}$$

$$EMW = \frac{EMS \cdot XW \cdot MW}{MS\ (1 - XW)} \tag{3.6}$$

$$WC = EMW + UFWC \tag{3.7}$$

3.1.2. Thermal Conductivity

Kopelman (1967) derived mathematical models to predict thermal conductivity in food products for both isotropic and anisotropic systems. The model for an isotropic system in a two component product is

$$k = k_c \left(\frac{1 - Q}{1 - Q(1 - M)}\right) \tag{3.8}$$

$$Q = M^2\ (1 - k_d/k_c) \tag{3.9}$$

The first step in the use of the Kopelman equation has water considered as the continuous phase for the water-ice system. Then, the water-ice mixture is treated as a continuous phase while the product solids is taken as discontinuous phase for the second use of the equation.

3.1.3. Product Density

The product density decreases according to the proportional changes of the mixture and can be expressed in the following manner (Heldman and Gorby, 1974a)

$$\bar{V} = 1/PD = WC/DW + MI/DI + EMS/DS \qquad (3.10)$$

For the computer program, the density of solids before freezing must be obtained by substituting initial product density, initial water content and MI = 0 into equation (3.10)

$$DS = 1/(1/IPD - WC/DW) \qquad (3.11)$$

Then, the product density at any given time is solved by using equation (3.10) and unfrozen water content as computed according to Section 3.1.1.

3.1.4. Enthalpy and Apparent Specific Heat

The enthalpy of the food product can be obtained based on the specific heat of product components and the unfreezable water content. Utilizing a reference temperature of -40°C, Lescano and Heldman (1973) expressed the enthalpy as

$$H = EMS \cdot CPS \cdot (T + 40) + WC \cdot LW + WC \cdot CPW \cdot (T + 40) + MI \cdot CPI \cdot (T + 40) - UFWC \cdot LW \quad (3.12)$$

The multiplication of water content by its latent heat of fusion, WC•LW, accounts for the heat released during phase-change inside the food product. The specific heat of solids can be determined by solving the equation

$$ICP = IWC \cdot CPW + MS \cdot CPS \quad (3.13)$$

while CPI is obtained from Dickerson equation (Dickerson, 1969)

$$CPI = A + B \cdot T \quad (3.14)$$

where

$A = 1.9507941$

$B = 0.00206153$ for T as absolute temperature

WC in equation (3.12) is calculated by solving equations (3.5) - (3.7), while MI is obtained as follows

$$MI = 1 - WC - MS \quad (3.15)$$

Assuming the relationship between enthalpy with temperature is a continuous function, the apparent specific heat of a food product can be expressed as differential change in enthalpy

$$CPA = \Delta H/\Delta T \tag{3.16}$$

For this study, $\Delta T = 0.003°C$ was used in the numerical solution.

3.2. Governing Equations, Initial and Boundary Conditions

In food freezing, heat transfer occurs primarily by conduction. This research dealt with two-dimensional heat transfer in eliptical and trapezoidal shapes. The governing differential equation for heat conduction in isotropic bodies is known as the Fourier heat conduction equation (Carslaw and Jaeger, 1959). For two-dimensional heat transfer, the equation is as follows

$$c_p \rho \frac{\partial T}{\partial t} = \frac{\partial}{\partial x}[k_{xx} \frac{\partial T}{\partial x}] + \frac{\partial}{\partial y} [k_{yy} \frac{\partial T}{\partial y}] + Q' \tag{3.17}$$

The body is at uniform temperature initially

$$T = T_o \text{ at } t = 0 \tag{3.18}$$

The boundary conditions are

$$k_{xx}[\frac{\partial T}{\partial x}] + k_{yy}[\frac{\partial T}{\partial y}] + h\ (T - T_\infty) = 0 \tag{3.19}$$

at the convective surface and for $t > 0$

and

$$\left.\frac{\partial T}{\partial y}\right|_{y=0} = 0 \text{ at the insulated surface and for any given time} \qquad (3.20)$$

Further assumptions regarding the modes of heat transfer are listed below:

1. Heat transfer from the freezing medium (air) to the product occurs by convection and heat moves by conduction within the product.
2. Energy transports occur only in x and y direction.
3. The rate of heat transfer within the food is uniform along the x and y direction. Thus, $k_{xx} = k_{yy}$.
4. The surface heat transfer coefficient is a function of location along the surface; however, it remains constant at a given position during the freezing process.
5. The surrounding temperature and velocity of freezing medium are constant and uniform.
6. Water vapor transport from the product to the air is negligible. Thus, mass transfer within the product and on the product surface are neglected.

The governing differential equation, initial and boundary conditions for axisymmetrical heat transfer in trapezoidal bodies are expressed in equations (3.21) - (3.24)

$$c_p \rho \frac{\partial T}{\partial t} = \frac{1}{r} k_{rr} \frac{\partial T}{\partial r} + \frac{\partial}{\partial r} [k_{rr} \frac{\partial T}{\partial r}] + \frac{\partial}{\partial z} [k_{zz} \frac{\partial T}{\partial z}] + Q' \tag{3.21}$$

Initial condition

$$T = T_o \quad \text{at} \quad t = 0 \tag{3.22}$$

Boundary conditions

$$k_{rr} [\frac{\partial T}{\partial r}] + k_{zz} [\frac{\partial T}{\partial z}] + h (T - T_\infty) = 0 \tag{3.23}$$

along the convective surface and for $t > 0$

and $$\left.\frac{\partial T}{\partial r}\right|_{r=0} = 0 \text{ at the insulated surface for any given time} \tag{3.24}$$

The assumption made for axisymmetric heat transfer are nearly the same as for two-dimensional, except for surface heat transfer coefficient and surface temperature:

1. Heat transfer from the freezing medium to the product occurs by convection and by conduction within the product.
2. Energy transports occur only in r and z directions.

3. The rate of heat transfer within the food is uniform along the r and z directions. Thus, $k_{rr} = k_{zz}$.

4. The surface temperature is a function of time and location along the surface.

5. Velocity of freezing medium is stable and uniform.

6. Mass transfer within the product and on the product surface are neglected.

3.3. Finite Element Formulation

3.3.1. Development of the Model for Two-Dimensional Heat Transfer in Elliptical Geometry

In the finite element method for field problems such as heat conduction, the integral of a function is minimized using the calculus of variations (Segerlind, 1976). The governing equation for two-dimensional heat transfer (3.17) and its boundary conditions (3.19) and (3.20) can be formulated as follows

$$\chi = \int_V \frac{1}{2} [k_{xx} (\frac{\partial T}{\partial x})^2 + k_{yy} (\frac{\partial T}{\partial y})^2 - 2Q'T + 2c_p \rho T \frac{\partial T}{\partial t}] \, dV + \int_S \frac{h}{2} (T - T_\infty)^2 \, ds \tag{3.25}$$

where T_∞ is ambient temperature while V denotes the total volume of the body and s is surface area.

The advantage of calculation of temperature dependent thermal properties using freezing point depression as described in 3.1. is that it has taken change of phase into account. Specific heat of product is derived as differential change in enthalpy which is a function of latent heat, thus the specific heat is also a function of latent heat. Since latent heat has been incorporated into thermal properties of product (k, c_p, and ρ), the term for heat generation inside the body, Q', can be eliminated.

$$\chi = \int_V \frac{1}{2} [k_{xx}(\frac{\partial T}{\partial x})^2 + k_{yy} (\frac{\partial T}{\partial y})^2 + 2c_p\rho T \frac{\partial T}{\partial t}] \, dV + \int_s \frac{h}{2} (T - T_\infty)^2 \, ds \tag{3.26}$$

Defining two matrices

$$\{g\}^T = [\frac{\partial T}{\partial x} \quad \frac{\partial T}{\partial y}] \tag{3.27}$$

and

$$[D] = \begin{bmatrix} k_{xx} & 0 \\ 0 & k_{yy} \end{bmatrix} \tag{3.28}$$

Equation (3.26) can be rewritten as

$$\chi = \int_V \frac{1}{2} (\{g\}^T [D] \{g\}) \, dV + \int_V c_p\rho T \frac{\partial T}{\partial t} \, dV + \int_s \frac{h}{2} [T^2 - 2T\cdot T_\infty + T_\infty^2] \, ds \tag{3.29}$$

Since the function for T is defined over individual sub-regions called elements, $T^{(e)}$, equation (3.29) can be transformed to a sum of the integrals over the total number of elements, E.

$$\chi = \sum_{e=1}^{E} \int_{V^{(e)}} \frac{1}{2}(\{g^{(e)}\}^T \; [D^{(e)}] \; \{g^{(e)}\})dV$$

$$+ \int_{V^{(e)}} c_p \rho \frac{\partial T}{\partial t} \, dV + \int_{S^{(e)}} \frac{h}{2}(T^{(e)}T^{(e)} - 2T^{(e)}T_\infty$$

$$+ T_\infty^2) \, ds$$

or $$\chi = \sum_{e=1}^{E} \chi^{(e)} \tag{3.30}$$

To minimize the function which is equating the summation of derivatives of $\chi^{(e)}$ with respect to T with zero, it is necessary to express the equation in terms of nodal values of temperature {T}. Utilizing two-dimensional simplex elements (Figure 3.1.a), then

$$T^{(e)} = [N^{(e)}] \; \{T\} \tag{3.31}$$

or $$T^{(e)} = N_i T_i + N_j T_j + N_k T_K \tag{3.32}$$

where N_β is a shape function, and i, j, k are denoting nodes of each triangular element whose equations are given by

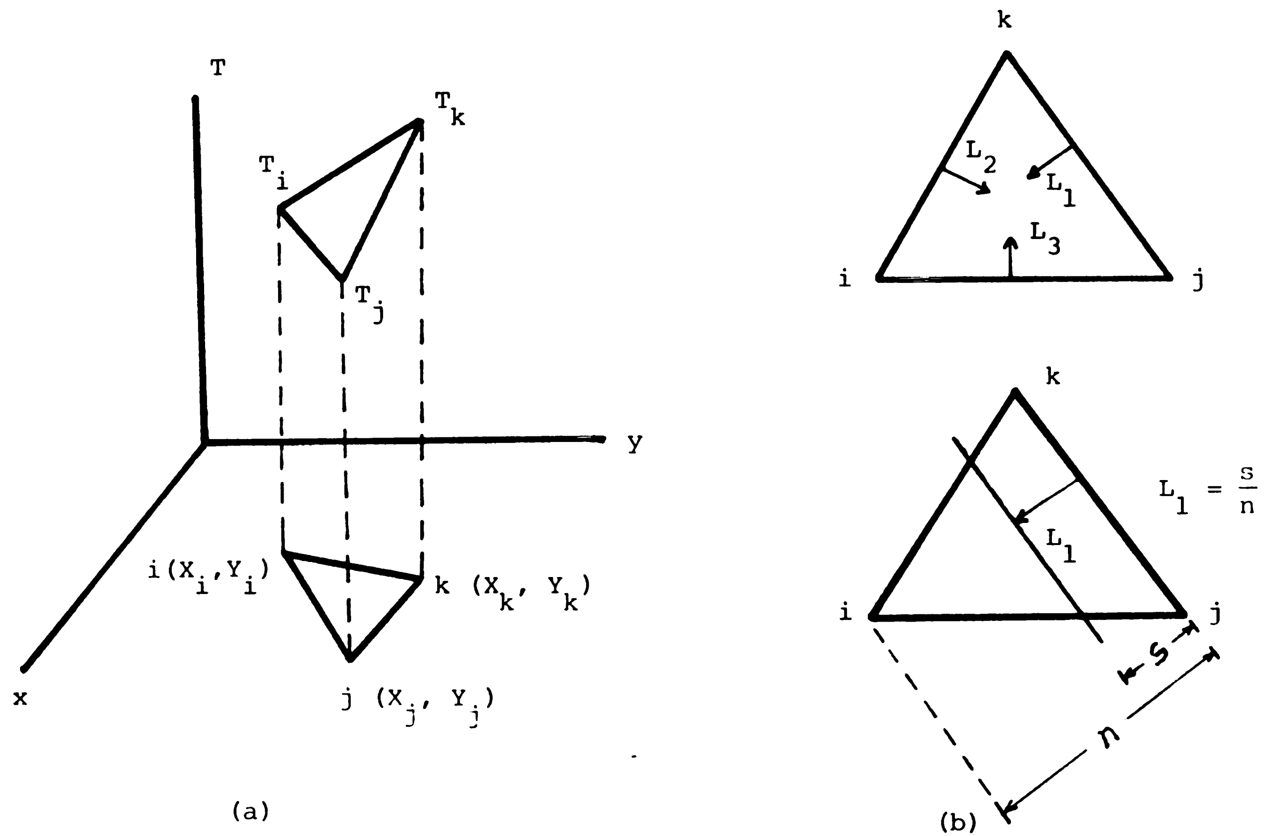

Figure 3.1. Simplex two-dimensional element and area coordinates.

$$N_i = \frac{1}{2A}(a_i + b_i x + c_i y)$$
$$N_j = \frac{1}{2A}(a_j + b_j x + c_j y) \quad (3.33)$$
$$N_k = \frac{1}{2A}(a_k + b_k x + c_k y)$$

$$a_i = x_j y_k - x_k y_j \qquad b_i = y_j - y_k \qquad c_i = x_k - x_j$$
$$a_j = x_k y_i - x_i y_k \qquad b_j = y_k - y_i \qquad c_j = x_i - x_k \quad (3.34)$$
$$a_k = x_i y_j - x_j y_i \qquad b_k = y_i - y_j \qquad c_k = x_j - x_i$$

$$A = \frac{1}{2}\begin{bmatrix} 1 & x_i & y_i \\ 1 & x_j & y_j \\ 1 & x_k & y_k \end{bmatrix} \quad (3.35)$$

Introducing the area coordinates L_1, L_2, L_3 (Figure 3.1.b) as values indicating the area, equation (3.33) can be expressed as follows

$$L_1 = N_i = \frac{1}{2A}(a_i + b_i x + c_i y)$$
$$L_2 = N_j = \frac{1}{2A}(a_j + b_j x + c_j y) \quad (3.36)$$
$$L_3 = N_k = \frac{1}{2A}(a_k + b_k x + c_k y)$$

Substituting equations (3.31) and (3.33) into equations (3.27) and (3.30)

$$\{g^{(e)}\} = \begin{Bmatrix} \dfrac{\partial T^{(e)}}{\partial x} \\ \\ \dfrac{\partial T^{(e)}}{\partial y} \end{Bmatrix} = \begin{bmatrix} \dfrac{\partial N_i^{(e)}}{\partial x} & \dfrac{\partial N_j^{(e)}}{\partial x} & \dfrac{\partial N_k^{(e)}}{\partial x} \\ \\ \dfrac{\partial N_i^{(e)}}{\partial y} & \dfrac{\partial N_j^{(e)}}{\partial y} & \dfrac{\partial N_k^{(e)}}{\partial y} \end{bmatrix} \begin{Bmatrix} T_i \\ T_j \\ T_k \end{Bmatrix} \qquad (3.37)$$

Or $$\{g^{(e)}\} = [B^{(e)}]\ \{T\} \qquad (3.38)$$

$$\begin{aligned} \chi^{(e)} = & \int_{V^{(e)}} \frac{1}{2}\{T\}^T\ [B^{(e)}]^T[D^{(e)}]\ [B^{(e)}]\{T\}\ dV \\ & + \int_{V^{(e)}} c_p \rho [N^{(e)}]\ \{T\}\ [N^{(e)}]\ dV\ \frac{\partial\{T\}}{t} \\ & + \int_{s^{(e)}} \frac{h}{2}\{T\}^T\ [N^{(e)}]^T\ [N^{(e)}]\{T\}\ ds \\ & - \int_{s^{(e)}} h\ T_\infty\ [N^{(e)}]\{T\} ds \\ & + \int_{s^{(e)}} \frac{h}{2}\ T_\infty^2\ ds \end{aligned} \qquad (3.38)$$

where $[B^{(e)}]$ is called the gradient matrix and is defined as

$$[B^{(e)}] = \frac{1}{2A} \begin{bmatrix} b_i & b_j & b_k \\ \\ c_i & c_j & c_k \end{bmatrix} \qquad (3.39)$$

The minimization of χ becomes

$$\frac{\partial \chi}{\partial \{T\}} = \sum_{e=1}^{E} \frac{\partial \chi^{(e)}}{\partial \{T\}} = \int_V [B]^T [D]\ [B]\{T\}\ dV$$

$$+ \int_V c_p \rho\ [N]^T [N]\ dV\ \frac{\partial \{T\}}{\partial t}$$

$$+ \int_s h\ [N]^T [N]\{T\}\ ds$$

$$- \int_s h\ T_\infty [N]^T\ ds = 0 \qquad (3.40)$$

Equation (3.40), in compact form, can be formulated as follows

$$[C]\ \{\dot{T}\} + [K]\ \{T\} = \{F\} \qquad (3.41)$$

where $[C] = \Sigma \int_V c_p \rho\ [N]\ dV$, capacitance matrix,

$$[K] = \Sigma (\int_V [B]^T\ [D]\ [B]\ dV$$

$$+ \int_s h\ [N]^T [N]\ ds),\text{ stiffness matrix,}$$

$$\{F\} = \Sigma \int_s h\ T_\infty\ [N]^T\ ds,\text{ force vector.}$$

Evaluating the integral of the first term of matrix [K] for a triangular element

$$\int_{V^{(e)}} [B^{(e)}]^T \; [D^{(e)}] \; [B^{(e)}] \; dV =$$

$$\frac{k_{xx}}{4A} \begin{bmatrix} b_i b_i & b_i b_j & b_j b_k \\ b_j b_i & b_j b_j & b_j b_k \\ b_k b_i & b_k b_j & b_k b_k \end{bmatrix}$$

$$+ \; \frac{k_{yy}}{4A} \begin{bmatrix} c_i c_i & c_i c_j & c_i c_k \\ c_j c_i & c_j c_j & c_j c_k \\ c_k c_i & c_k c_j & c_k c_k \end{bmatrix} \qquad (3.42)$$

Heat loss by convection along the body surface occurs in the second term of the stiffness matrix [K]. Using area coordinates, it is formulated as (Segerlind, 1976)

$$\int_s h \; [N]^T \; [N] \; ds =$$

$$h \int_{\mathcal{L}_{i,j,k}} \begin{bmatrix} L_1 L_1 & L_1 L_2 & L_1 L_3 \\ L_2 L_1 & L_2 L_2 & L_2 L_3 \\ L_3 L_1 & L_3 L_2 & L_3 L_3 \end{bmatrix} d\mathcal{L} \qquad (3.43)$$

Assuming the heat loss is along side ij of a triangular element, it gives

$$\int_s h\ [N]^T[N]\ ds = h\int_{\ell_{ij}} \begin{bmatrix} L_1L_1 & L_1L_2 & 0 \\ L_2L_1 & L_2L_2 & 0 \\ 0 & 0 & 0 \end{bmatrix} d\ell$$

$$= \frac{h}{6}\ell_{ij} \begin{bmatrix} 2 & 1 & 0 \\ 1 & 2 & 0 \\ 0 & 0 & 0 \end{bmatrix} \qquad (3.44)$$

where $\ell_{ij} = \sqrt{(x_i - x_j)^2 + (y_i - y_j)^2}$

The force vector in equation (3.41) becomes

$$\{f^{(e)}\} = \int_s h\ T_\infty\ [N]^T\ ds = \frac{h\ T_\infty}{2}\ell_{ij} \begin{Bmatrix} 1 \\ 1 \\ 0 \end{Bmatrix} \qquad (3.45)$$

The capacitance matrix can be expressed also in terms of area coordinates

$$[c^{(e)}] = c_p\rho \int_{\ell_{i,j,k}} \begin{bmatrix} L_1L_1 & L_1L_2 & L_1L_3 \\ L_2L_1 & L_2L_2 & L_2L_3 \\ L_3L_1 & L_3L_2 & L_3L_3 \end{bmatrix} d\ell$$

$$= \frac{c_p\rho A}{12} \begin{bmatrix} 2 & 1 & 1 \\ 1 & 2 & 1 \\ 1 & 1 & 2 \end{bmatrix} \qquad (3.46)$$

Equation (3.41) must be solved for each time step. Implementing a central difference rule will result in

$$([K] + \frac{2}{\Delta t}[C])\ \{T_{t+\Delta t}\} = (\frac{2}{\Delta t}[C] - [K])\ \{T_t\} - (\{F_{t+\Delta t}\} + \{F_t\}) \tag{3.47}$$

The thermal properties of food products are higher order functions of temperature (Figure 2.3) and are computed numerically as described in Section 3.1. An attempt to substitute the property functions into equation (3.26) would give complicated derivative of χ with respect to T in the minimization step. Thus, the values of k, c_p and ρ are computed for each element at every time step and new capacitance and stiffness matrices are assembled.

3.2.2. Development of the Model for Axisymmetrical Heat Transfer in Trapezoidal Geometry

The development of the model for axisymmetrical heat transfer is similar to two-dimensional heat transfer except for coordinates changed from x and y to r and z throughout equations (3.33) to (3.35). Figure (3.2) illustrates an axisymmetric triangular element. The shape function of an axisymmetric triangular element is transformed into

$$[N] = [N_i\ N_j\ N_k] = [L_1\ L_2\ L_3] \tag{3.48}$$

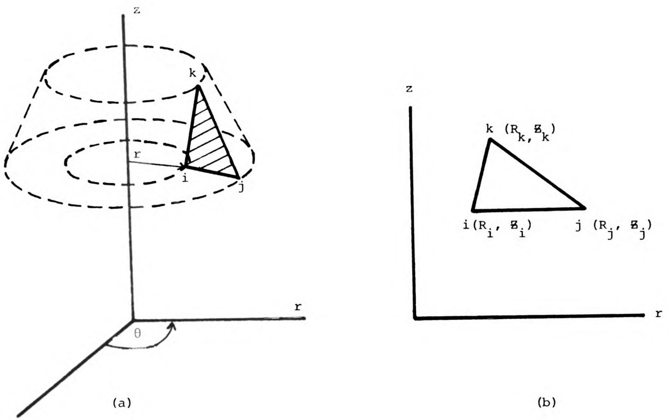

Figure 3.2. Simplex triangular axisymmetric element.

$$\text{where} \quad r = [L_1 \ L_2 \ L_3] \begin{Bmatrix} R_i \\ R_j \\ R_k \end{Bmatrix} \tag{3.49}$$

The stiffness and force matrices in equation (3.41) for the axisymmetrical body, assuming heat loss by convection along the ij side of a triangular element, are changed into

$$[k^{(e)}] = \frac{2\pi\bar{r}\ k_{rr}}{4A} \begin{bmatrix} b_i b_i & b_i b_j & b_i b_k \\ b_j b_i & b_j b_j & b_j b_k \\ b_k b_i & b_k b_j & b_k b_k \end{bmatrix}$$

$$+ \frac{2\pi\bar{r}k_{zz}}{4A} \begin{bmatrix} c_i c_i & c_i c_j & c_i c_k \\ c_j c_i & c_j c_j & c_j c_k \\ c_k c_i & c_k c_j & c_k c_k \end{bmatrix}$$

$$+ \frac{2\pi h\mathcal{L}_{ij}}{12} \begin{bmatrix} (3R_i + R_j) & (R_i + R_j) & 0 \\ (R_i + R_j) & (R_i + 3R_j) & 0 \\ 0 & 0 & 0 \end{bmatrix} \tag{3.50}$$

where $\bar{r} = \frac{1}{3}(R_i + R_j + R_k)$

$$[c^{(e)}] = \frac{2\pi A c_p \rho}{60} \begin{bmatrix} 2(3\bar{r} + 2R_i) & (3\bar{r} + R_i + R_j) & (3\bar{r} + R_i + R_k) \\ (3\bar{r} + R_i + R_j) & 2(3\bar{r} + 2R_j) & (3\bar{r} + R_j + R_k) \\ (3\bar{r} + R_k + R_i) & (3\bar{r} + R_k + R_j) & 2(3\bar{r} + 2R_k) \end{bmatrix} \tag{3.51}$$

$$\{f^{(e)}\} = \frac{2\pi h \mathcal{L}_{ij} T_\infty}{6} \begin{bmatrix} 2 & 1 & 0 \\ 1 & 2 & 0 \\ 0 & 0 & 0 \end{bmatrix} \begin{Bmatrix} R_i \\ R_j \\ R_k \end{Bmatrix} \tag{3.52}$$

For a horizontal triangle as seen in Figure 3.2.b

$$\mathcal{L}_{ij} = R_j - R_i \tag{3.53}$$

3.4. Computer Implementation and Finite Element Grid

Computer programs were developed from the finite element models to solve the phase-change in food freezing for both two-dimensional elliptical heat transfer and axisymmetrical trapezoidal heat transfer as described previously. The programs were modified from the computer simulation written by Krutz and Segerlind (1978) to predict the temperature distribution in welded joints. The modification took into account the non-linear function of physical properties versus temperature as developed by Heldman and Gorby (1974). Furthermore, the program incorporated boundary variations surrounding the surface of the food product. Convective heat transfer coefficients were defined as a function of location for elliptical products (Appendix C), while local temperature was varied along the surface for trapezoidal bodies (Appendix D). A change from two-dimensional simplex triangular element coordinates to axisymmetric triangular element coordinates was incorporated for the axisymmetrical trapezoidal heat transfer problems. The structure of the whole program is illustrated in Figure 3.3. The function of subroutines are described below.

SETFL : Setting the dimension of a column vector A containing $\{T_t\}$, $\{T_{t+\Delta t}\}$, $\{F\}$, $[K]$ and $[C]$.

SETMAT : Computing the matrices $\{F\}$, $[K]$, and $[C]$ at each time step.

READ 1 : Reading and calculating the initial physical properties of food product.

PROP 1 : Computing the physical properties of food product at each time step.

TVAR : Performing the calculation of the local temperature along the surface on the trapezoidal geometry.

HVAR : Performing the calculation of the convective heat transfer coefficient at each location along the surface on the elliptical geometry.

DCMPBD : Decomposing the term $([K] + \frac{2}{\Delta T} [C])$ from equation (3.47) into an upper triangle matrix using Gaussian elimination

TRANSIENT : Computing $T_{t+\Delta t}$ and writing the output.

MULTBD : Multiplying the matrix $(\frac{2}{\Delta T} [C] - [K])$ by $\{T_t\}$ in equation (3.47)

SLVBD : Solving $T_{t+\Delta t}$ in the above equation by backward substitution.

The flow diagrams of subroutines READ 1, SETMAT, PROP 1, TVAR, HVAR, and TRANSIENT are outlined in Figures 3.4 - 3.6. Subroutines DCMPBD, MULTBD, and SLVBD were given in Segerlind (1976) and are available in computer packages from the CDC 6500 at Michigan State University. Both computer programs are fully printed in Appendix A.

A GRID program was used to generate the input data of element node numbers and their respective coordinates. The program, as developed by Segerlind (1976), performs the plot of the finite element grid designed for specific geometry of food products and cards punched with triangular elements data related to the grid. Figures 3.7 and 3.8 illustrate the finite element grid for elliptical and trapezoidal geometry.

The input parameters and variables for computer program can be divided into four categories: product thermal properties; physical properties of water, ice, and gas; freezing medium properties; and finite element parameters resulted from the grid program. All required input parameters and variables are listed in Table B.3. The mean surface heat transfer coefficients (h) for various air velocities were obtained from an experiment conducted by Chavarria (1978) for freezing of ground beef in the wind tunnel. Their values were 61.7, 70.6, and 142.5 W/m^2 K for air velocities of 7.4, 11.3, and 15.2 m/s, respectively.

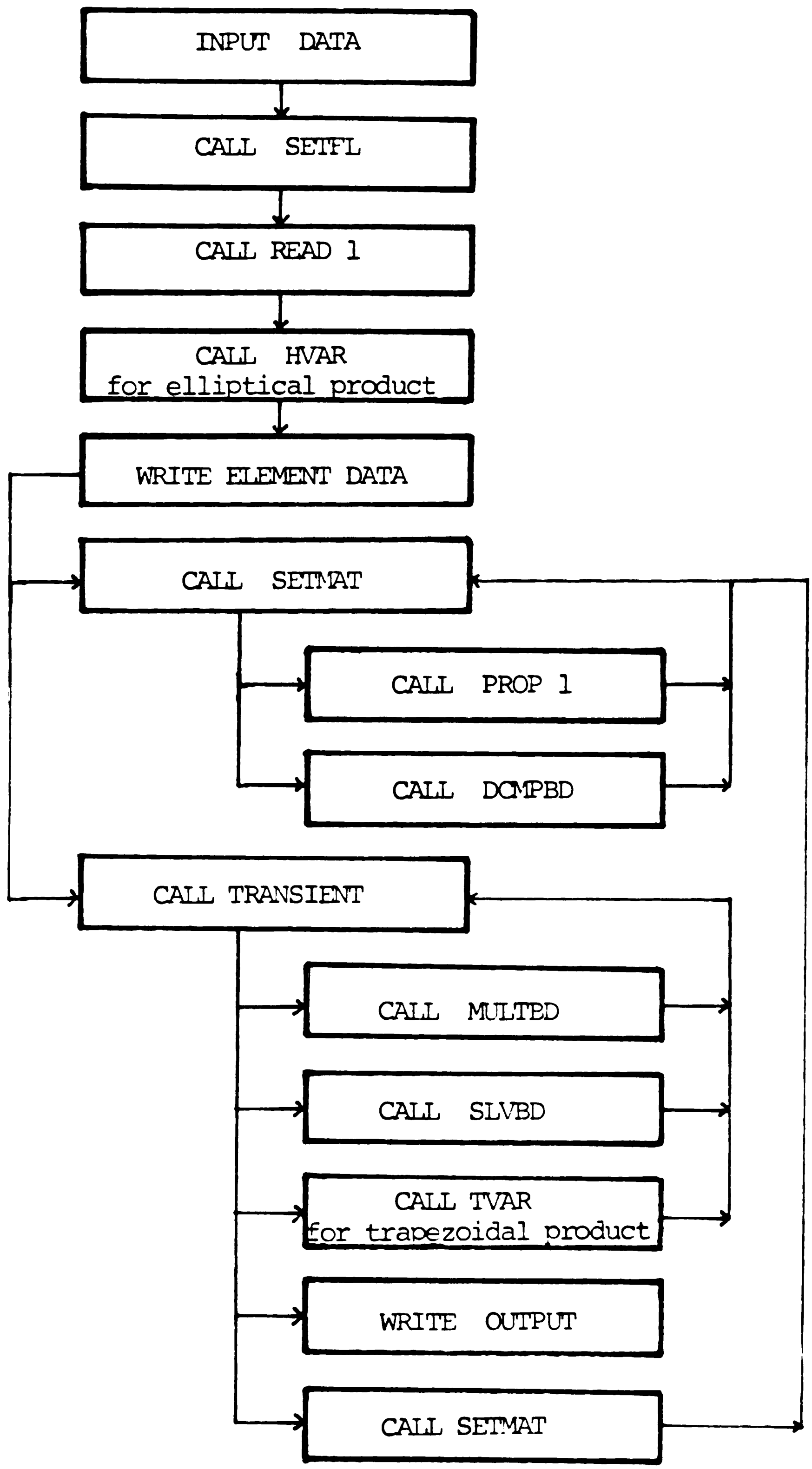

Figure 3.3. Flow diagram of Main Program.

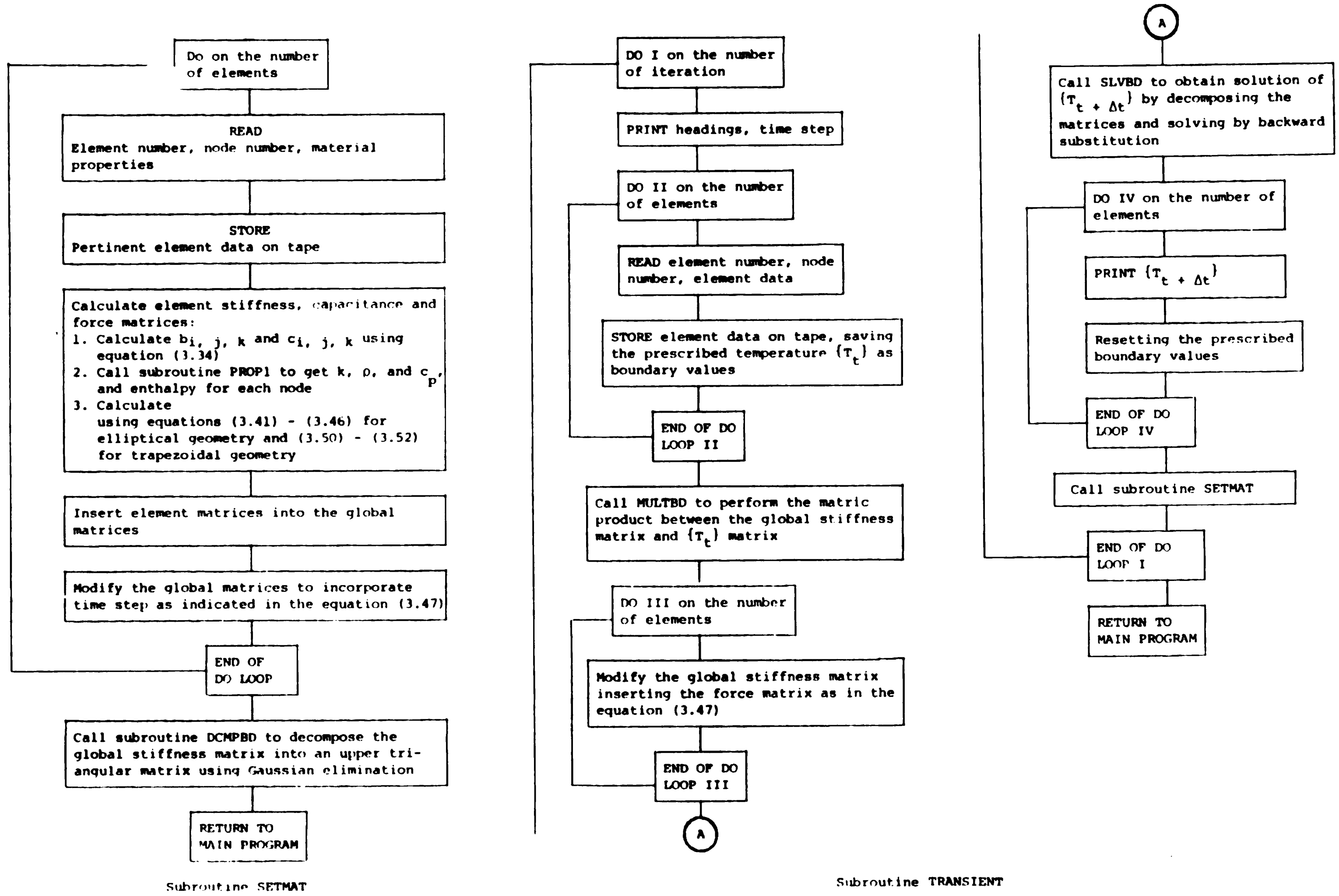

Figure 3.4. Flow diagram of subroutines SETMAT and TRANSIENT.

READ
Input initial values R, LW, DW, DI, TO, KI, CPW, IWC, TF, UFWC, ICP, IK, MW

CALL SUBROUTINE PARAM 1
Calculate the initial parameters necessary DS, KS, MS, CPS

DS is solved from equation (3.11)

KS is solved from equations (3.8) and (3.9) using water-solid system

$KS = [KW\ (VFS^{2/3} - Q)]/VFS^{2/3}$

$Q = (KW - IK)/(VFS^{1/3} \cdot IK + KW - IK)$

$VFS = EMS \cdot PD/DS$

MS is obtained by solving XW in equation (3.1) and utilizing equations (3.2) and (3.3)

CPS is calculated using equation (3.13)

$CPS = (ICP - IWC \cdot CPW)/EMS$

RETURN TO
MAIN PROGRAM

Subroutine READ 1

Calculate WC and MI
1. Solve XW from equation (3.5)
2. Solve EMW from equation (3.6)
3. Solve WC from equation (3.7)
4. Solve MI from equation (3.15)

Solve PD utilizing equation (3.10)
$PD = 1/(WC/DW + MI/DI + EMS/DS)$

Calculate VFD for ice-water system

$VFS = VFI/(VFI + VFW)$

where $VFI = MI \cdot PD/DI$,

$VFS = EMS \cdot PD/DS$

$VFW = 1 - (VFI + VFS)$

Calculate KD for ice-water system applying equations (3.8) and (3.9)

$KD = KW\ [(1 - Q)/(1 - Q(1 - VFD^{1/3}))]$

where $Q = VFD^{2/3}(1 - KI/KW)$

Calculate K for food product using equations (3.8) and (3.9)

$K = KD\ [(1-Q)/(1-Q(1-VFS^{1/3}))]$

where $Q = VFS^{2/3}(1-KS/KD)$

Solve CPI and H using equations (3.14) and (3.12)
Solve CPA using equation (3.16)

RETURN TO SUBROUTINE
SETMAT

Subroutine PROP 1

Figure 3.5. Flow diagram of subroutines READ 1 and PROP 1.

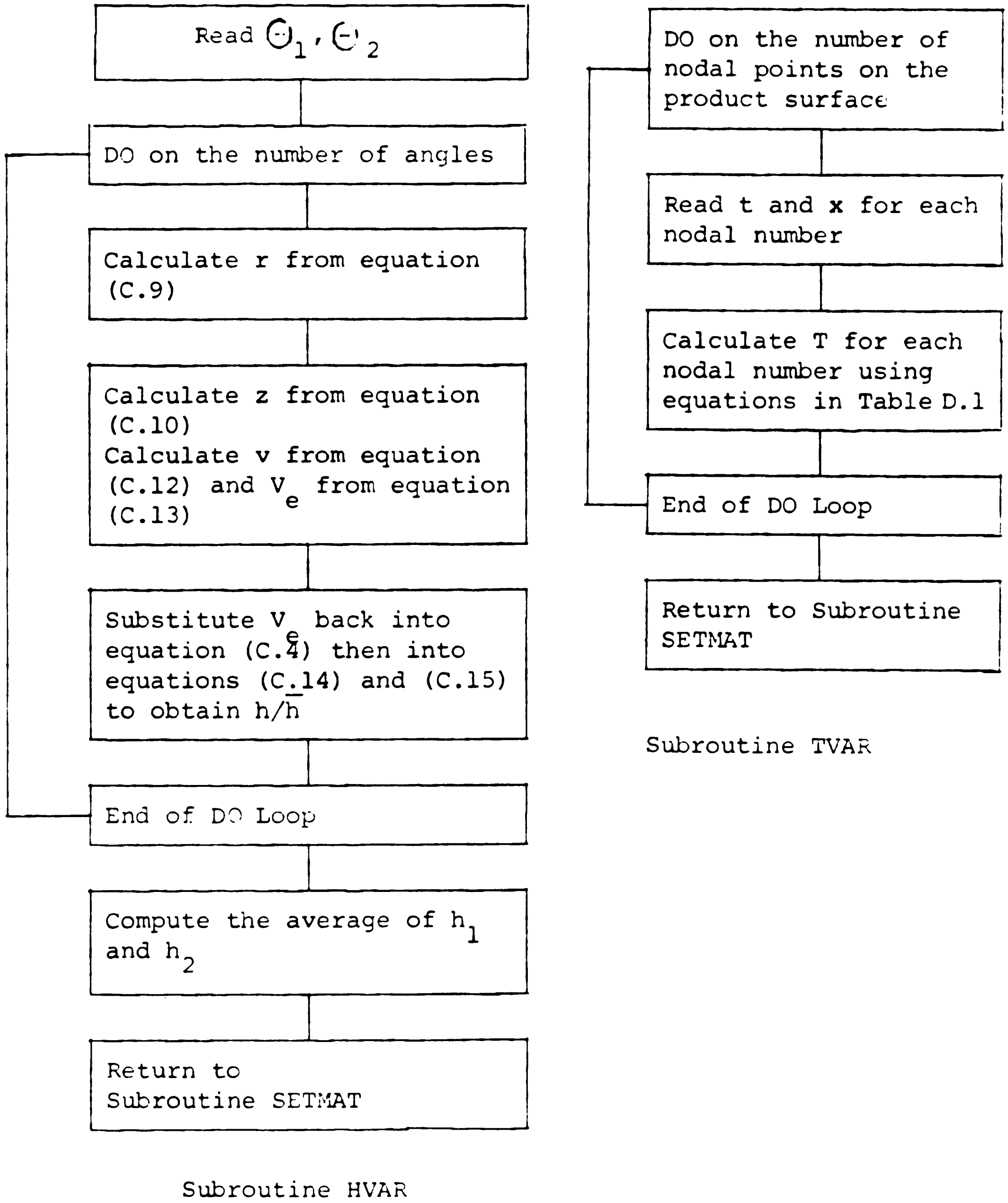

Figure 3.6. Flow diagram of subroutines HVAR and TVAR.

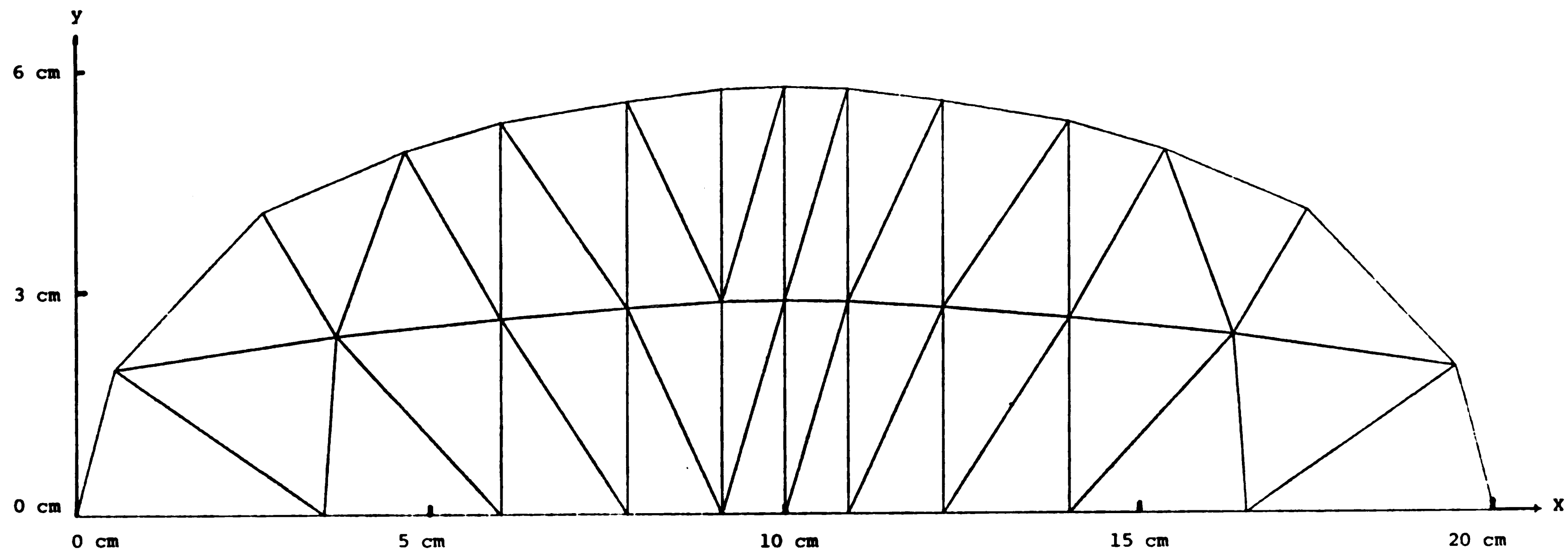

Figure 3.7. The two-dimensional elliptical finite element grid with simplex triangular elements.

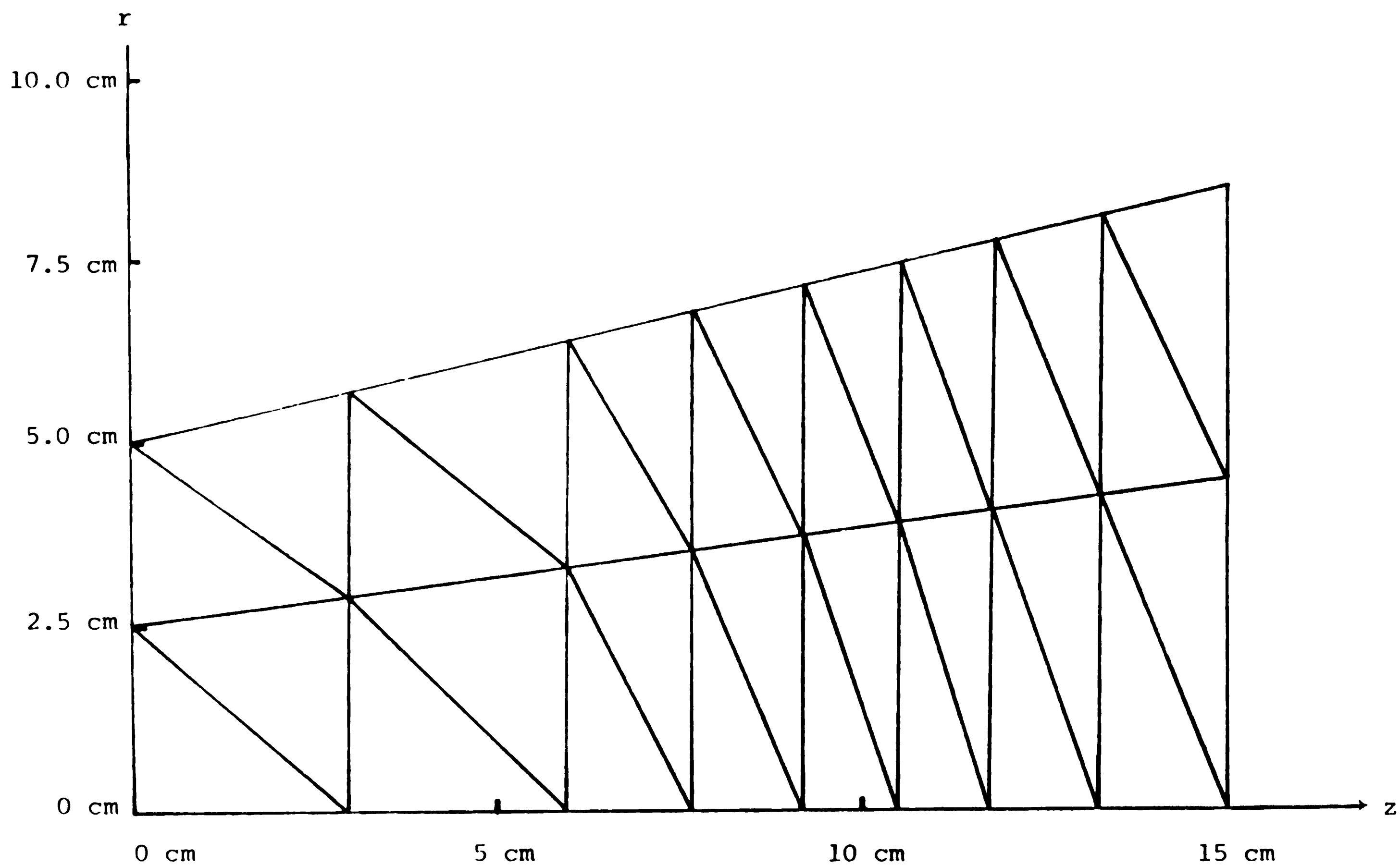

Figure 3.8. The axisymmetrical trapezoidal finite element grid with simplex triangular elements.

4. EXPERIMENTAL

4.1. Equipment

An air-blast wind tunnel located in a low-temperature room was used to freeze the food product as illustrated in Figure 4.1. The length of the wind tunnel was 3.8 m with circular cross section of 46 cm I.D. The fan drew air into the tunnel using a three-phase electric motor of 3.73 KW; 440/220 Volt. The air speed was controlled by a circular opening with baffles which were regulated by a lever and positioned in front of the fan. The internal size of the freezing room was 6.7 m x 1.8 m x 2.4 m. Two evaporators provided the refrigeration effect to reduce the temperature in the room to as low as -34.4°C with a deviation of ±1.8°C when the fan was not operating.

The food product, supported by a styrofoam plate was placed at the center of the wind tunnel. The styrofoam support plate had dimensions of 46 cm x 35 cm x 5 cm, and functioned as an insulator to avoid heat losses through the bottom and edge of the food products (Figure 4.2). The boundary conditions in equations (3.17) and (3.21) were satisfied by the design of the plate. A sharp leading edge was designed on the side of the

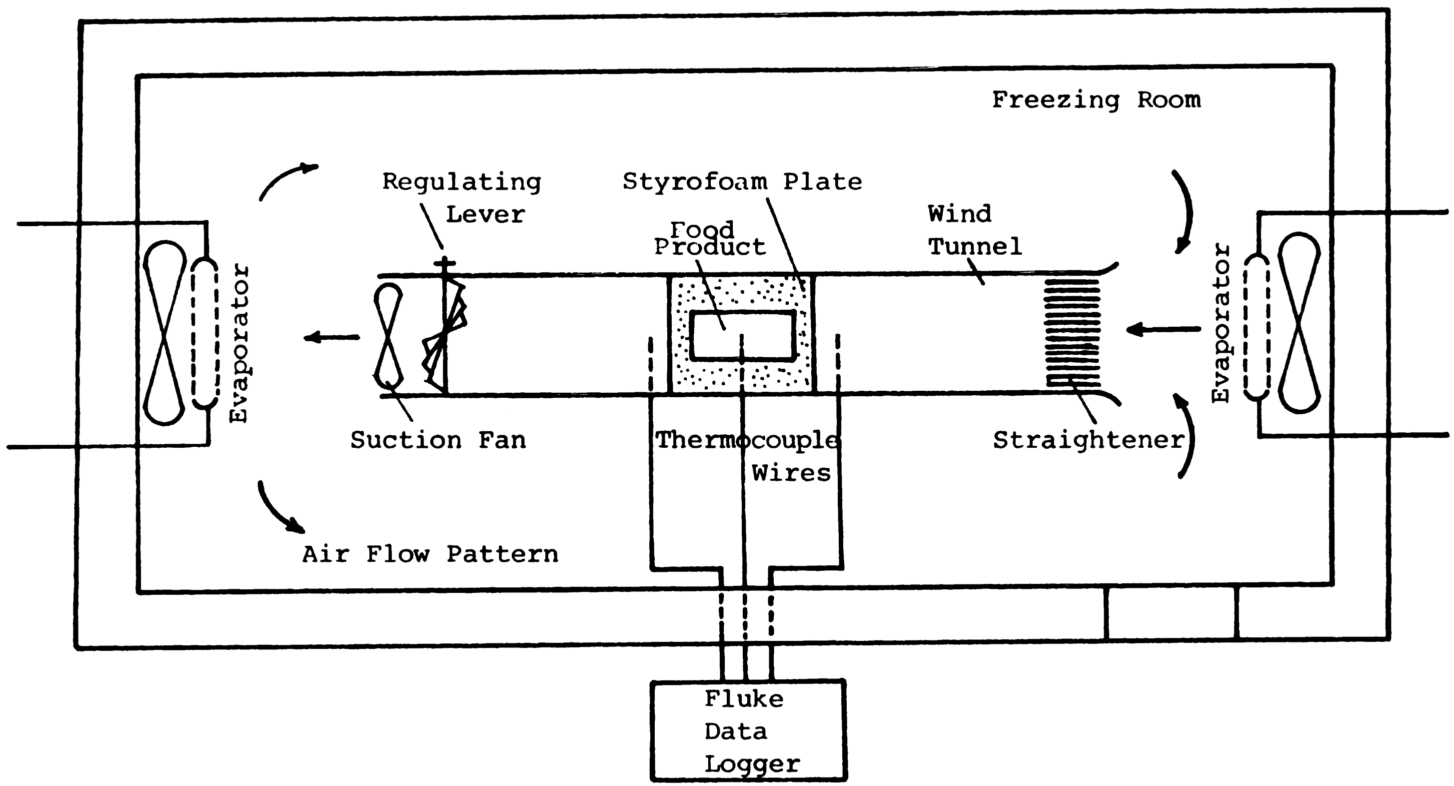

Figure 4.1. Schematic diagram of the experimental setups for freezing process (top view).

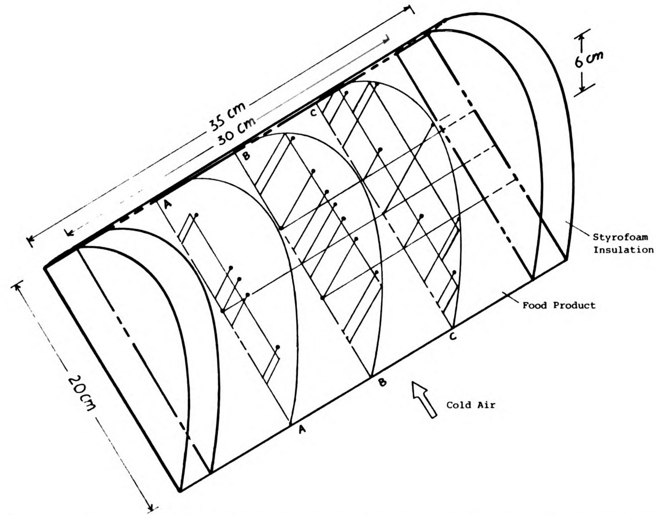

Figure 4.2. Elliptical geometric product with thermocouple junctions and wire structure.

styrofoam support plate facing the air flow to reduce turbulence created by air flow over the support plate and product.

Unsheathed fine copper-constantan thermocouple wires (beaded by Omega Engineering, Inc.) were utilized to sense the temperature of the product. The thermocouple had precision of ± 0.417°C in the temperature range from -59.444°C to 93.333°C, and the diameter of each wire was 0.0125 cm. The wires were sheathed by teflon tubes with 0.055 cm I.D. to avoid direct contact with product. Copper-constantan thermocouple extension wires (gauge 20; 0.08 cm diameter) with polyvinyl insulation were used to connect the sensing thermocouple wire to the temperature recording instrumentation. The precision of the extension wires was the same as the sensing wires. The connectors were heavy-duty copper constantan miniature thermocouple connectors designed with fine gauge thermocouple wires.

Two different types of product shape were investigated in this study, a two-dimensional elliptical geometry (Figure 4.2) and an axisymmetric trapezoidal geometry (Figure 4.4). The nodal locations measured by the thermocouple junctions are illustrated in Figure 4.3 for the elliptical shape and Figure 4.5 for the trapezoidal shape. The teflon sheathed thermocouple wires were partially

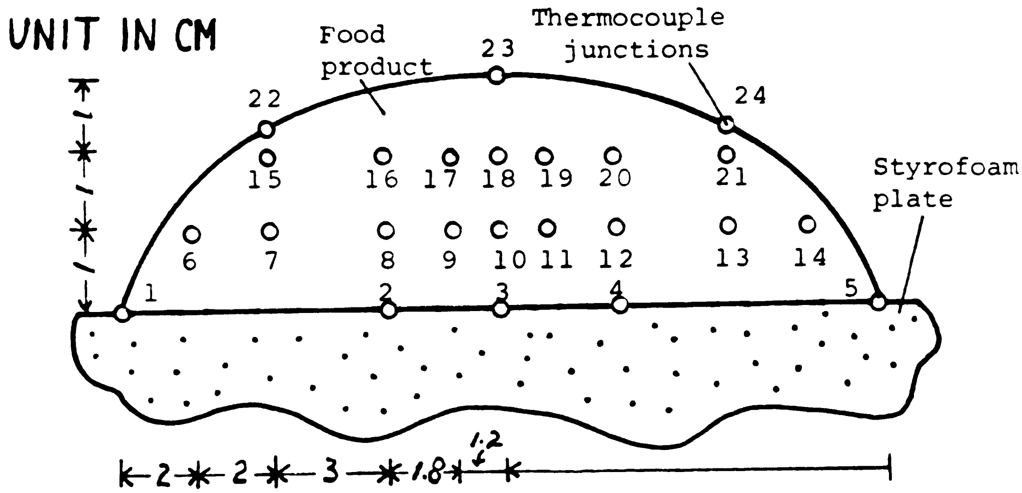

(a) Overall locations

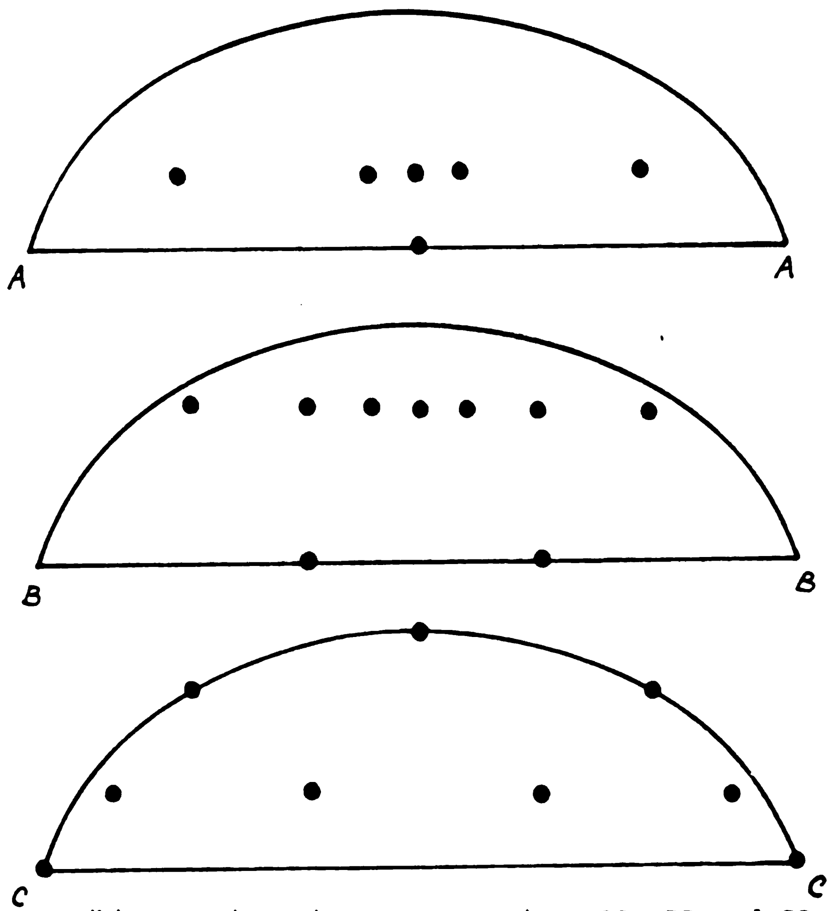

(b) Locations in cross-sections AA, BB and CC (Figure 4.2)

Figure 4.3. Nodal locations of thermocouple junctions on the cross-sectional area in elliptical product.

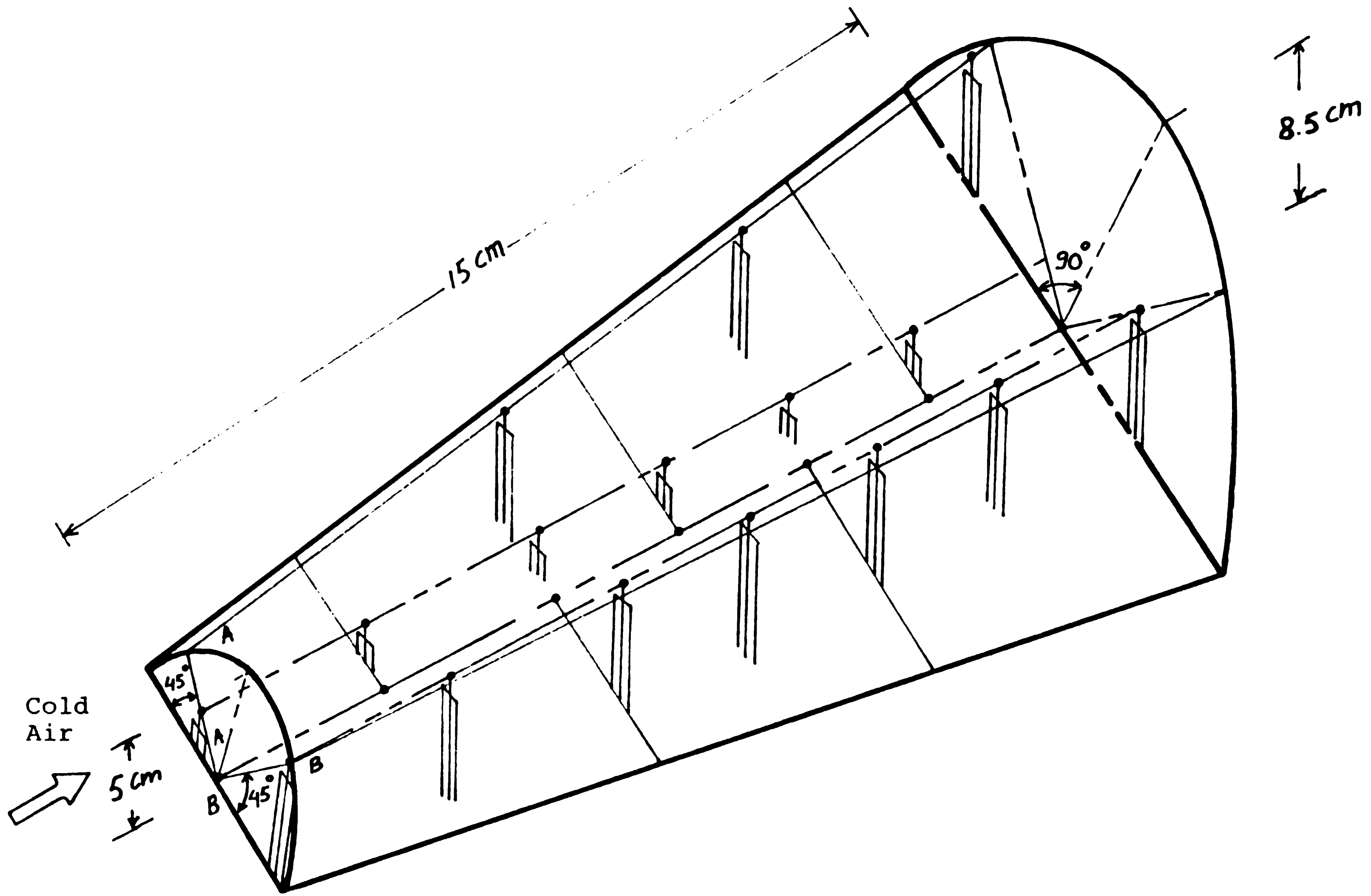

Figure 4.4. Trapezoidal geometric product with thermocouple junctions and wire structure.

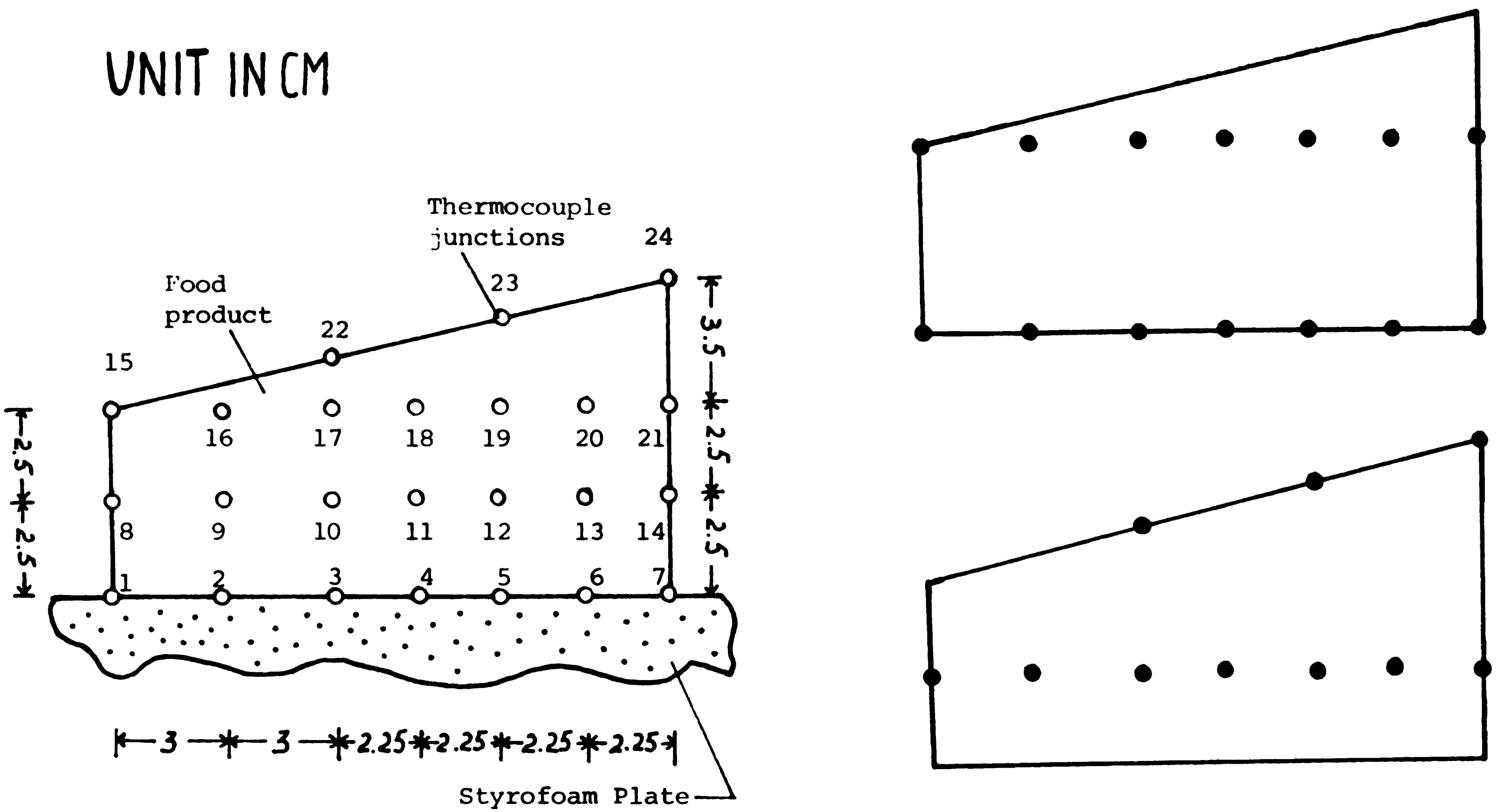

(a) Overall locations

(b) Locations in cross-sections AA and BB (Figure 4.4)

Figure 4.5. Nodal locations of thermocouple junctions on the cross-sectional area in trapezoidal product.

imbedded in the styrofoam plate and partially supported by a 0.05 cm diameter copper wire structure inside the product. Since the teflon sheathed wires and the copper wire structure had different thermal properties from the product, there was concern that the 24 nodal measurements located in one cross-section might influence heat conduction within the product and produce significant error. To eliminate this possibility, the measured locations were installed in three different cross-sections (Figures 4.3 and 4.5) assuming that heat transfer occurred uniformly along the length of the elliptical body and along the circumference of the trapezoidal body. Three other thermocouple junctions were positioned to detect the air temperature at three locations near the product.

The temperature measurements were recorded by the Fluke Model 2240A Data Logger with scanning speed capacity of 2.5 channels per second or about 11 seconds for one cycle containing 27 nodal readings. The output was printed in degrees centigrade for each nodal location and for each time step. The system accuracy was ± 0.5°C in the temperature range of -130°C to 0°C, and ± 0.4°C in the temperature range from 0°C to 400°C when copper-constantan thermocouple wires were employed.

4.2. Material for Food Product

Ground beef was used as the food product in the freezing process experiments for two considerations: (1) it was easily molded and shaped into the desired geometry and (2) it responded to the assumption of product homogeneity since its fibers and tissues had been broken during the grinding process. Ground beef was purchased as commercial lean ground beef from a local grocery store.

Thermal conductivity values and initial freezing point of ground beef were obtained from literature references. Density of ground beef was determined by weighing the product before and after freezing. By calculating the volume of the product shapes and dividing the weight by the volume, the density of unfrozen and frozen meat was established (Table B.1). Specific heat of ground beef was calculated using Dickerson's formula (1965) and the moisture content of meat (MC)

$$c_p = 4.185\ (0.4 + 0.006\ MC) \tag{4.1}$$

where c_p is in J/g K and MC is in percent. Charm (1971) suggested more elaborate equations to compute the specific heat of a food product

$$c_p = 4.184\ (0.5\ X_f + 0.3\ X_s + 1.0\ X_m) \tag{4.2}$$

and $$c_p = 4.184\ (0.34\ X_c + 0.37\ X_p + 0.4\ X_f + 0.2\ X_a + 1.0\ X_m) \qquad (4.3)$$

where X was the weight fraction and subscripts a, c, p, f, s, and m indicated ash, carbohydrate, protein, fat, solid and moisture content of food, respectively. However, the comparison of the results from equations (4.1), (4.2), and (4.3) for specific heat of beef product illustrated only ± 2 percent deviation (Heldman, 1975).

In this investigation, equation (4.1) was used after the moisture content of lean ground beef was determined experimentally according to AOAC procedure (AOAC, 1975). Three samples of ground beef, each 2 g, from each freezing treatments, were placed in aluminum dishes and dried for 4 hours in a Precision Scientific Model 625-A oven at 125°C temperature. The dishes were covered with lids to avoid contact with moist air when removed from the oven and cooled inside a desiccator prior to being weighed. The moisture content of samples for each treatment are listed in Table B.1, and other physical properties of ground beef are presented in Table B.2.

4.3. Procedures

The freezing experiments were conducted for three magnitudes of air velocity for both elliptical and trapezoidal shapes. Each experiment was repeated three times. Air velocities at the center of the wind tunnel had been monitored by Chavarria (1978) utilizing a micromanometer and a Pitot tube. The air speeds used in this investigation are presented in Table B.1 along with the air temperatures. The air temperature fluctuated during the freezing process due to the effect of turbulence within the closed circuit air pattern inside the freezing room and motor heat dissipation. The magnitude of fluctuation varied from ± 0.8°C to ± 2.0°C for an air temperature of -20.0°C (Table B.1).

The data from the experiments were needed to verify the results of computer simulation program described in Chapter 3. The operation of each experiment included the following steps:

1. Setting the freezing room temperature at -20°C at least 24 hours before the experiment.
2. Tempering the ground beef to a uniform initial temperature of 18°C to satisfy the initial condition for the governing heat transfer equations.
3. Molding the ground beef into either elliptical or trapezoidal shape on the styrofoam support plate.

4. Programing the Fluke Data Logger and supplying the input parameters, number of channels, and scanning intervals.
5. Placing the styrofoam support plate and the product at the center of the wind tunnel.
6. Connecting the sensing thermocouple wires with the extension thermocouple wires by matching the nodal number with the channel number of the Fluke Data Logger.
7. Starting the electric motor and the fan to initiate the freezing process and, at the same time, starting the Fluke Data Logger to monitor the temperature history.
8. Removing the ground beef model from the wind tunnel and refrigerating room after freezing process.

5. RESULTS AND DISCUSSION

5.1. Comparison of Numerical Simulation Model with Finite Difference Method During Food Freezing

The numerical simulation was compared with experimental data and results from the finite difference analysis used by Lescano (1973) to describe freezing of codfish fillets in a flat plate geometry. Since Lescano's investigation was conducted for one-dimensional heat transfer and the finite element program was for two-dimensional, some modifications were made to accommodate the comparison. A rectangular geometry of codfish fillets with a ratio of length to thickness being 12 was used (Figure 5.1) and insulated boundaries were applied in all sides except the product surface. This resulted in heat conduction along x-direction being negligible compared to the y-direction, which was the product thickness and a one-dimensional heat transfer problem could be assumed in the product.

Using the same product parameters, the predicted temperature history using finite element method was compared to results from Lescano's prediction and experimental data in Figure 5.2. In general, the results indicated that the finite element prediction was in good

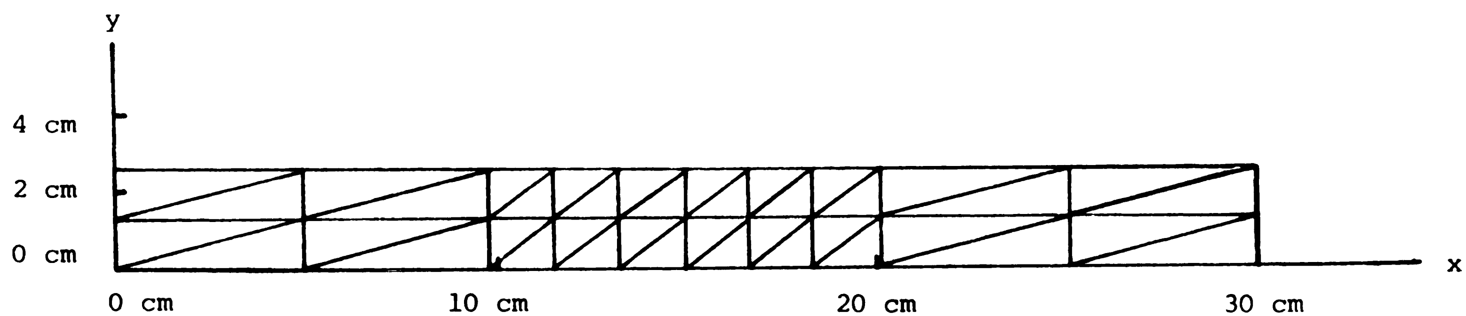

Figure 5.1. The two-dimensional finite element grid for slab geometry with simplex triangular elements.

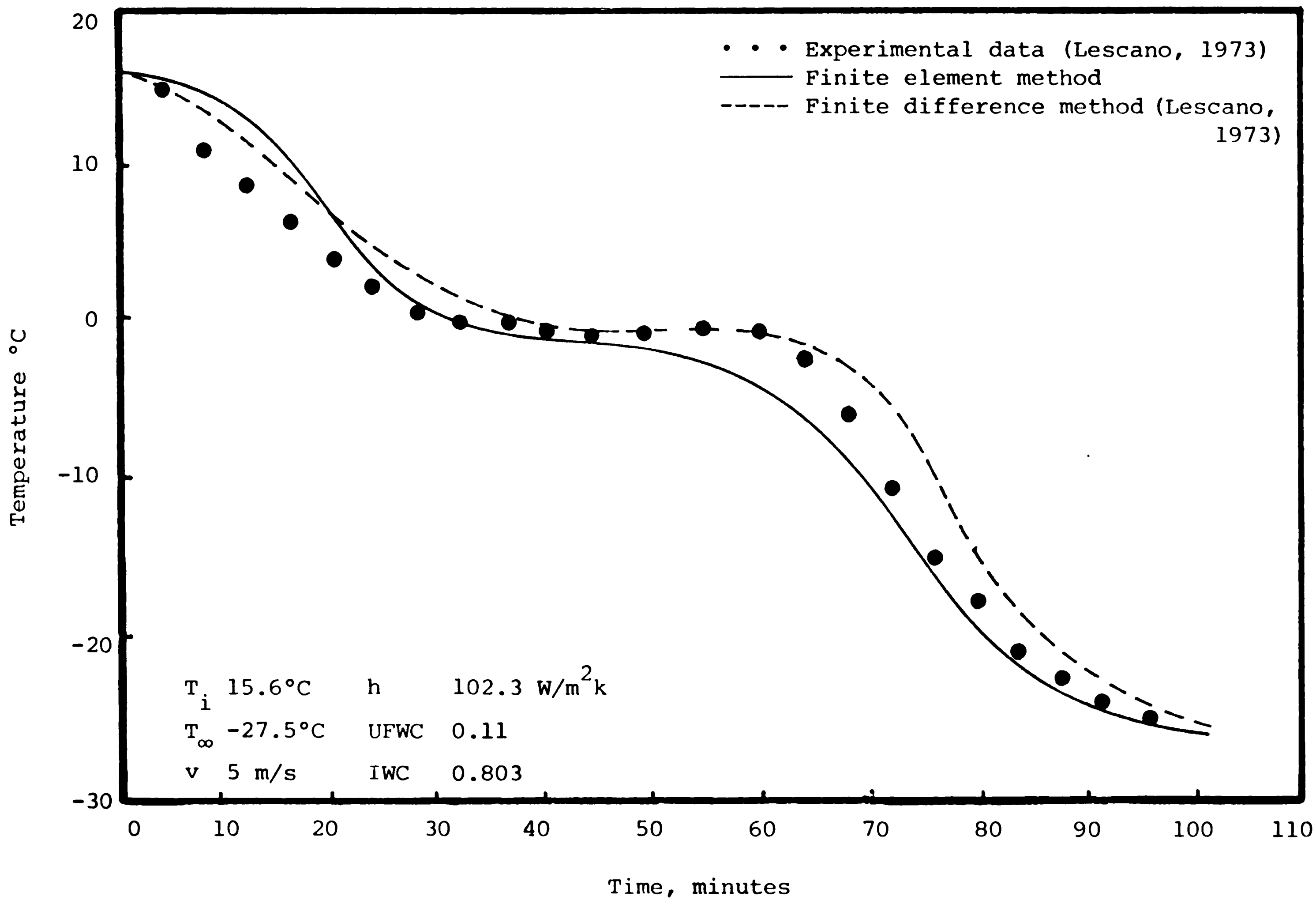

Figure 5.2. Temperature history of codfish fillets during freezing.

agreement with both experimental data and the finite difference method.

The "Student t-test" (Netter and Wasserman, 1974) was used to quantify the differences among the experimental data, the predicted temperature by finite difference and predicted results from the finite element simulation. The results (Table 5.1) indicate that the finite element method provides more favorable agreement with experimental data than the finite difference method. The finite element method will predict the same temperature as experimental data at the confidence level of 95 percent.

TABLE 5.1.--The "Student t-test" for Experimental and Predicted Temperature in Codfish Freezing

Treatment	Calculated t	Degree of Freedom	t-table* (α=0.05)
Experimental vs finite element method	0.48	24	2.064
Experimental vs finite difference method	-5.25+	24	2.064
Finite element vs finite difference method	-2.29+	24	2.064

*t for two-tail test (Neter and Wasserman, 1974).

It has been observed that the finite element method gives more accurate results than finite difference method and converges to an exact solution in heat conduction problem (Emery and Carson, 1971; Bruch and Zyvoloski, 1974). Hence, the results predicted in this study (Figure 5.2 and Table 5.1) are similar to the previous publication.

5.2. Verification of Computer Simulation with Experimental Data

5.2.1. Freezing of Product with Elliptical Geometry

The results of computer simulation using the finite element method to predict temperature history of elliptical geometry product are presented in Figures 5.3-5.5 at various air velocities; 7.4, 11.3, and 15.2 m/s. The predicted temperatures were compared to data obtained experimentally from 3 replications at each air velocity. Experimental data were tabulated in Table B.4. Temperature histories are illustrated at three node locations including the center of the ellips (node 1), 4 cm above the center (node 2) and at the surface adjacent to the product center (node 3). The standard deviations of the temperature measurements at one hour time step were computed and presented with the experimental curves. The results indicate that the standard deviations varied from ± 0.1°C to ± 3.5°C. Higher deviations occurred at the

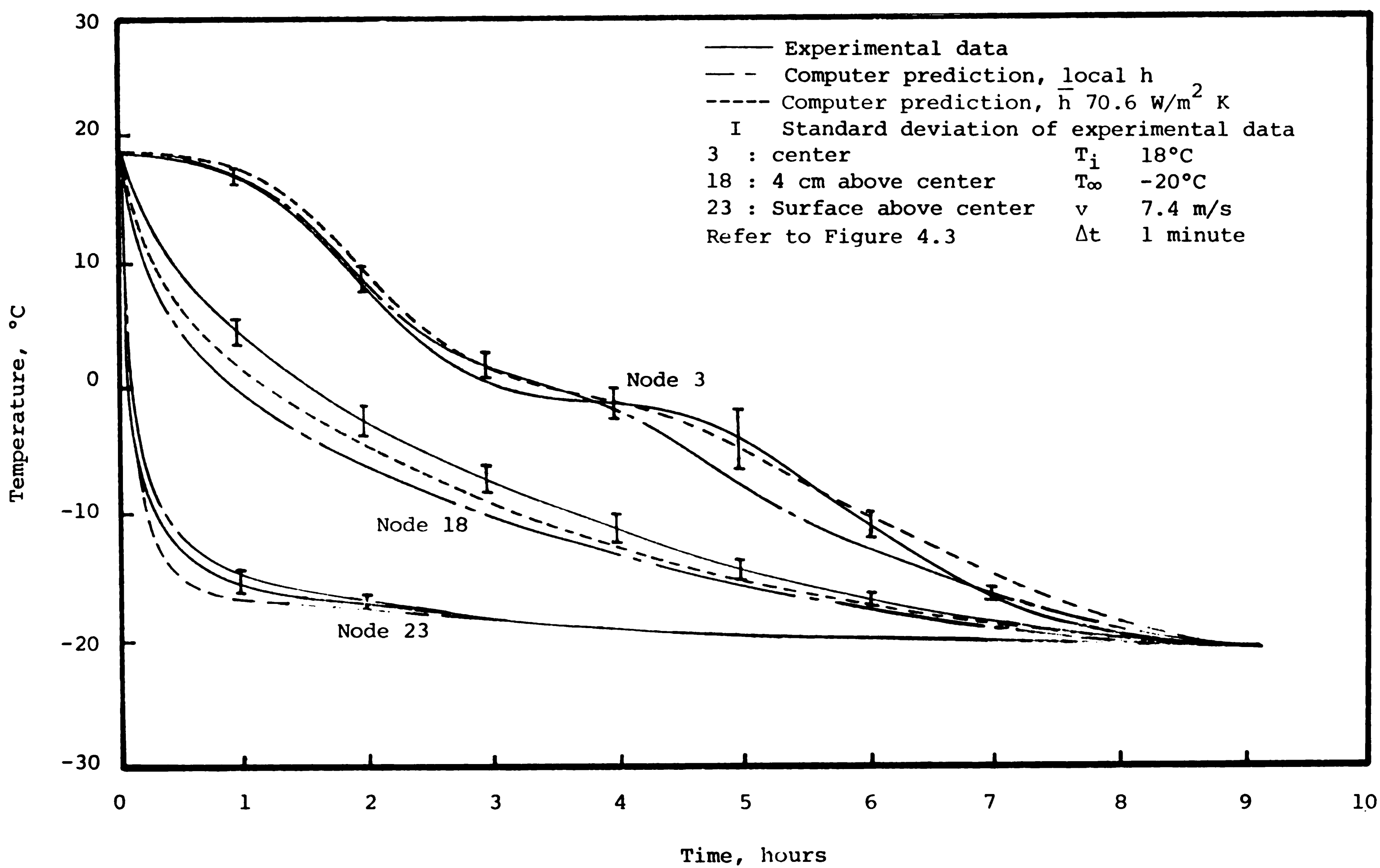

Figure 5.3. The time-temperature history of elliptical product during freezing at air speed 7.4 m/s.

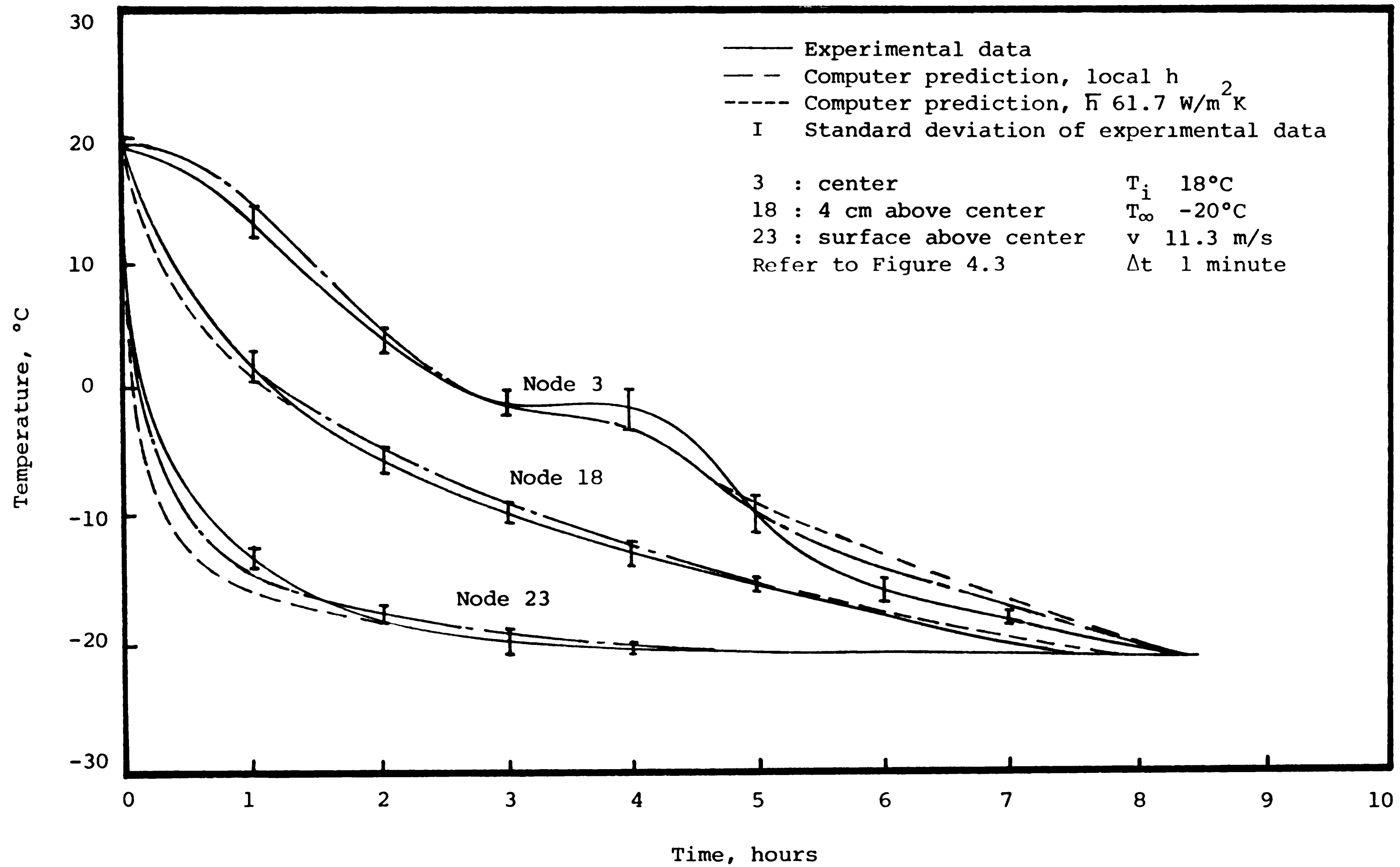

Figure 5.4. The time-temperature history of elliptical product during freezing at air speed 11.3 m/s.

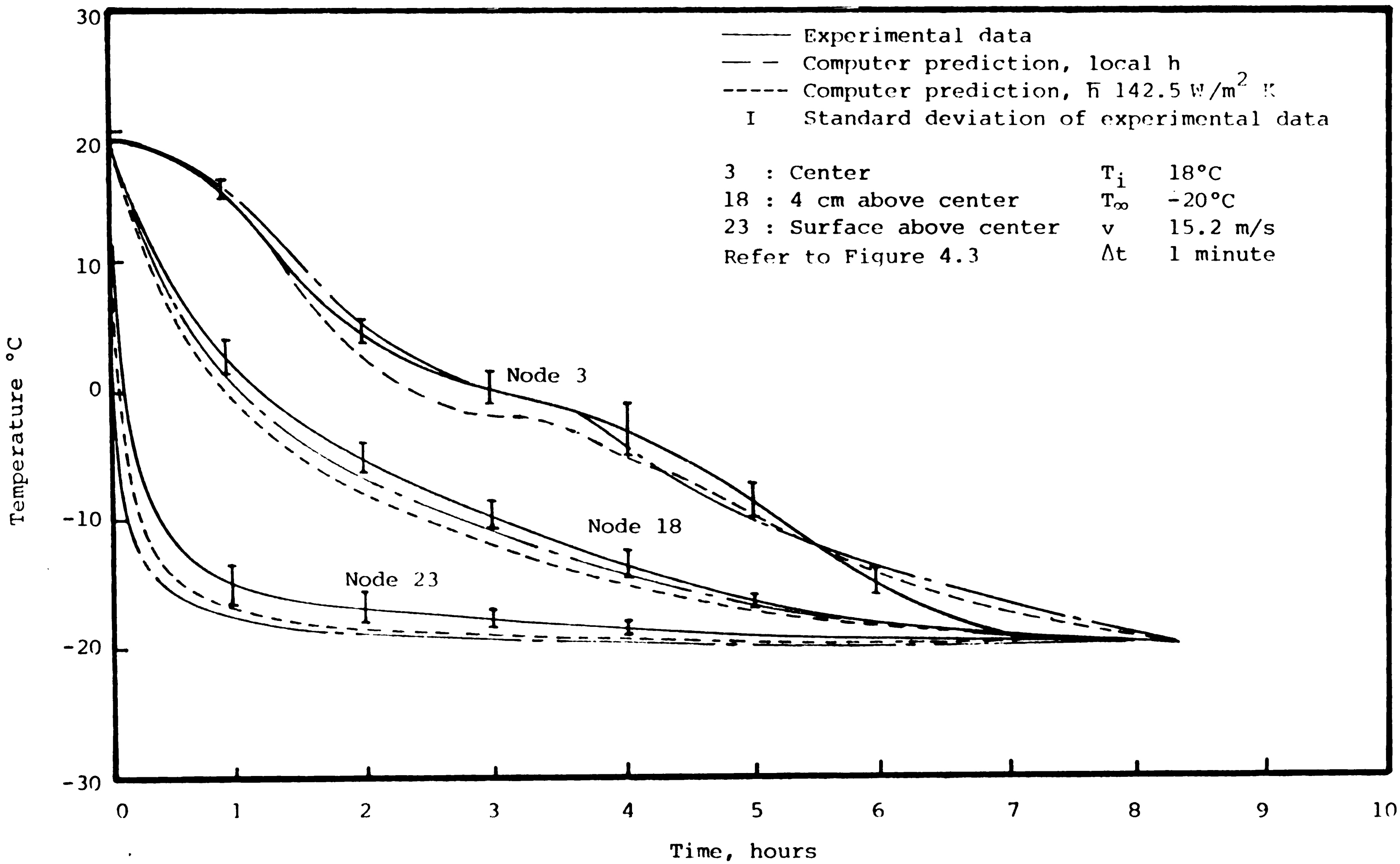

Figure 5.5. The time-temperature history of elliptical product during freezing at air speed 15.2 m/s.

initial freezing point of food product and decreased when the flat plateau of the freezing curve ended and the slope began to increase.

In general, the computer prediction was in close agreement with experimental data. By introducing variable local surface heat transfer coefficients, a better simulation was obtained than when the surface heat transfer coefficient was constant along the surface of the product with elliptical shape. The discrepancy between the simulated and experimental curves can be attributed to fluctuating air temperature (± 2.0°C), as indicated in Table B.l., and inconsistency of product density which might have occurred during the shaping of product into the elliptical geometry. Measured surface temperatures (node 3) were higher than predicted values due to placement of thermocouple junctions on the product surface. It is anticipated that the temperature sensors will give higher temperature reading if their locations are not exactly on the product surface but several millimeters under.

A statistical test was conducted using the t-distribution to evaluate the agreement between experimental and predicted temperature history at the center of the elliptical shape. The results in Table 5.2 indicate a good agreement between the experimental data and computer simulation. The finite element simulation predicts the

TABLE 5.2.--The Results of "Student t-test" to Evaluate Agreement Between Experimental and Predicted Temperature at the Slowest Freezing Point Location

General Shape	Air Speed m/s	Calculated t	Degree of Freedom	t Table* (α=0.05)
Elliptical	7.4	-1.63	16	2.12
	11.3	0.89	15	2.13
	15.2	0.95	15	2.13
Trapezoidal	7.4	-3.59+	10	2.23
	11.3	-4.49+	10	2.23
	15.2	-1.44	10	2.23

*t for two-tail test (Neter and Wasserman, 1977).

same temperature as the experimental data at the confidence level of 95 percent.

The isothermal fields at 2.5 hours after the freezing process started are illustrated in Figures 5.6 to 5.8. The shape of the isothermal fields from the experiment are closer to the slowest freezing point for the portion of the product facing the cold air stream, indicating a higher convective heat transfer on the surface of the upstream portion compared to the surface of the downstream portion of the elliptical product. Comparison of experimental data and the computer predicted isothermal fields using average surface heat transfer

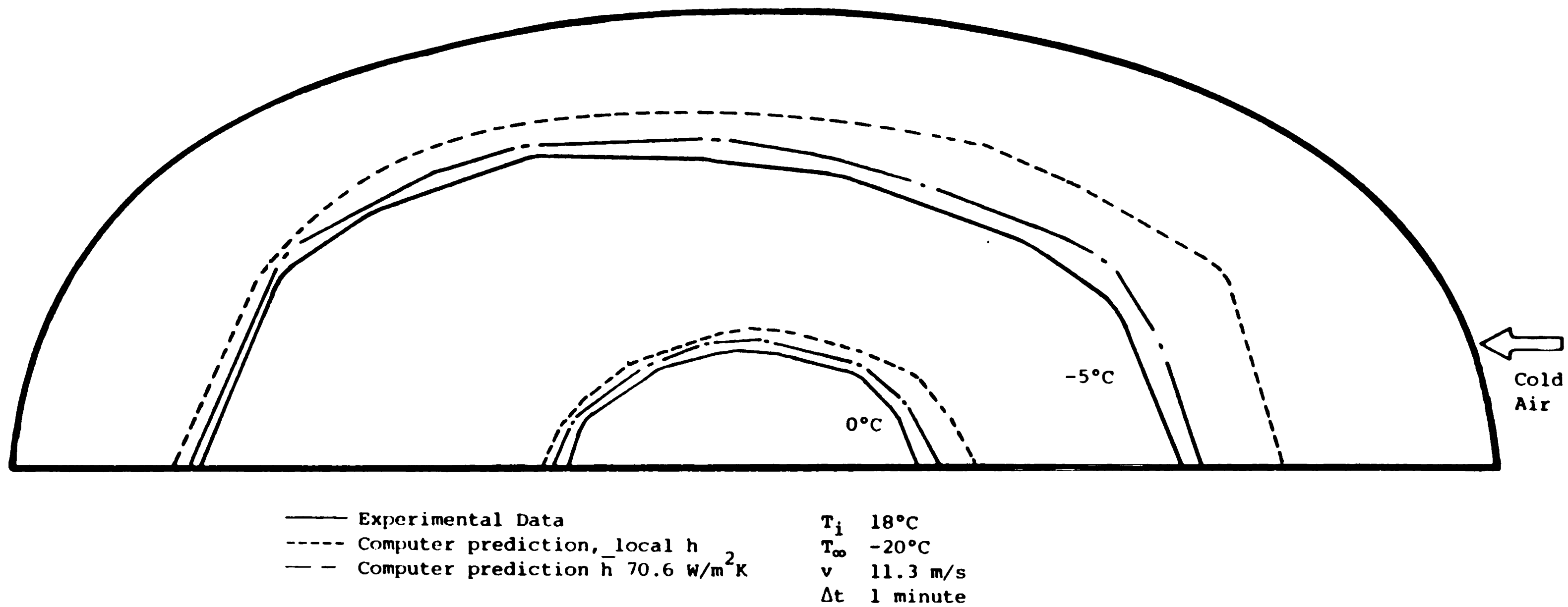

Figure 5.6. The isothermal fields inside elliptical geometry product after 2.5 freezing hours at air speed 11.3 m/s.

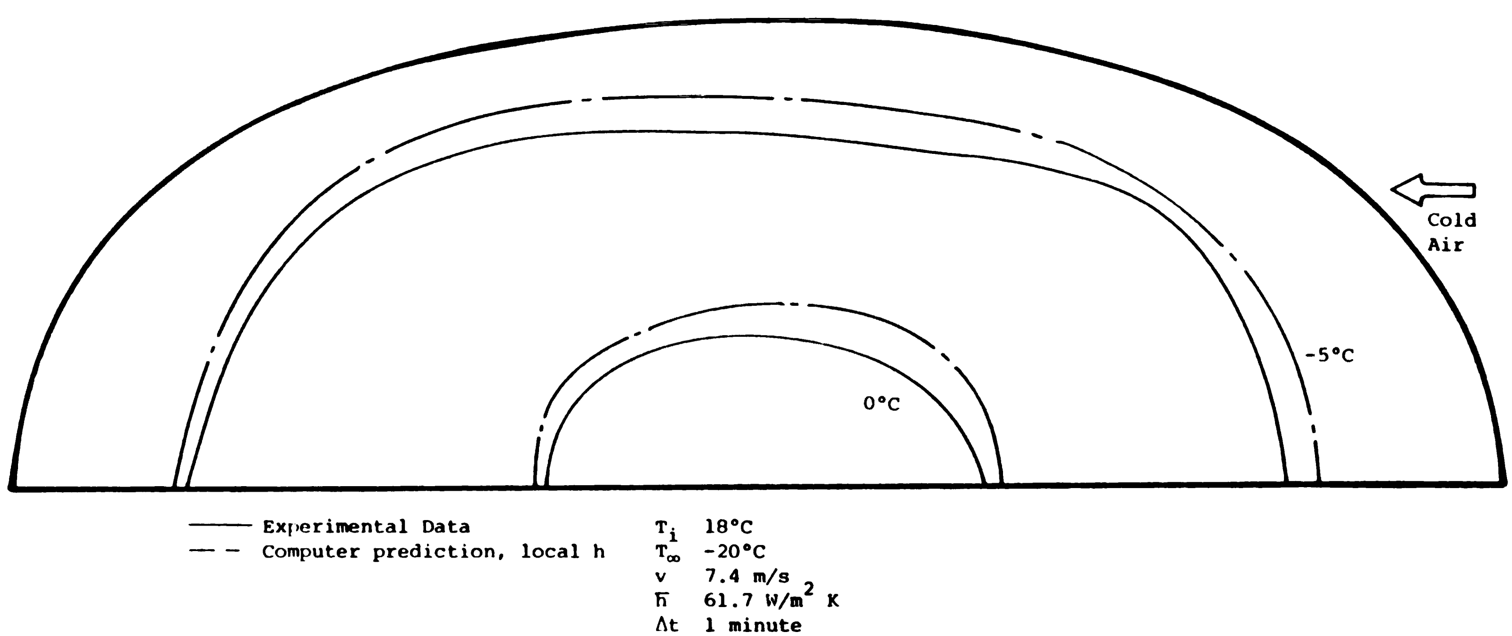

Figure 5.7. The isothermal fields inside elliptical geometry product after 2.5 freezing hours at air speed 7.4 m/s.

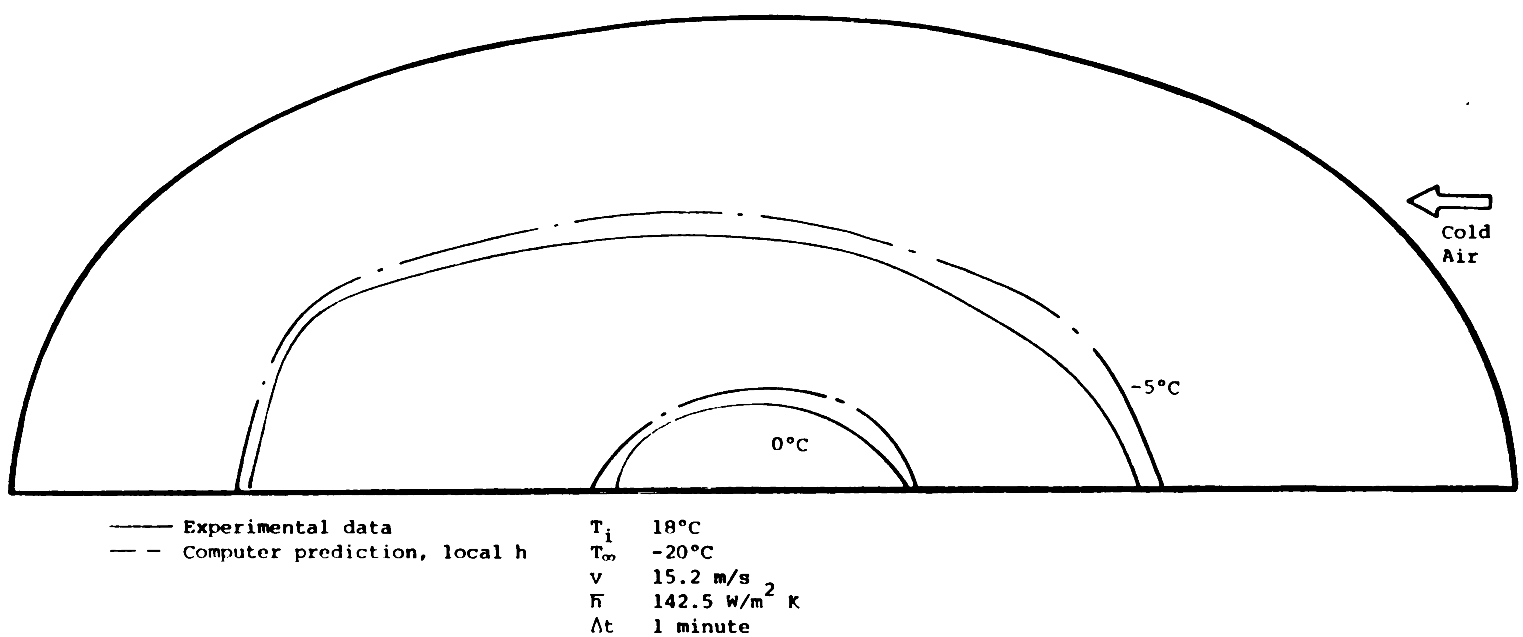

Figure 5.8.--The isothermal fields inside elliptical geometry product after 2.5 hours freezing at air speed 15.2 m/s.

coefficient and local surface heat transfer coefficient revealed that local heat transfer coefficient was in favor over average heat transfer coefficient. This was supported by the result of mathematical analysis using Katinas' data (Katinas et al., 1976) as described in Appendix C.

5.2.2. Freezing of Product with Trapezoidal Geometry

The temperature history, during the freezing process of trapezoidal geometry product measured in the laboratory was compared to the computer prediction in Figures 5.9 to 5.11. The results of the numerical model was in close agreement with experimental; the standard deviation varied from ± 0.1°C to ± 3.1°C. More favorable results were observed from utilizing local surface temperature (Appendix D) than uniform surface temperature. This implies that the heat transfer coefficient varies as a function of location on the product surface.

The isothermal fields presented in Figures 5.12 to 5.14 indicate that the heat transfer depends on the local surface temperature. The numerical model incorporating the surface temperature as a function of location and time gave more exact results to experimental data compared to the model using uniform surface temperature.

The t-tests for trapezoidal (Table 5.2) indicate that the predicted temperature at the slowest freezing

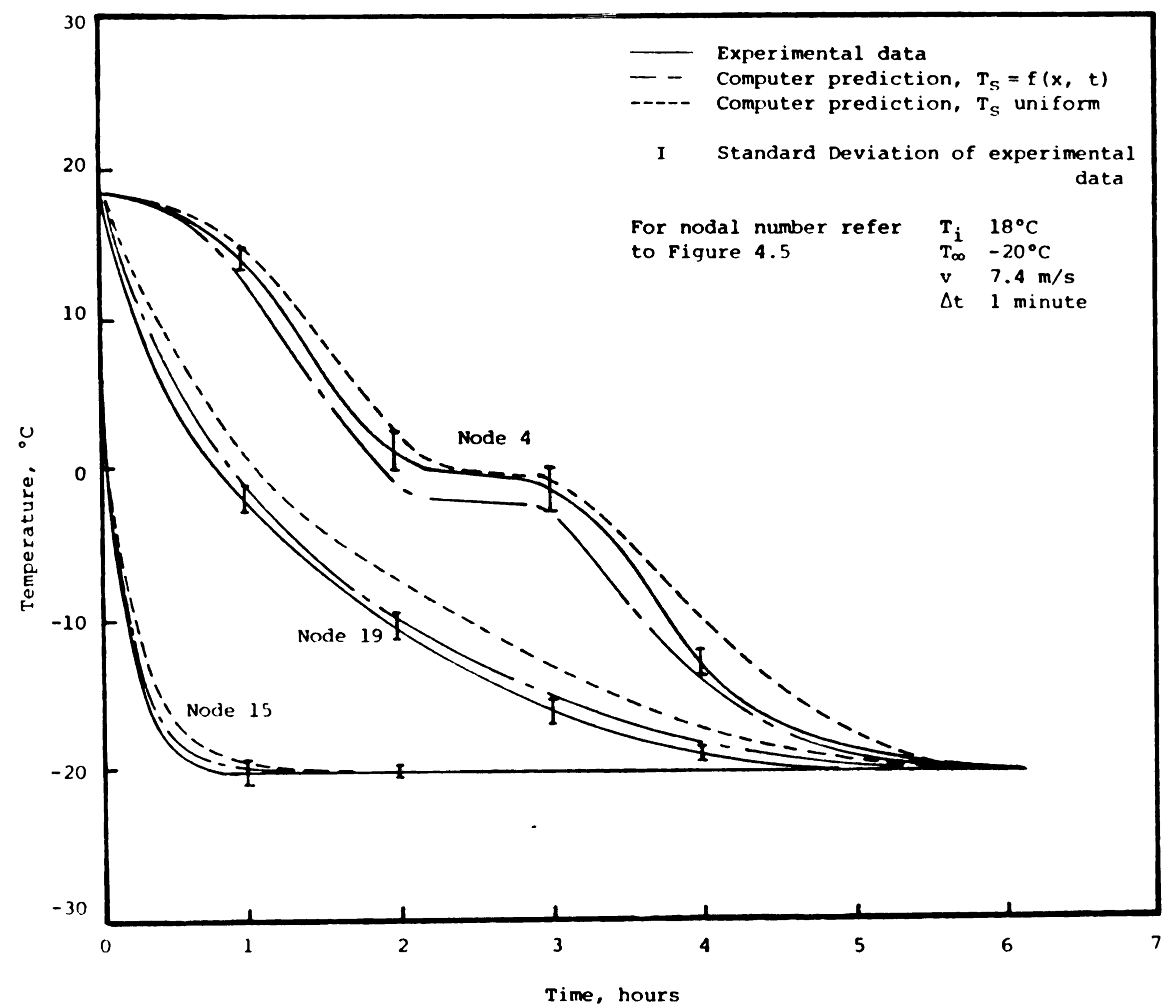

Figure 5.9. The time-temperature history of trapezoidal product during freezing at air speed 7.4 m/s.

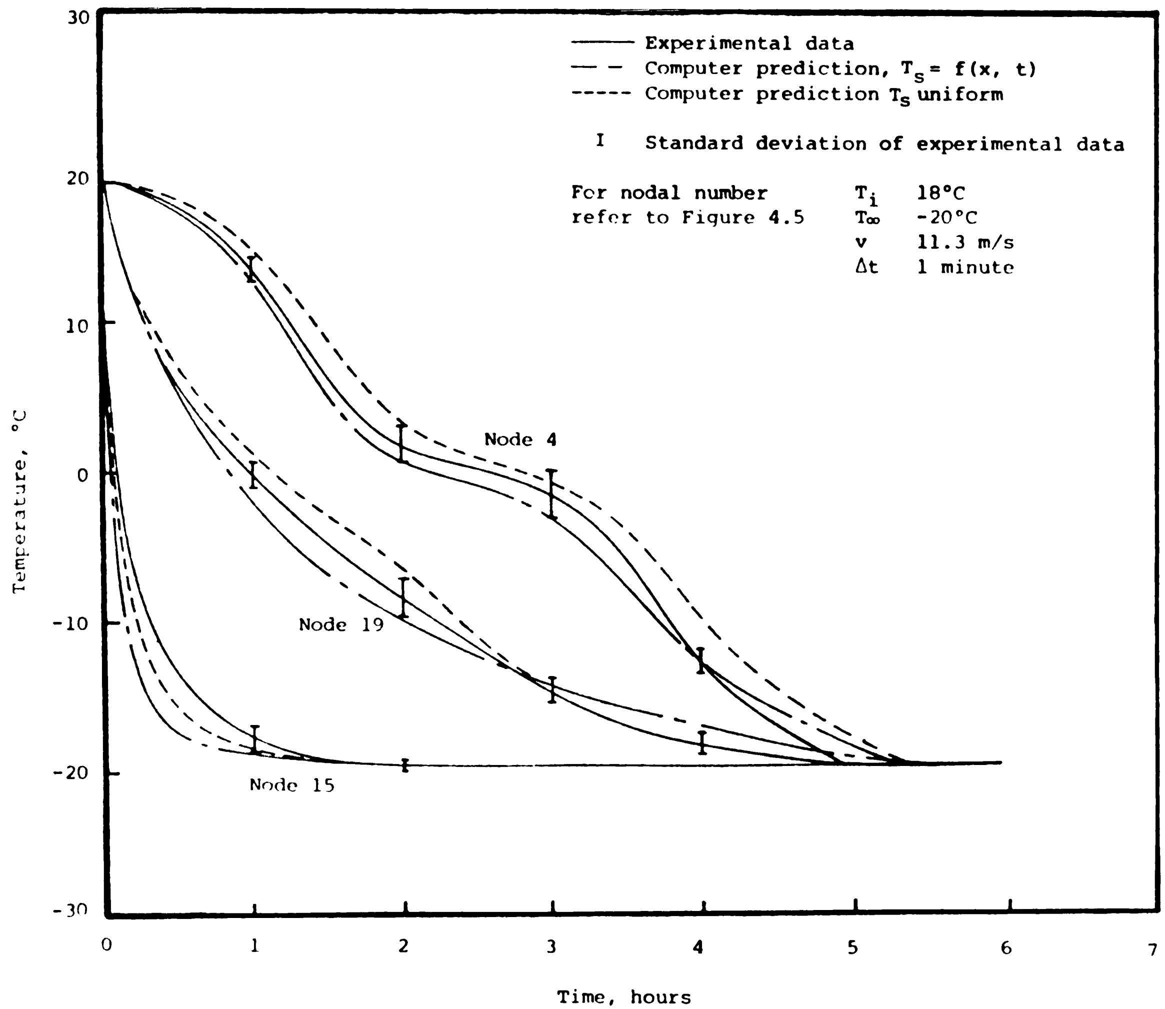

Figure 5.10. The time-temperature history of trapezoidal product during freezing at air speed 11.3 m/s.

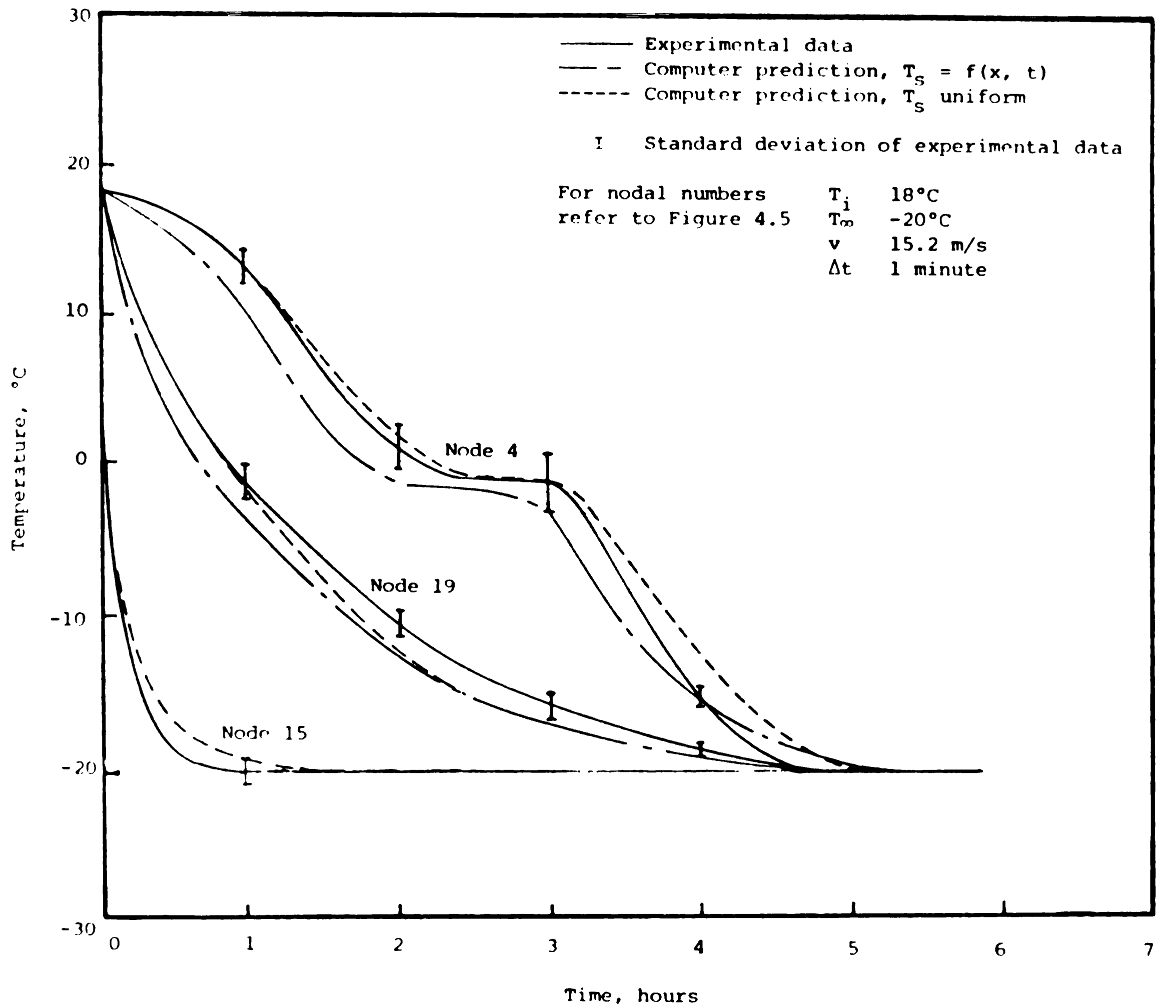

Figure 5.11. The time-temperature history of trapezoidal product during freezing at air speed 15.2 m/s.

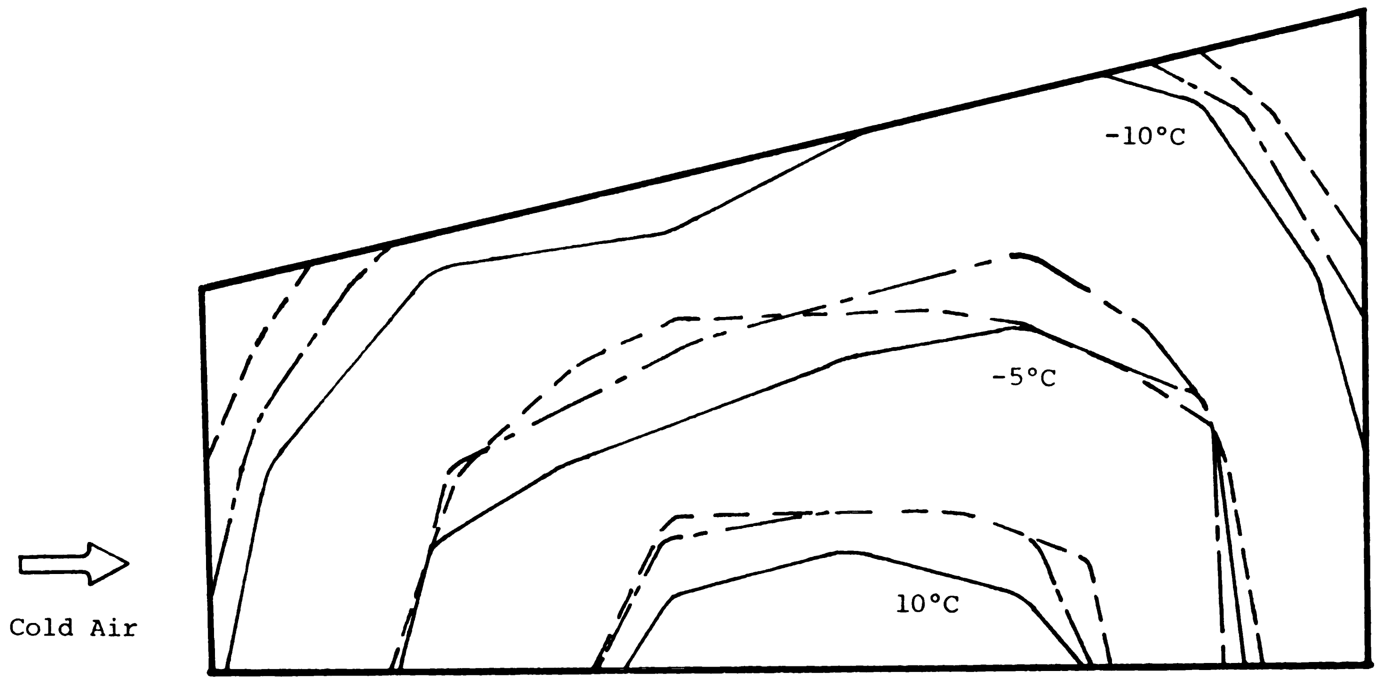

——— Experimental data

— — Computer prediction $T_s = f\ (x,\ t)$

----- Computer prediction, T_s uniform

T_i	18°C
T_∞	-20°C
v	11.3 m/s
$\overline{h}$	70.6 $W/m^2\ K$

Figure 5.12. The isothermal fields inside trapezoidal product after 1.0 freezing hour at air speed 11.3 m/s.

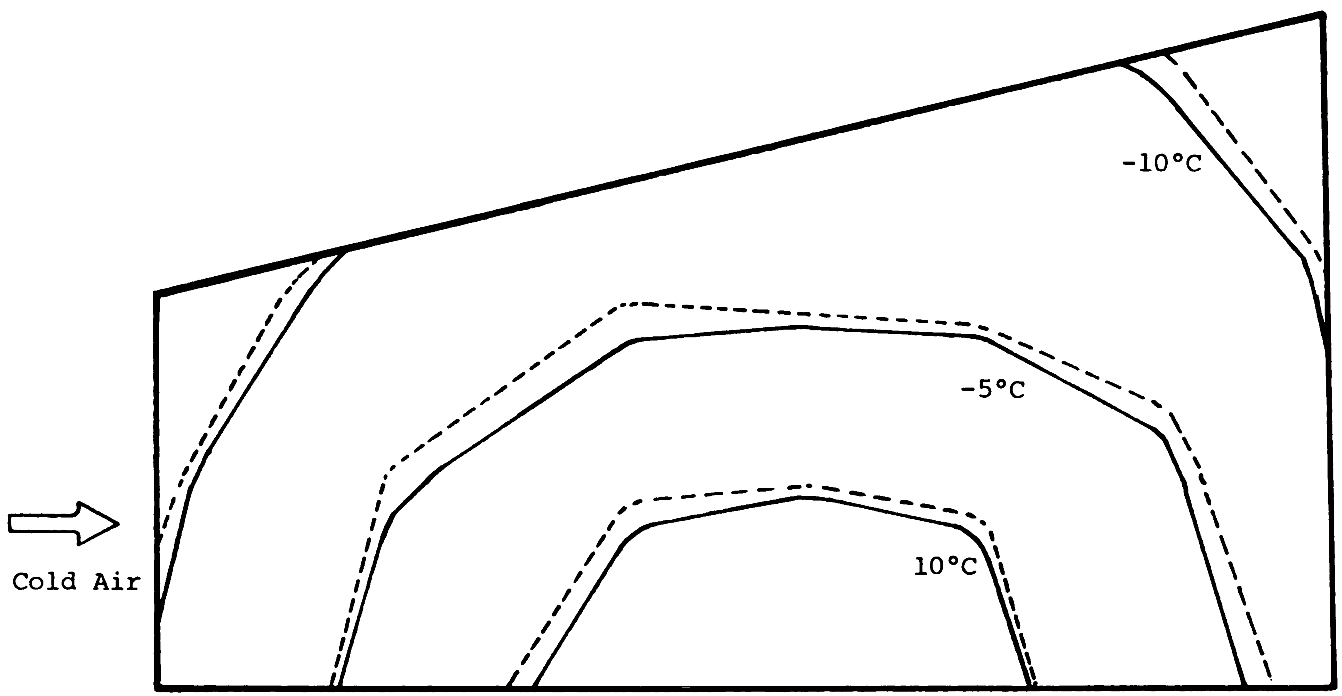

—— Experimental Data — T_i 18°C — v 7.4 m/s

– – – Computer prediction, $T_s = f(x,t)$ — T_∞ -20°C — Δt 1 minute

Figure 5.13. The isothermal fields inside trapezoidal product after 1.0 freezing hour at air speed 7.4 m/s.

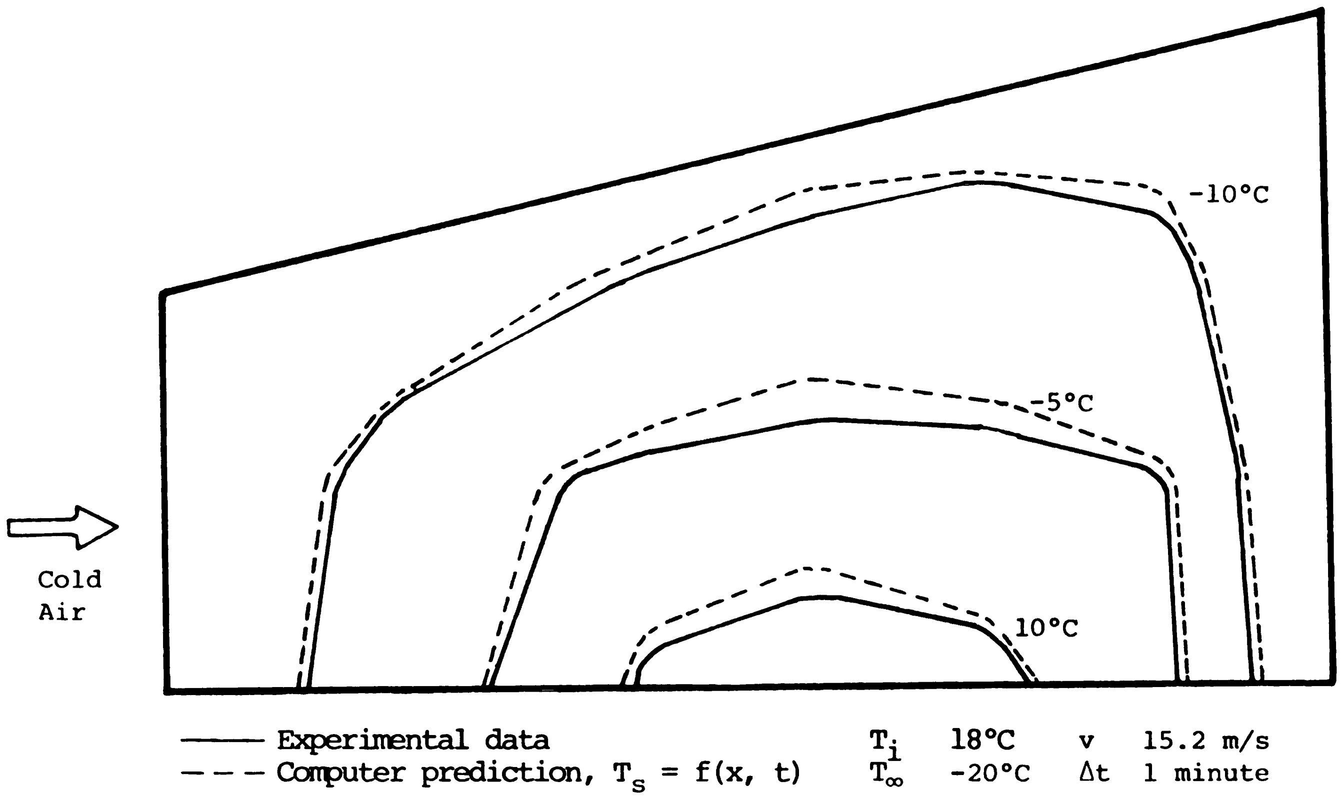

Figure 5.14. The isothermal fields inside trapezoidal product after 1.0 freezing hour at air speed 15.2 m/s.

point location, for air speeds of 7.4 and 11.3 m/s, do not give results as good as for 15.2 m/s air speed. The discrepancies can be attributed to the method used to average the thermal product properties of a triangular finite element after the initial freezing point was achieved. While this averaging method may provide insignificant error for a small size triangle, the error will increase as the size of the triangular element becomes larger. Thus, the predicted curves tend to be decreasing slower than the experimental curves beyond the thermal arrest time.

5.3. Influence of Area Average Enthalpy on Freezing Time

Freezing time can be predicted conventionally by expressing the temperature history at the slowest freezing point location in the product or by using the total heat content (enthalpy) of the food product. The conventional method for predicting freezing time represents the length of process required to achieve a temperature equal to the desired storage temperature at the slowest freezing point location.

An alternate criteria involves time required for the food product enthalpy to be reduced to an enthalpy equivalent to the storage temperature (Gorby, 1974). When the freezing process is stopped at this point, the product temperature will equilibrate uniformly to the storage temperature with the heat content from the portion with higher temperature transferring to the portion of the product with lower temperature. The mass average enthalpy, $\bar{H}_m$ can be expressed as follows

$$H_m = \frac{1}{m} \int_m H dm \tag{5.1}$$

Implementing the above equation into the finite element method, an area average enthalpy was used as a criteria to determine the freezing time

$$\bar{H}_A = \frac{1}{\sum_{e=1}^{E} A^{(e)}} \sum_{e=1}^{E} H^{(e)} A^{(e)} \tag{5.2}$$

The predicted freezing times were compared for both conventional method and area average enthalpy (Table 5.3) at various product geometries and air speeds. The storage temperature used for these comparisons was -17.0°C. The average enthalpy method predicts lower freezing times, ranging from 10.7 to 24.7 percent compared to conventional method. These results may encourage the use of the average enthalpy method to predict the freezing time in order to achieve a more efficient process and to reduce energy consumption.

TABLE 5.3.--Experimental and Predicted Freezing Time for Various Shapes and Air Speeds*

General Shape	Air Speed m/s	Predicted Freezing Time, Hours	
		Based on Conventional Method	Based on Area Average Enthalpy Method
Elliptical	7.4	8.1	6.25
	11.3	7.6	5.72
	15.2	7.3	5.50
Trapezoidal	7.4	5.0	4.25
	11.3	4.5	4.02
	15.2	4.3	3.78

*Storage temperature -17°C.

At time periods after the freezing process is stopped, the equilibration period required to achieve storage temperature will occur at a reduced rate compared to the freezing rate. From microbiological and food quality standpoint, this phenomena might be a matter of concern. However, the temperature at the end of the freezing process is well below -10°C and the product portion with temperature above the storage temperature, -17.0°C, is only about 30-35 percent of the total product as seen on Figures 5.15 and 5.16.

5.4. Sensitivity Analysis

5.4.1. Geometric Size

Geometric size has a significant influence on the freezing rate as illustrated in Figures 5.17 and 5.18. For an elliptical shape the freezing time increases 173 percent as the product size becomes 1.5 times larger and decreased by 53 percent as the size is reduced by 0.5 as compared to the size used for experimental measurements (a = 10 cm, b = 6.5 cm). These values for the trapezoidal shape are 164 percent and 59 percent, respectively. It is interesting to note that the flat plateau indicating the region where a major portion of the latent heat is removed, becomes less evident as the size becomes smaller.

The relationship between the multiplication factor for geometric size to the freezing time could provide

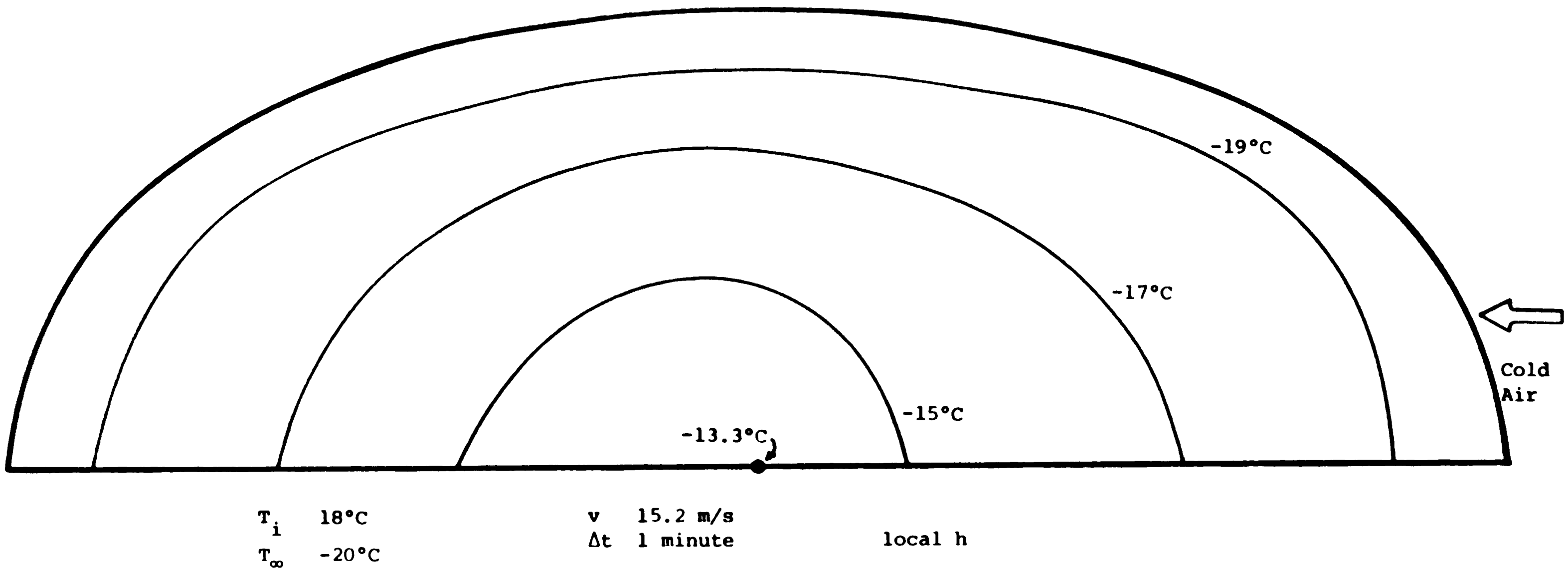

Figure 5.15. The isothermal fields inside elliptical product at the time the freezing process terminated based on area average enthalpy (v = 15.2 m/s).

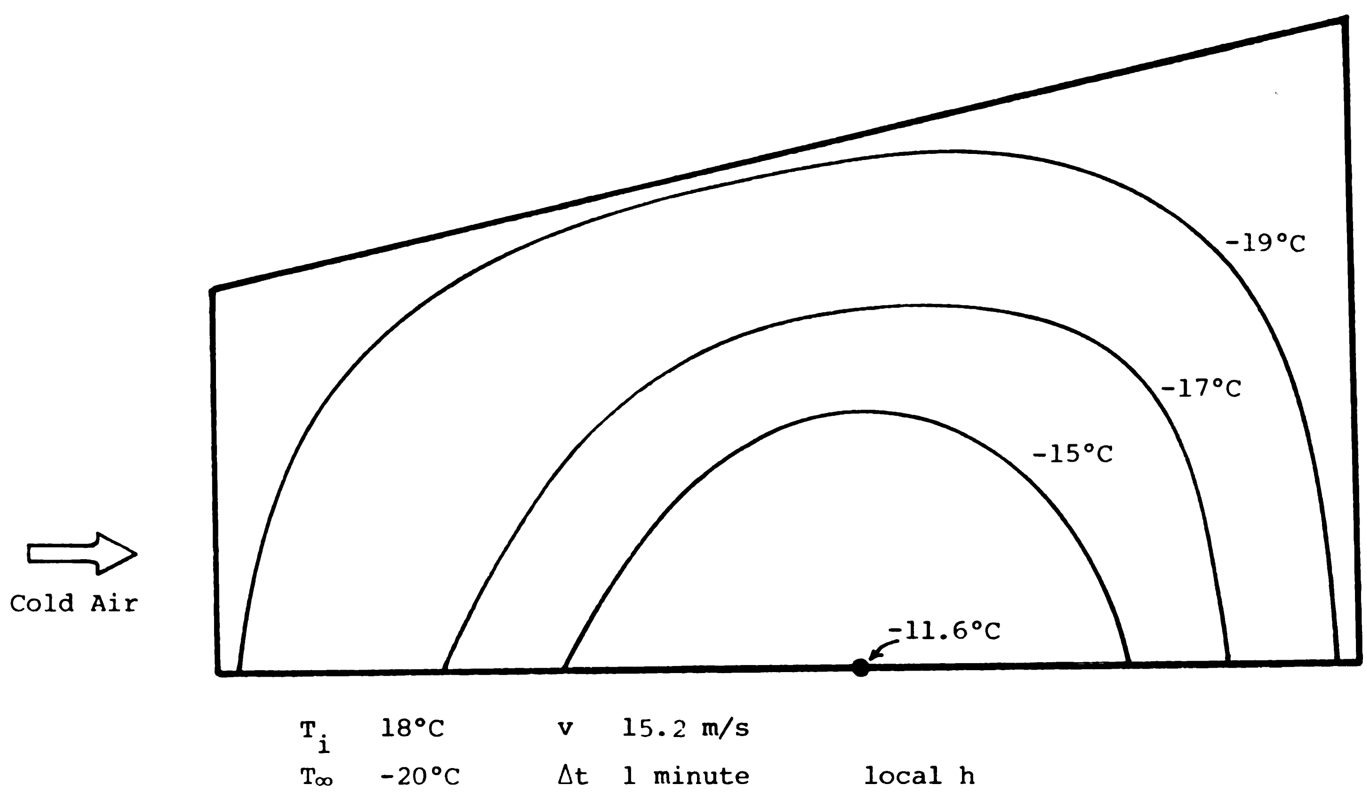

Figure 5.16. The isothermal fields inside trapezoidal product at the time the freezing process terminated based on area average enthalpy (v = 15.2 m/s).

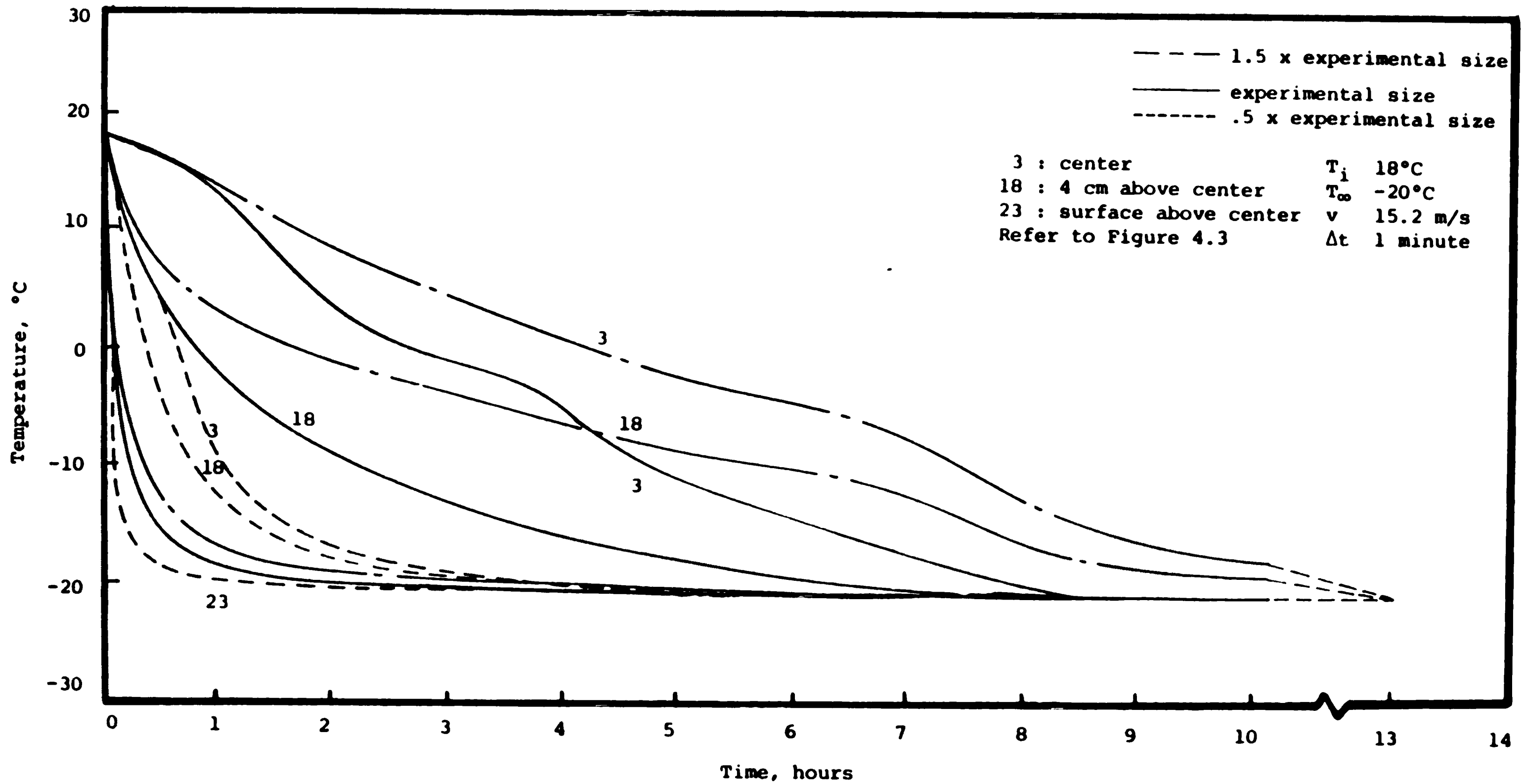

Figure 5.17. The influence of geometrical size on the freezing rate of elliptical product.

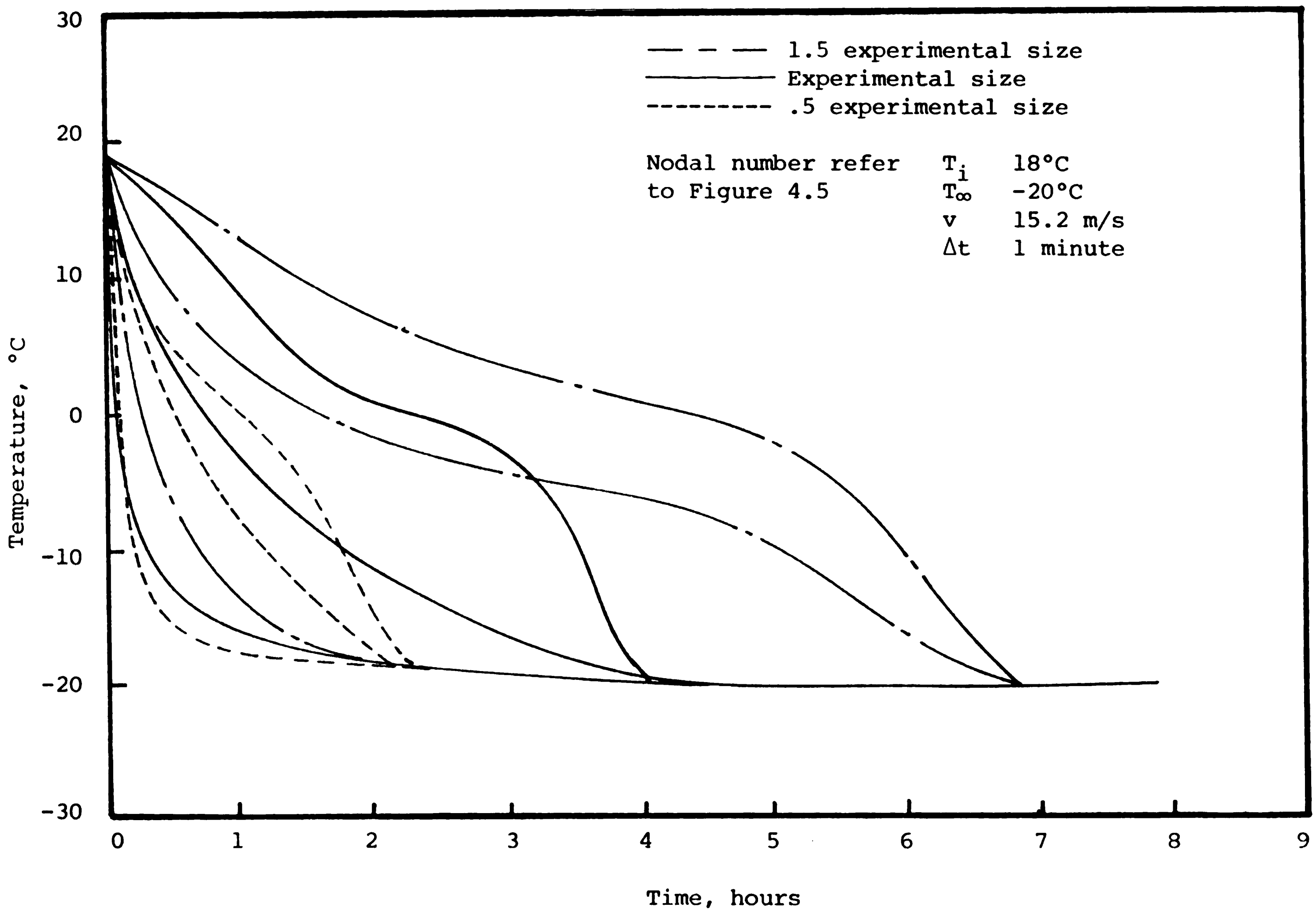

Figure 5.18. The influence of geometrical size on the freezing rate of trapezoidal product.

useful information in the selection of optimum size and conditions for efficient freezing time.

5.4.2. Initial Product Temperature

A sensitivity analysis was conducted to determine the effect of initial product temperature on the freezing time. Initial temperatures of 22°C and 14°C were compared to 18°C, which was initial temperature used to generate the experimental results. The results, presented in Figures 5.19 to 5.22, indicate that initial product temperature does not influence freezing time significantly. The isothermal field after 2.5 hours illustrates a deviation in the range of ± 2.0°C for elliptical shape and ± 1.5°C for trapezoidal shape. The results, presented in Figures 5.19 to 5.22, indicate that the freezing time is about the same for various initial product temperatures. The freezing rate curves converge to 7.5 hours of freezing time for elliptical product and to 4.0 hours of freezing time for trapezoidal product. In general, it could be concluded that initial product temperature has small influence on freezing time.

5.4.3 Time Step

Time increment, Δt, has been known as an important factor in the stability of numerical analysis. Two

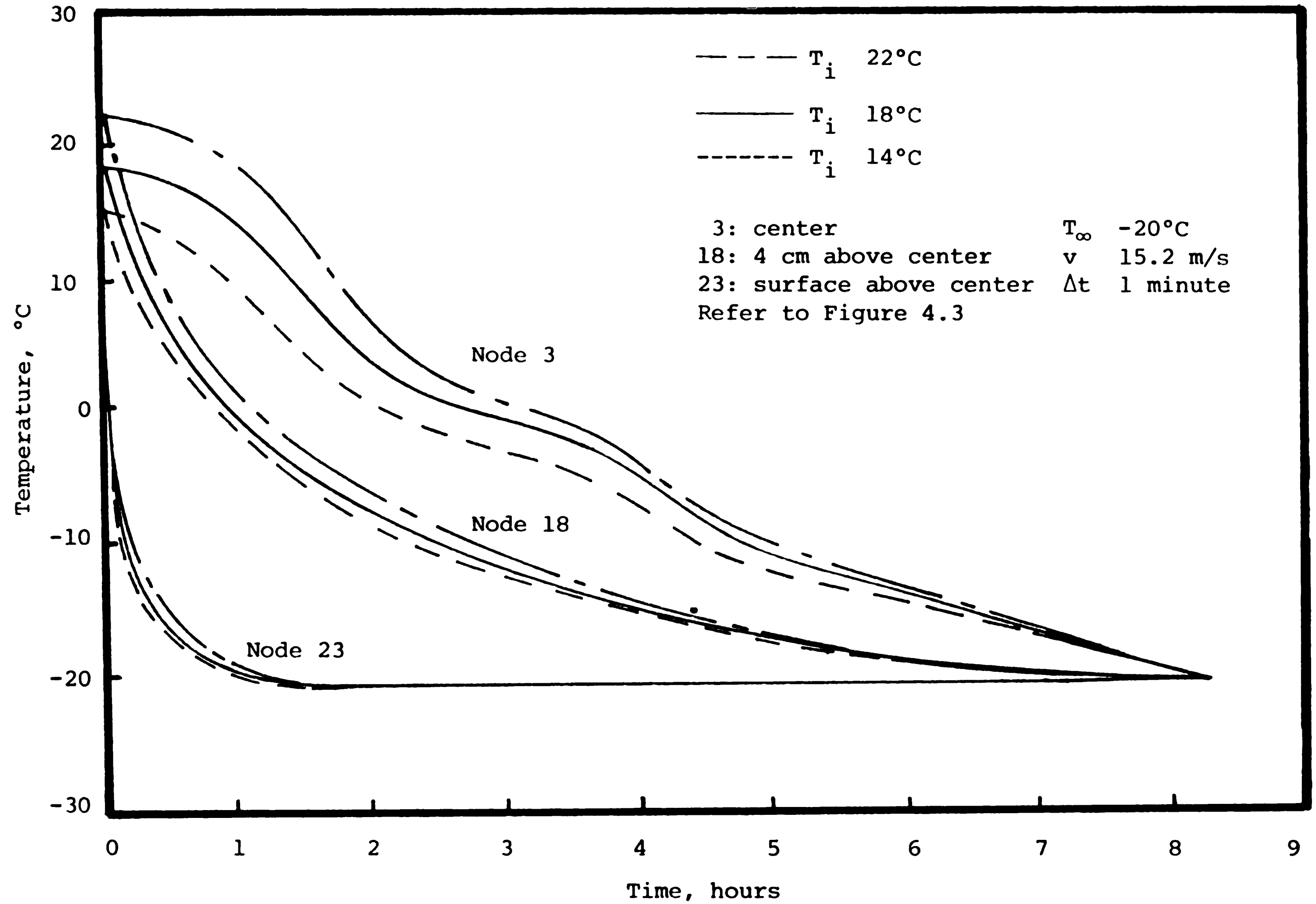

Figure 5.19. The influence of initial temperature on the freezing rate of elliptical product.

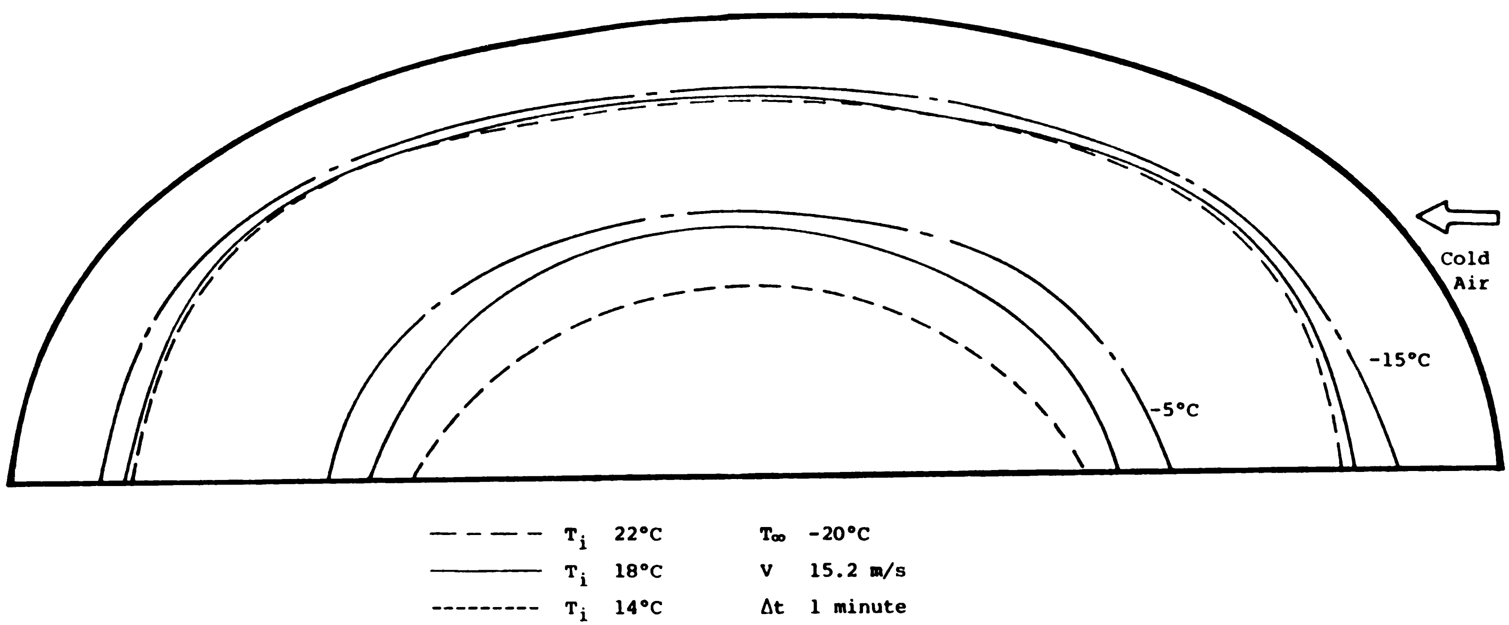

Figure 5.20. The isothermal fields for various initial temperatures in the elliptical product after 2.5 freezing hours.

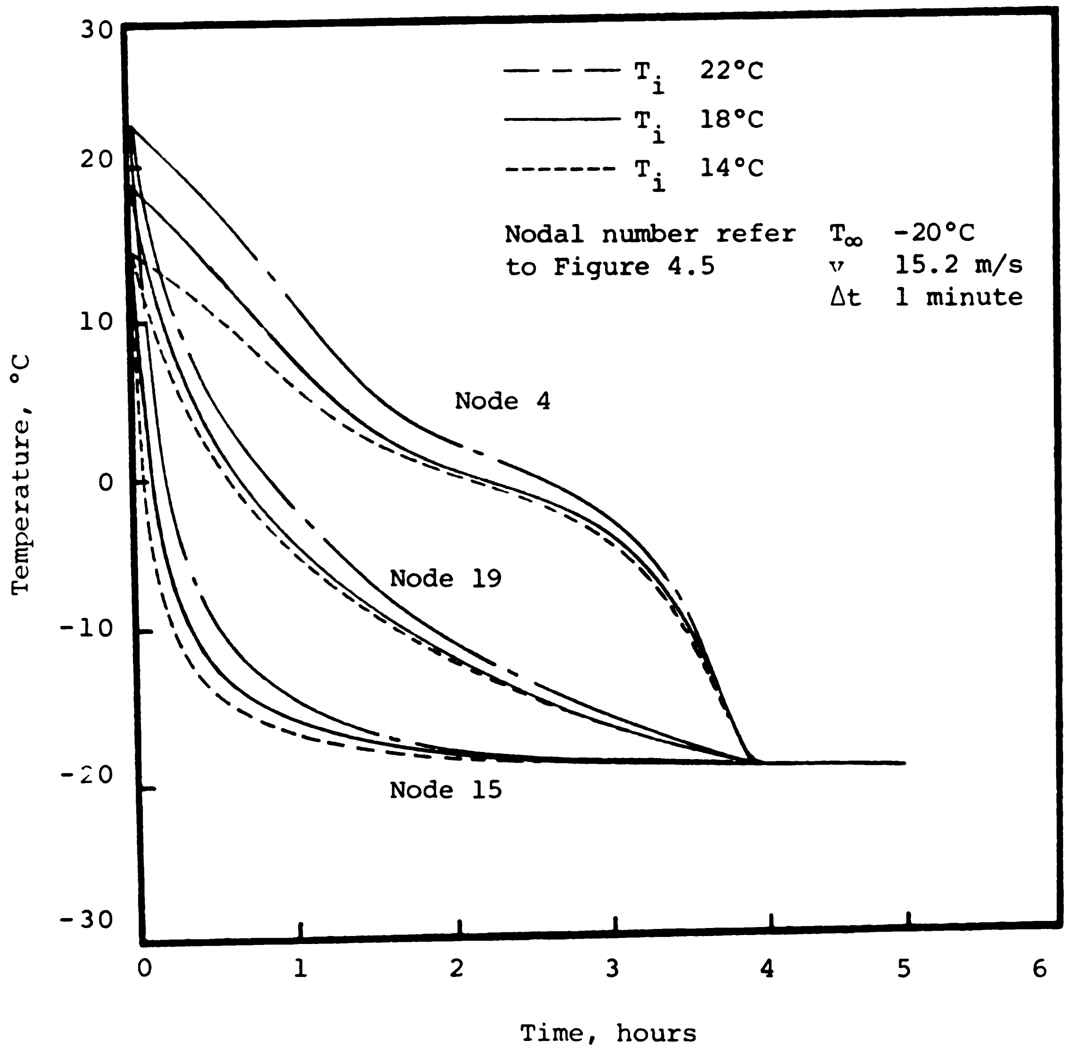

Figure 5.21. The influence of initial temperature on the freezing rate of trapezoidal product.

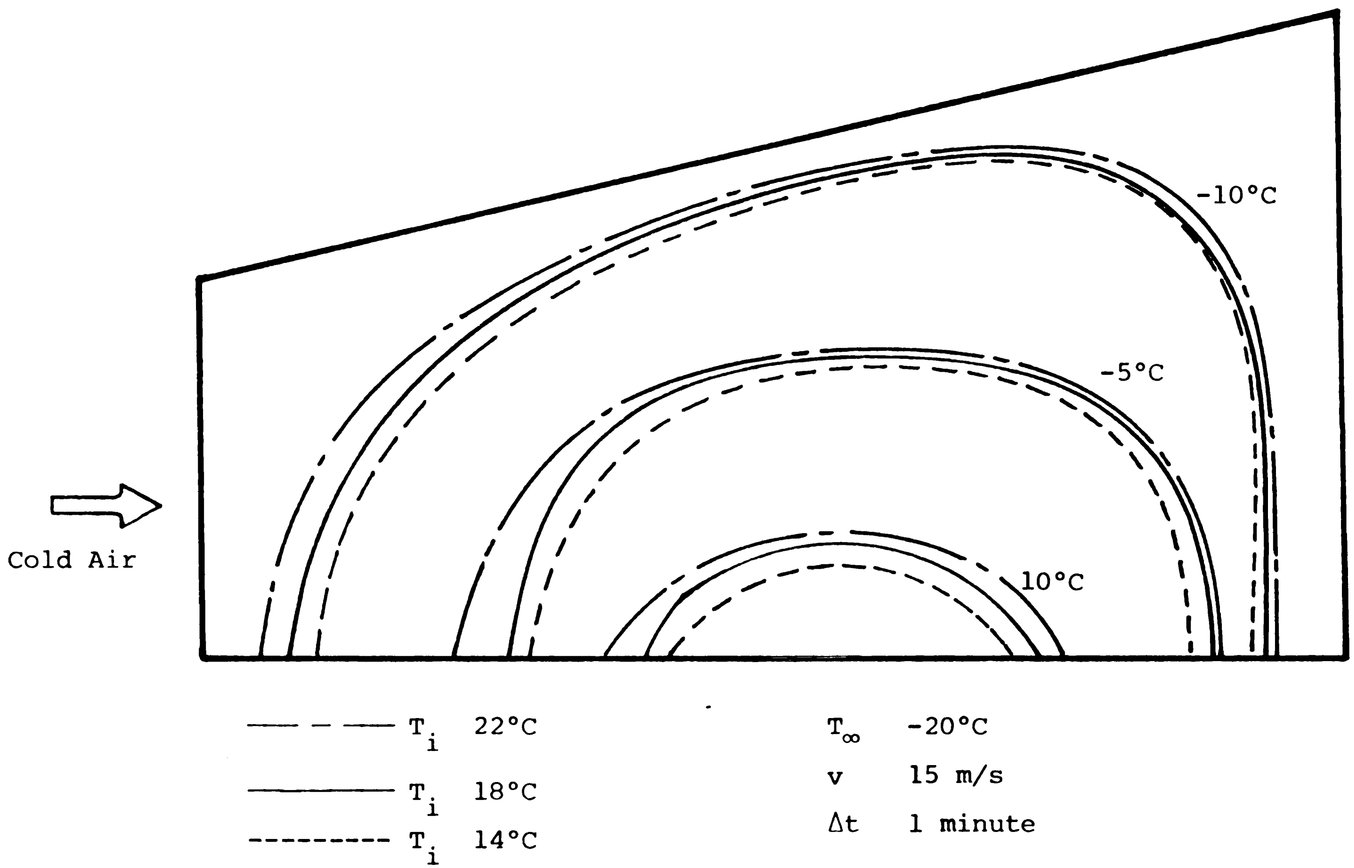

Figure 5.22. The isothermal fields for various initial temperatures in the trapezoidal product after 1.0 freezing hour.

different types of time step, one minute and three minutes, were supplied to the simulation program. Figures 5.23 to 5.26 indicate that the numerical solution remains stable, at least in the range of Δt equal to one to three minutes. The discrepancies shown are small and insignificant; 0.0 to 1.0°C for the trapezoidal shape and 0.0 to 0.5°C for the elliptical shape.

Isothermal fields indicate that discrepancies exist between the time step of one minute and three minutes on the product portion facing the cold air stream (Figure 5.26). This phenomena can be attributed to the fact that thermal properties of product were computed at each time step in the simuation. Large time step will provide inaccuracy which becomes more significant for higher temperature difference between the product and the cold air occurred at the upstream portion than the downstream portion.

5.5. Application of the Numerical Model in the Food Freezing Process

The finite element simulation model has been verified by the experimental data as described in previous sections. The application of the model in food freezing is not restricted to trapezoidal and elliptical geometry but to other anomalous shapes as well. For practical value, an observation of size parameter influence on

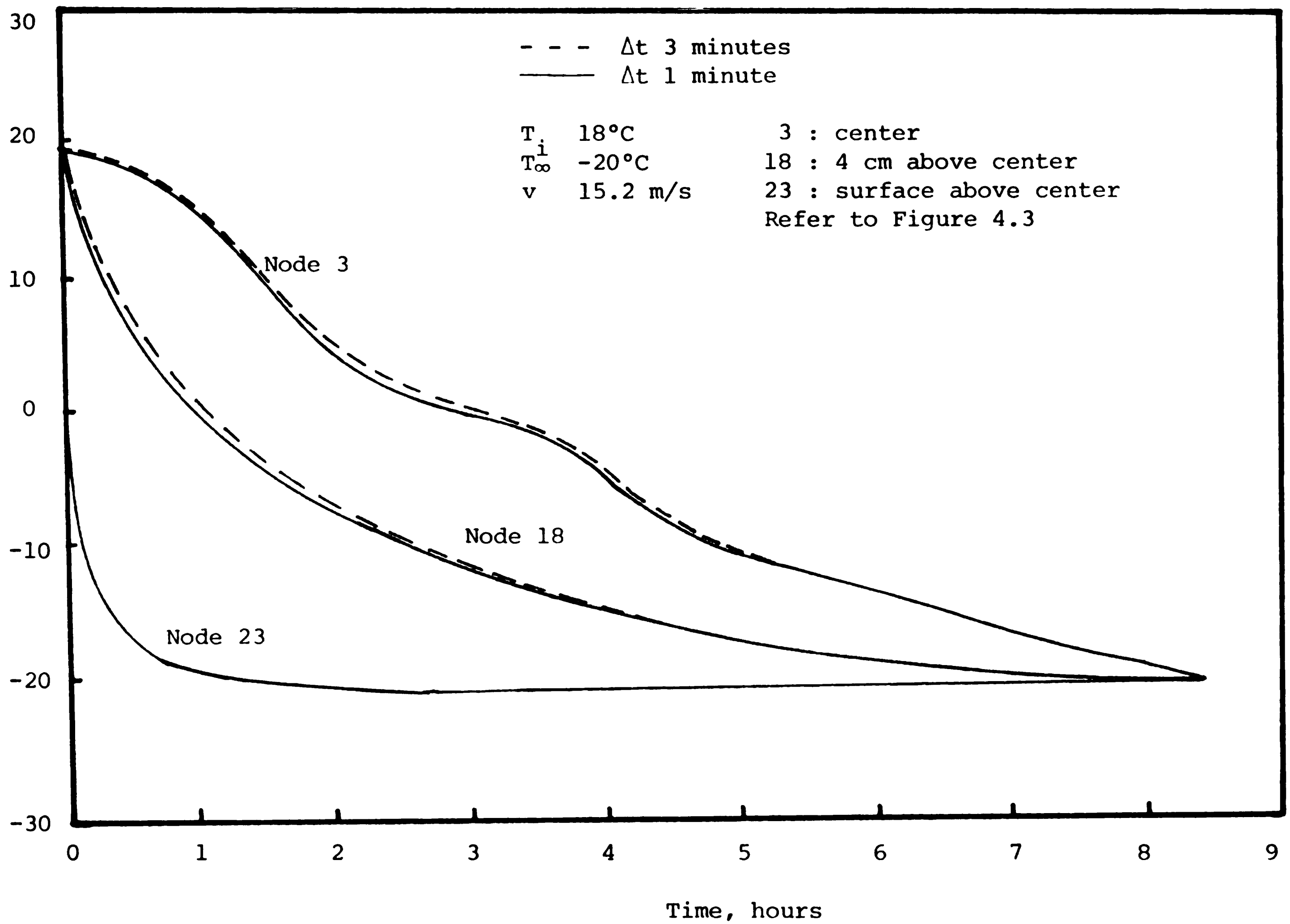

Figure 5.23. The effect of time step used in numerical scheme on the freezing rate of elliptical product.

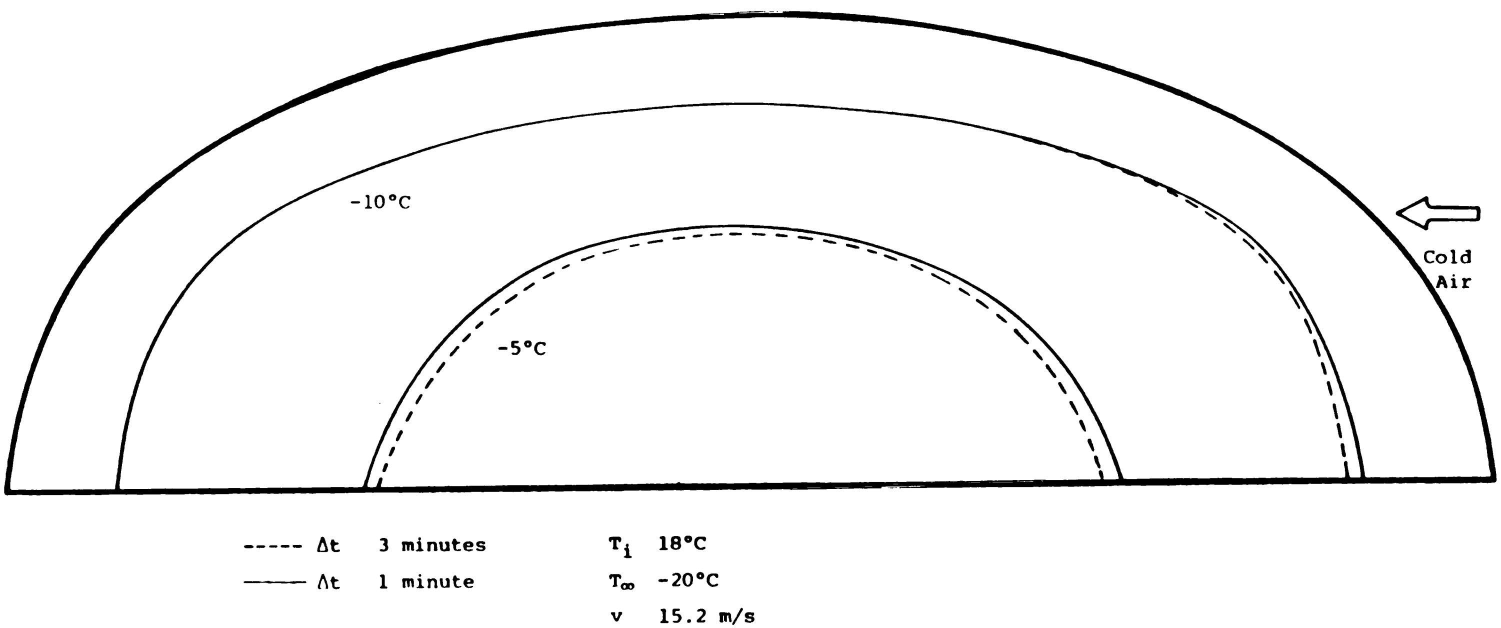

Figure 5.24. The isothermal fields for two different time steps in the elliptical product after 2.5 freezing hours.

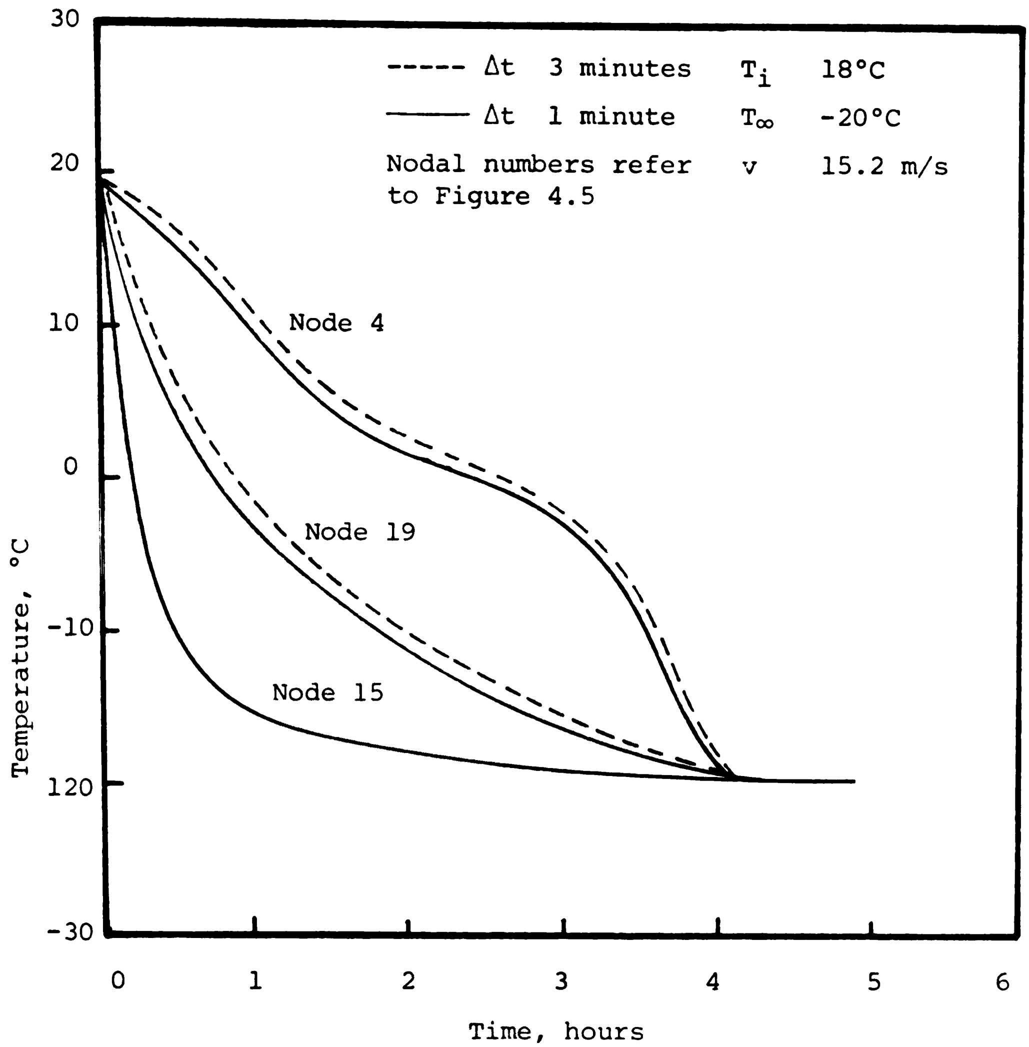

Figure 5.25. The effect of time step used in numerical scheme on the freezing rate of trapezoidal product.

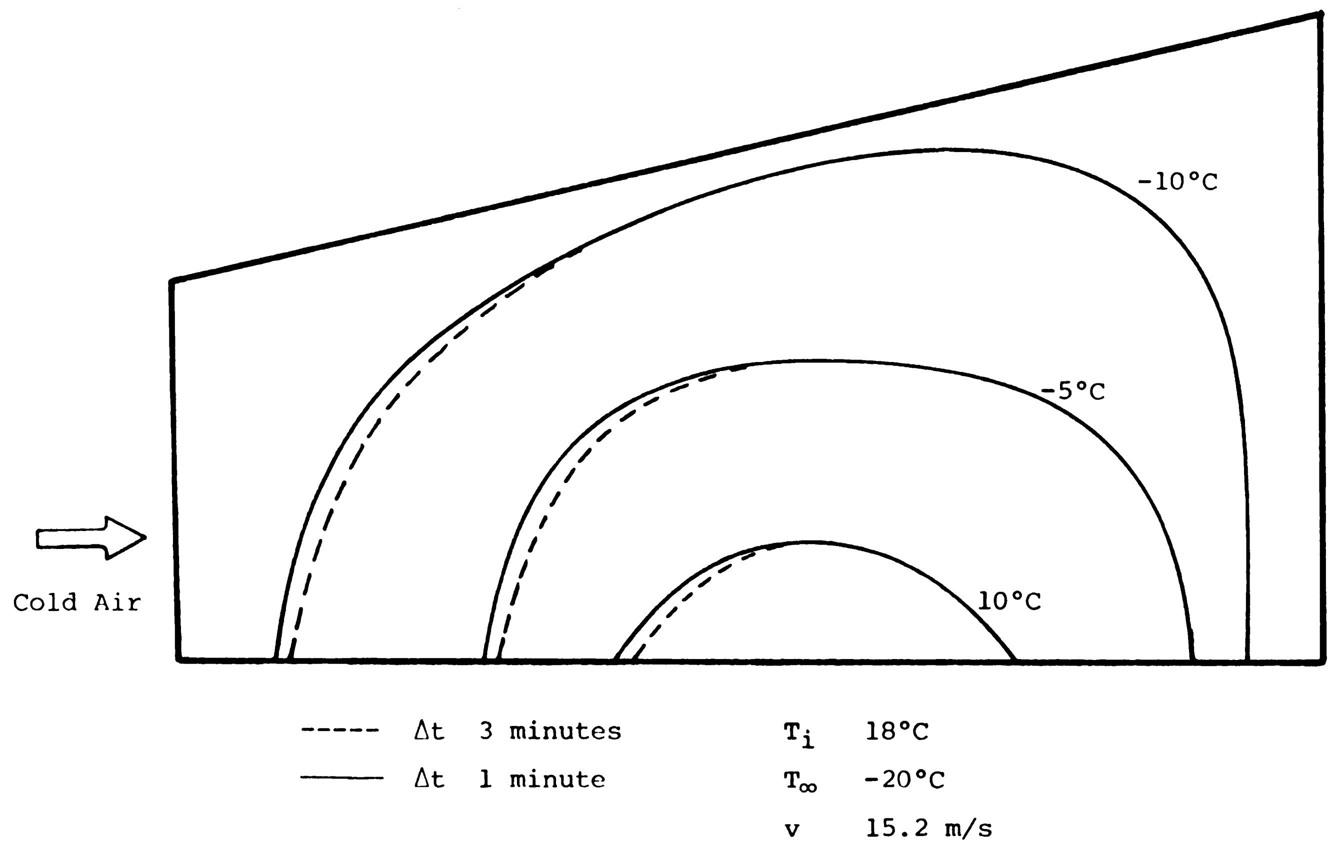

Figure 5.26. The isothermal fields for two different time steps in the trapezoidal product after 1.0 freezing hour.

freezing time can be conducted for any given product shape. Then a chart illustrating the relationships among freezing time, size and shape can be developed and a convenient method to select freezing times for desired product, shape, and size would result.

Requirements that must be satisfied when using the numerical model include:

1. The initial product thermal properties must be available either from literature or experimental measurements. These properties include thermal conductivity, specific heat, and product density of unfrozen product and freezing point, water content and unfreezable water content.

2. Average heat transfer coefficient should be known or measured accordingly over a range of air velocities.

3. A finite element grid should be developed for the given product configuration. Again careful judgment must be made since the coarseness of the grid might affect the accuracy of the estimated freezing process. Smaller grid will use more core memory in the computer and produce long execution time and in turn high computer cost. For example, the elliptical grid in this study used 360 to 390 seconds execution time and the trapezoidal grid 140 to 190 seconds for total computation at the CDC 6500 computer.

4. Computer facilities must be close at hand to run the computation.

The finite element analysis has advantages and limitations when used to simulate the freezing process. The advantages include:

1. Easiness in changing the input boundary conditions and parameters including product properties and freezing environment.
2. Readiness to accommodate various product shapes and sizes.

The limitations to applying the simulation model approach are:

1. Modifications are needed for a specific anomalous shapes and for non-homogeneous materials.
2. The model is valid for food freezing utilizing air velocities in laminar region with Reynolds Numbers smaller than 2.1×10^5.
3. Required more computer time than finite difference method, thus higher computer cost.
4. The method used in averaging nodal product thermal properties for a triangular element causes some error in the simulation scheme as previously discussed especially in large grids.

6. CONCLUSIONS

1. A computer simulation utilizing the finite element method to predict the freezing rate for food products with elliptical and trapezoidal shapes has been developed and verified by experimental data.

2. The computer simulation using the finite element method has the ability to accommodate various boundary conditions as well as the non-linearity of product thermal properties during phase-change, and different product geometries.

3. The utilization of local convective heat transfer coefficients over the product surface as boundary condition in the computer model provides better simulation of the actual freezing process as compared to an average surface heat transfer coefficient.

4. The predicted freezing times based on area-average enthalpy method are 10.7 to 24.7 percent lower than the predicted times based on the conventional method --the slowest freezing point location.

5. Geometric size affects the freezing time significantly, while the influence of initial product temperature over the range of 14.0 to 22.0°C can be considered negligible.

6. The stability of the finite element algorithm is not influenced by the magnitude of time step at Δt from one to three minutes.

7. RECOMMENDATIONS FOR FURTHER STUDY

1. To develop a chart illustrating the relationship between freezing time and various product shapes and sizes. This chart would have practical value in selecting the optimum size of a given product shape for an efficient freezing process.

2. To modify the computer program in order to accommodate the ability to simulate the freezing process for non-homogeneous food products.

3. To determine the ratio of local to average surface convective heat transfer coefficient for product shape other than flat plate, circle, and ellips.

4. To utilize higher order elements and a non-consistent capacitance matrix to investigate the possibility of getting more accurate and stable results than using a simplex triangular element and a consistent capacitance matrix.

APPENDICES

APPENDIX A

COMPUTER PROGRAM TWODFR AND AXISFR

TWODFR FORTRAN LISTING FOR ELLIPTICAL PRODUCT

--TWO DIMENSIONAL FREEZING

```
      PROGRAM TWODFR(INPUT,OUTPUT,PUNCH,TAPE60=INPUT,TAPE61=OUTPUT,TAPE6
     12=PUNCH,TAPE1,TAPE2,TAPE3,TAPE67)
      DIMENSION NS(3),X(3),Y(3),ISIDE(3)
      COMMON/TLE/TITLE(20)
      COMMON MC(625)
      COMMON A(1)
      COMMON/PROP/DI,RI,HS,DW,CI,TJ,KI,KW,CPW,TF,LHC,UFWC,CS,KS,MS,CPS,
     $LK,ICP,LFD
      COMMON/HSF1/HSF(40)
      REAL KXX,KYY,LO
CCC
C  DEFINITION OF THE CONTROL PARAMETERS
C       NP - NUMBER OF GLOBAL TEMPERATURES, NE - NUMBER OF
C       ELEMENTS, NBW - BAND WIDTH, KXX - CONDUCTIVITY IN X DIRECTION,
C       KYY - CONDUCTIVITY IN Y DIRECTION, H - CONVECTION COEFFICIENT,
C       TINF - FLUID TEMPERATURE
C     CRHO=SPECIFIC HEAT*DENSITY
C     DT=TIME STEP    NIT=NO. OF ITERATIONS
C     INTR=ITERATIONS BEFORE PRINTING
CCC
      IO=61
      NCL=1
      IZ=67
      KK=1
CCC
C  INPUT OF THE TITLE CARD AND THE CONTROL PARAMETERS
C  GRAVE = INITIAL TEMPERATURE
CCC
      READ(IZ,3) TITLE
    3 FORMAT(20A4)
      READ(IZ,2) NP,NE,NBW,NIT,INTR,KXX,KYY,H,TINF,DT,CRHO
    2 FORMAT (5I3,6F10.4)
      REWIND 2
      DO 510 INO=1,NP
      GRAVE=64.
      WRITE(2,1005) GRAVE
 1005 FORMAT (E17.5)
  510 CONTINUE
CCC
C  CALCULATION OF POINTERS AND INITIALIZATION OF THE COLUMN VECTORAA
CCC
      JTN=NP
      JGF=2*NP
      JGSM=JGF+NP
      JGCM=JGSM+NP*NBW
      JEND=JGCM+NP*NBW
      CALL SETFL(A(JEND))
      DO13I=1,JEND
   13 A(I)=0.0
CCC
C  OUTPUT OF TITLE AND DATA HEADINGS
CCC
      WRITE(IO,4) TITLE,KXX,KYY,H,TINF
    4 FORMAT(1H1,//,/,1X,20A4//1X,5HKXX =,F9.4,10X,5HKYY =,F9.4/1X,16HCO
     1NVECTION COEFF =,F9.4/1X,12HFLUID TEMP =,F9.4//1X,17HNEL   NODE NU
     2MBER,6X,4HX(1),6X,4HY(1),6X,4HX(2),6X,4HY(2),6X,4HX(3),6X,4HY(
     33)
      WRITE(IO,82) CRHO,DT,NIT,INTR
   82 FORMAT(2X,21HT C RHO             =,F10.5/2X,11HTIME STEP =,F10.5/
     12X,19HNO. OF ITERATIONS =,I4/2X,30HITERATIONS BETWEEN PRINTING =,
     2I4)
CCC
C  INPUT AND ECHO PRINT OF ELEMENT DATA
CCC
      REWIND 1
      DO 77 KK=1,NE
      READ(IZ,1) NEL,NS,X(1),Y(1),X(2),Y(2),X(3),Y(3),ISIDE
    1 FORMAT(4I3,6F10.4,3I2)
      WRITE (1,3002) NEL,NS,X(1),Y(1),X(2),Y(2),X(3),Y(3),ISIDE
 3002 FORMAT (4I3,6F10.4,3I2)
   77 CONTINUE
      CALL REAL 1
CCC
C  CALCULATION OF LOCAL SURFACE
C  HEAT TRANSFER COEFFICIENT
CCC
      CALL HVAR
      CALL SETMAT(A,CRHO,KXX,KYY,H,TINF,NP,JGSM,JGCM,DT,NE,NN,NBW,JEND,
     1NCL,NIT,INTR,KK)
      CALL TRANSLT(A(JGSM+1),A(JGCM+1),A(JGF+1),A(JTN+1),A(1),NP,NBW,NCL
     1,DT,NIT,INTR,NN,CRHO,KXX,KYY,H,TINF,JGSM,JGCM,NE,JEND,AS)
      STOP
      END
```

```
      SUBROUTINE SETMAT(A,CRHO,KXX,KYY,H,TINF,NP,JGSM,JGCM,CT,NE,NN,NBW,
     1JEND,NCL,NLT,IHTS,KK)
      DIMENSION A(JEND),NS(3),B(3),C(3),ECM(3,3),ESM(3,3),EF(3),ISIDE(3)
      DIMENSION X(3),Y(3)
      DIMENSION TVAL(4I)
      DIMENSION TJ(3),CIJ(3),KJ(3),PDJ(3)
      DIMENSION EH1(3)
      COMMON/PROF/BI,RI,HS,DW,DI,TO,KI,KW,CFW,TF,LWC,UFWC,DS,KS,MS,CFS,
     $IK,IOP,LFD
      COMMON/HSF1/HSF(40)
      REAL KXX,KYY,KJ,LG
      CF=0.82
      RHO=56.
      SH1=0.
      SA=0.
      REWIND 2
      DO 510 JEO=1,NP
      READ (2,1005) TVAL (JEO)
 1005 FORMAT (E17.5)
      A(JEO)=TVAL(JEO)
  510 CONTINUE
      REWIND 1
      DO 7 IE=1,NE
      READ(1,1004) NEL,NS(1),NS(2),NS(3),X(1),Y(1),X(2),Y(2),X(3),Y(3),
     1ISIDE(1),ISIDE(2)
 1004 FORMAT (4I3,6F10.4,2X,2I2)
      X(1)=X(1)/30.24
      X(2)=X(2)/30.24
      X(3)=X(3)/30.24
      Y(1)=Y(1)/30.24
      Y(2)=Y(2)/30.24
      Y(3)=Y(3)/30.24
      B(1)=Y(2)-Y(3)
      B(2)=Y(3)-Y(1)
      B(3)=Y(1)-Y(2)
      C(1)=X(3)-X(2)
      C(2)=X(1)-X(3)
      C(3)=X(2)-X(1)
      AR4=(X(2)*Y(3)+X(3)*Y(1)+X(1)*Y(2)-X(2)*Y(1)-X(3)*Y(2)-X(1)*Y(3))
     1*2.
      NE1=NS(2)
      NE2=NS(3)
      NE3=NS(1)
      TJ(1)=TVAL(NE1)
      TJ(2)=TVAL(NE2)
      TJ(3)=TVAL(NE3)
CCC
C     CALCULATION OF ELEMENT PROPERTIES
C     AS FUNCTIONS OF TEMPERATURE
CCC
      IF (TJ(1)-32.) 3011,3011,1007
 1007 IF (TJ(2)-32.) 3011,3011,1008
 1008 IF (TJ(3)-32.) 3011,3011,1009
 3011 DO 3001 N=1,3
      T=TJ(N)
      IF (T.GT.32.) GO TO 3002
      CALL PROP1(T,CPA,AK,PD,H1)
      CIJ(N)=CPA
      KJ(N)=AK
      PDJ(N)=PD
      IF (KK-210) 3001,311,311
  311 EH1(N)=H1
      GO TO 3001
 3002 CIJ(N)=CF
      KJ(N)=KXX
      PDJ(N)=RHO
 3001 CONTINUE
      KYY=KXX=(KJ(1)+KJ(2)+KJ(3))/3.
      CRHO=(CIJ(1)*PDJ(1)+CIJ(2)*PDJ(2)+CIJ(3)*PDJ(3))/3.
CCC
C     SUMMATION OF AREA ENTHALPY AND TOTAL
C     AREA OF ELEMENT
CCC
      IF (KK-210) 1009,811,811
  811 AH1=(EH1(1)+EH1(2)+EH1(3))/3.
      SH1=SH1+AH1*AR4/4.
      SA=SA+AR4/4.
 1009 CONTINUE
      DO5I=1,3
      DO5J=1,3
      TK=1.
      IF (I.EQ.J) TK=2.
      ECM(I,J)=CRHO*AR4*TK/48.
    5 ESM(I,J)=(KXX*B(I)*B(J)+KYY*C(I)*C(J))/AR4
      DO11I=1,3
   11 EF(I)=0.0
```

```
CCC
C     CALCULATION OF THE CONVECTION RELATED QUANTITIES
CCC
      DO10I=1,2
      IF(ISIDE(I).LE.0) GOTO8
      H=H*HSF(NEL)
      J=ISIDE(I)
      M=J+1
      IF(J.EQ.3) M=1
      LG=SQRT((X(M)-X(J))**2+(Y(M)-Y(J))**2)
      HL=H*LG
      EF(J)=EF(J)+HL*TINF/2.
      EF(M)=EF(M)+HL*TINF/2.
      ESM(J,J)=ESM(J,J)+HL/3.
      ESM(J,M)=ESM(J,M)+HL/6.
      ESM(M,J)=ESM(J,M)
   10 ESM(M,M)=ESM(M,M)+HL/3.
CCC
C     INSERTION OF ELEMENT PROPERTIES INTO THE GLOBAL STIFFNESS MATRIX
CCC
    8 DO 7 I=1,3
      II=NS(I)
      J5=2*NP+II
      A(J5)=A(J5)+EF(I)
      DO17J=1,3
      JJ=NS(J)
      JJ=JJ-II+1
      IF(JJ)17,17,16
   16 J5=JGSM+(JJ-1)*NP+II
      J6=JGSM+(JJ-1)*NP+II
CCC
C     AJ5=A MATRIX
C     AJ6=P MATRIX
C     A*T(NEW)=P*T(OLD)-2*F
CCC
      A(J5)=A(J5)+ESM(I,J)+2./DT*ESM(I,J)
      A(J6)=A(J6)+2./DT*ESM(I,J)-ESM(I,J)
   17 CONTINUE
    7 CONTINUE
CCC
C     CALCULATION AND OUTPUT OF AREA
C     AVERAGE ENTHALPY
CCC
      IF (KK-210) 711,712,712
  712 AGM=SH1/CM
      PRINT 4111,AGM
 4111 FORMAT (* *,*AREA AVERAGE ENTHALPY*,F10.4)
  711 CONTINUE
CCC
C     DCMPBD DECOMPOSED A INTO UPPER TRIANGLE MATRIX
CCC
      CALL DCMPBD(A(JGSM+1),NP,NBW)
      RETURN
      END
```

```
      SUBROUTINE TRANSNT(GCM,GMM,P,TR,XI,NP,NBW,NCL,DT,NIT,INTR,NN,CRHO,
     1KXX,KYY,H,TINF,JCSM,JGCM,NE,JEND,A)
      COMMON/TLE/TITLE(20)
      COMMON/PROF/BI,RL,HS,DW,DI,TO,KI,KW,CPW,TF,IWC,UFWC,DS,KS,MS,CPS,
     $IK,ICP,IPD
      DIMENSION GCM(NP,NBW),GMM(NF,NBW),P(NP,1),TR(NF,1)
      DIMENSION A(JEND),BDYPHI(23),IB(23),IPSV(23)
      DIMENSION XV(4,2),NO(4,2)
      DIMENSION XI(NF,1)
      DIMENSION XF(33)
      REAL KXX,KYY
      ID=1
      SDT=0.0
      DO 6001 I=1,NP
      XF(I)=18.
 6001 XI(I,1)=64.
      WRITE(61,6) TITLE
    6 FORMAT(1H1,//1X,18HTRANSIENT ANALYSIS//1X,20A4)
      WRITE(61,7) SDT,(I,XF(I),I=1,NP)
    7 FORMAT(//1X,6HTIME =,F9.4/(1 X,I3,3X,E17.6,5X,I3,3X,E17.6,5X,I3,3X
     1,E17.6,5X,I3,3X,E17.6))
      LCOUNT=NP/5+4
      DO90 N=1,23
   90 IB(N)=0
      KN=0
CCC
C     CALCULATION OF PHI(I+1) FROM PHI(I)
CCC
      DO 13 KK=1,NIT
      IF(KN.EQ.0) GO TO 22
      DO 16 JJ=1,KN
 16   IPSV(JJ)=IB(JJ)
CCC
C     SAVING OF PRESCRIBED BOUNDARY VALUES IN BDYPHI
CCC
   22 IF(KN.EQ.0) GOTO15
      DO14I=1,KN
      J=IPSV(I)
   14 BDYPHI(I)=XI(J,1)
   15 CONTINUE
      SDT=SDT+DT
      CALL MULTBL(GMM,XI,TR,NF,NBW,NCL)
      DO9I=1,NF
    9 TR(I,1)=TR(I,1)+2.*P(I,1)
CCC
C     DECOMPOSES F AND SOLVES FOR TEMPERATURE
CCC
      CALL SOLVBD(GCM,TR,XI,NF,NBW,NCL,ID)
CCC
C     RESETTING OF THE PRESCRIBED BOUNDARY VALUES
CCC
      IF(KN.EQ.0) GOTO21
      DO20I=1,KN
      J=IPSV(I)
   20 XI(J,1)=BDYPHI(I)
   21 CONTINUE
      REWIND 2
      DO 510 ILK=1,NF
      WRITE (2,1005) XI(ILK,1)
 1005 FORMAT(E17.5)
  510 CONTINUE
CCC
C     OUTPUT OF THE RESULTS
CCC
      IF (((KK/INTR)*INTR).NE.KK) GO TO 6011
      DO 555 I=1,NP
  555 XF(I)=(XI(I,1)-32.)*5./9.
      WRITE (61,7) SDT,(I,XF(I),I=1,NP)
      LCOUNT=LCOUNT+NP/5+3
 6011 CONTINUE
      KCOUNT=3*NF+2*NP*NBW
      DO 501 I=1,KCOUNT
      A(I)=0.0
  501 CONTINUE
CCC
C     SET THE NEW ELEMENT MATRICES FOR
C     THE NEXT TIME STEP
CCC
      CALL SETMAT(A,CRHO,KXX,KYY,H,TINF,NF,JCSM,JGCM,DT,NE,NN,NBW,JEND,
     1NCL,NIT,INTR,KK)
      DO 430 IXM=1,NF
      XI(IXM,1)=A(IXM)
      TR(IXM,1)=0.0
      NLKD=IXM+NF*2
      P(IXM,1)=A(NLKD)
  430 CONTINUE
      LC1=3*NF+1
      LC2=3*NF+NBW*NP+1
      DO 431 I5=1,NBW
      DO 432 I6=1,NF
      GMM(I6,I5)=A(LC2)
      GCM(I6,I5)=A(LC1)
      LC2=LC2+1
      LC1=LC1+1
  432 CONTINUE
  431 CONTINUE
   13 CONTINUE
      RETURN
      END
```

```
      SUBROUTINE HVAR
      COMMON/HSF1/HSF(40)
      DIMENSION THETA1(15),NNN(14)
      READ 51,THETA1
   51 FORMAT (15F5.0)
      READ 52,NNN
   52 FORMAT (14I2)
      NN=1
      TH=THETA1(NN)
CCC
C   CALCULATION OF NEW THETA, SEE APPENDIX C
CCC
      CALL ZIVETH(TH,THZ)
      THC=THZ
   53 IF (NN-15) 57,55,55
   57 NN=NN+1
      KK=NN-1
      LL=NNN(KK)
CCC
C   CALCULATION OF H/H AVERAGE
CCC
      IF(NN-9)71,72,72
   72 TH=180.-THETA1(NN)
      GO TO 73
   71 TH=THETA1(NN)
   73 CALL ZIVETH(TH,THZ)
      THC=(THC+THZ)/2.
      IF (NN-9)74,54,54
   74 HSF(LL)=1.34+4.8[illegible]E-03*THC-5.21E-04*(THC**2)+1.58E-05*(THC**3)-2.6[illegible]
     1E-07*(THC**4)+1.91E-09*(THC**5)-4.86E-12*(THC**6)
      GO TO 56
   54 THC=180.-THC
      HSF(LL)=20.21-0.59*THC+5.23E-03*(THC**2)+[illegible].50E-06*(THC**3)-3.85E-0
     17*(THC**4)+2.15E-09*(THC**5)-3.83E-12*(THC**6)
   56 THC=THZ
      GO TO 53
   55 CONTINUE
      PRINT *,HSF
      RETURN
      END


      SUBROUTINE ZIVETH(TH,THZ)
      COMPLEX P,X
      VC=11.3
      AA=10.
      BB=5.
      PI=3.14159
      TH=TH*2.*PI/360.
      RR=(AA*BB)**2/((AA*SIN(TH))**2+(BB*COS(TH))**2)
      AR1=SQRT(RR)*COS(TH)
      AI1=SQRT(RR)*SIN(TH)
      AR2=((AR1)**2 -(AI1)**2-AA*AA+BB*BB)
      AI2=2.*(AR1)*(AI1)
      P=CMPLX(AR2,AI2)
      X=CSQRT(P)
      AR3=REAL(X)
      AI3=AIMAG(X)
      BR2=((AR1)*(AR3)+(AI1)*(AI3))/((AR3)**2+(AI3)**2)
      BI2=((AI1)*(AR3)-(AR1)*(AI3))/((AR3)**2+(AI3)**2)
      VE=VC*SQRT((AA-BB*BR2)**2+(BB*BI2)**2)/(AA-BB)
      PRINT *,VE
      VE1=1.-VE**2/(2.*VC**2)
      IF(VE1-0.)62,61,61
   62 VE1=-VE1
   61 THZ=0.5*ACOS(VE1)
      THZ=THZ*360./(2.*PI)
      RETURN
      END
```

AXISFR FORTRAN LISTING FOR TRAPEZOIDAL PRODUCT --AXISYMMETRICAL FREEZING

```
      PROGRAM AXISFR(INPUT,OUTPUT,PUNCH,TAPE60=INPUT,TAPE61=OUTPUT,TAPE6
     12=PUNCH,TAPE1,TAPE2,TAPE3,TAPE63)
      DIMENSION IS(3),X(3),Y(3),ISIDE(3)
      COMMON/TLE/TITLE(20)
      COMMON AC(351)
      COMMON A(1)
      COMMON/PROF/BI,RI,HS,DW,DI,TD,KI,KW,CPW,TF,IHC,UFHC,DS,KS,MS,CPS,
     &IK,ICP,IPL
      COMMON/VV1/VV(12)
      REAL KXX,KYY,LG
CCC
C   DEFINITION OF THE CONTROL PARAMETERS
C         NP - NUMBER OF GLOBAL TEMPERATURES, NE - NUMBER OF
C         ELEMENTS, NBW - BAND WIDTH, KXX - CONDUCTIVITY IN X DIRECTION,
C         KYY - CONDUCTIVITY IN Y DIRECTION, H - CONVECTION COEFFICIENT,
C         TINF - FLUID TEMPERATURE
C     CRHO=SPECIFIC HEAT*DENSITY
C     DT=TIME STEP     NIT=NO. OF ITERATIONS
C     ITWR=ITERATIONS BEFORE PRINTING
CCC
      IO=61
      NL=1
      IZ=63
      KK=1
CCC
C   INPUT OF THE TITLE CARD AND THE CONTROL PARAMETERS
C   GRAVE = INITIAL TEMPERATURE
CCC
      READ(IZ,3) TITLE
    3 FORMAT(20A4)
      READ(IZ,2) NP,NE,NBW,NIT,INTR,KXX,KYY,H,TINF,DT,CRHO
    2 FORMAT (5I3,6F10.4)
      INTR=10
      REWIND 2
      DO 510 IHO=1,NP
      GRAVE=64.
      WRITE(2,1005) GRAVE
 1005 FORMAT (E17.5)
  510 CONTINUE
CCC
C   CALCULATION OF POINTERS AND INITIALIZATION OF THE COLUMN VECTORAA
CCC
      JTN=NP
      JGF=2*NP
      JGSM=JGF+NP
      JGCM=JGSM+NP*NBW
      JEND=JGCM+NP*NBW
      CALL SETFL(A(JEND))
      DO 13 I=1,JEND
   13 A(I)=0.0
CCC
C   OUTPUT OF TITLE AND DATA HEADINGS
CCC
      WRITE(IO,4) TITLE,KXX,KYY,H,TINF
    4 FORMAT(1H1,///1X,20A4,/1X,5HKXX =,F9.4,10X,5HKYY = ,F9.4,1X,19HCO
     1NVECTION COEFF =,F9.4/1X,12HFLUID TEMP =,F9.4//1X,17HNODE    NODE NU
     2MBER,6X,4HX(1),6X,4HY(1),6X,4HX(2),6X,4HY(2),5X,4HX(3),5X,4HY(
     33)
      WRITE(IO,82) CRHO,DT,NIT,INTR
   82 FORMAT(2X,21HTCRHO                =,F10.5/2X,11HTIME STEP =,F10.5/
     12X,19HNO. OF ITERATIONS =,I4/2X,30HITERATIONS BETWEEN PRINTOFFS =,
     2I4)
CCC
C   INPUT AND ECHO PRINT OF ELEMENT DATA
CCC
      REWIND 1
      DO 77 KK=1,NE
      READ(IZ,1) NEL,NS,X(1),Y(1),X(2),Y(2),X(3),Y(3),ISIDE
    1 FORMAT(4I3,6F10.4,3I2)
      WRITE (1,3002) NEL,NS,X(1),Y(1),X(2),Y(2),X(3),Y(3),ISIDE
 3002 FORMAT (4I3,6F10.4,3I2)
      QCM=0.0
   77 CONTINUE
      CALL READ 1
      READ 41,(VV(II),II=1,12)
   41 FORMAT (12F5.0)
      CALL SETMAT(A,CRHO,KXX,KYY,H,TINF,NP,JGSM,JGCM,DT,NE,AN,NBW,JEND,
     1NEL,NIT,INTR,KK)
      CALL TRANSIT(A(JGSM+1),A(JGCM+1),A(JGF+1),A(JTN+1),A(1),NP,NBW,NEL
     1,DT,NIT,INTR,NH,CRHO,KXX,KYY,H,TINF,JGSM,JGCM,NE,JEND,AC)
      STOP
      END
```

```
      SUBROUTINE SETMAT (A,CRHO,KXX,KYY,H,TINF,NP,JGSM,JGIM,DT,NE,NN,NBW,
     1JEND,NCL,NIT,IWT,KK)
      DIMENSION A(JEND),NS(3),B(3),C(3),ECM(3,3),ESM(3,3),EF(3),ISIDE(3)
      DIMENSION X(3),Y(3)
      DIMENSION TVAL(44)
      DIMENSION TJ(3),CIJ(3),KJ(3),PDJ(3)
      DIMENSION Z(3),P(3)
      DIMENSION EH1(3)
      COMMON/PROP/BI,RI,HS,DW,DI,TS,KI,KW,CPW,TF,IMC,UFWS,DS,KS,MS,CPS,
     &IK,ICP,IPD
      COMMON/VV1/VV(12)
      REAL KXX,KYY,KJ,LG
      CF=0.82
      RHO=56.
      SH1=0.
      SA=0.
      REWIND 2
      DO 510 JEO=1,NP
      READ (2,1005) TVAL (JEO)
 1005 FORMAT (E17.5)
      A(JEO)=TVAL(JEO)
  510 CONTINUE
      REWIND 1
      DO 7 IE=1,NE
      READ(1,1004) NEL,NS(1),NS(2),NS(3),X(1),Y(1),X(2),Y(2),X(3),Y(3),
     1ISIDE(1),ISIDE(2)
 1004 FORMAT (4I3,6F10.4,2X,2I2)
      X(1)=X(1)/30.24
      X(2)=X(2)/30.24
      X(3)=X(3)/30.24
      Y(1)=Y(1)/30.24
      Y(2)=Y(2)/30.24
      Y(3)=Y(3)/30.24
      B(1)=Y(2)-Y(3)
      B(2)=Y(3)-Y(1)
      B(3)=Y(1)-Y(2)
      C(1)=X(3)-X(2)
      C(2)=X(1)-X(3)
      C(3)=X(2)-X(1)
      AR4=(X(2)*Y(3)+X(3)*Y(1)+X(1)*Y(2)-X(2)*Y(1)-X(3)*Y(2)-X(1)*Y(3))
     1*2.
      RBAR=(X(1)+X(2)+X(3))/3.
      AR=RBAR/AR4
      NE1=NS(2)
      NE2=NS(3)
      NE3=NS(1)
      TJ(1)=TVAL(NE1)
      TJ(2)=TVAL(NE2)
      TJ(3)=TVAL(NE3)
CCC
C     CALCULATION OF ELEMENT PROPERTIES
C     AS FUNCTIONS OF TEMPERATURE
CCC
      IF (TJ(1)-32.) 3011,3011,1007
 1007 IF (TJ(2)-32.) 3011,3011,1008
 1008 IF (TJ(3)-32.) 3011,3011,1009
 3011 DO 3001 N=1,3
      T=TJ(N)
      IF (T.GT.32.) GO TO 3002
      CALL PROP1(T,CPA,AK,PD,H1)
      CIJ(N)=CPA
      KJ(N)=AK
      PDJ(N)=PD
      IF (KK-135) 3001,311,311
  311 EH1(N)=H1
      GO TO 3001
 3002 CIJ(N)=CF
      KJ(N)=KXX
      PDJ(N)=RHO
 3001 CONTINUE
C     CONDUCTIVITY AS A FUNCTION OF TEMPERATURE
      KYY=KXX=(KJ(1)+KJ(2)+KJ(3))/3.
      CRHO=(CIJ(1)*PDJ(1)+CIJ(2)*PDJ(2)+CIJ(3)*PDJ(3))/3.
CCC
C     SUMMATION OF AREA ENTHALPY AND TOTAL
C     AREA OF ELEMENT
CCC
      IF (KK-135) 1009,811,811
  811 AH1=(EH1(1)+EH1(2)+EH1(3))/3.
      SH1=SH1+AH1*AR4/4.
      SA=SA+AR4/4.
 1009 CONTINUE
      DO5I=1,3
      DO5J=1,3
      TK=1.
      IF (I.EQ.J) TK=2.
      ECM(I,J)=CRHO*AR4*(TK/2.)*(3.*RBAR+X(I)+X(J))/120.
    5 ESM(I,J)=(KXX*B(I)*B(J)+KYY*C(I)*C(J))*AR
      DO11I=1,3
   11 EF(I)=0.0
```

```
CCC
C   CALCULATION OF THE CONVECTION RELATED QUANTITIES
CCC
       DO10I=1,2
       IF(ISIDE(I).LE.0) GOTO8
       J=ISIDE(I)
       M=J+1
       IF(J.EQ.3) M=1
       LG=SQRT((X(M)-X(J))**2+(Y(M)-Y(J))**2)
       HL=H*LG
       EF(J)=EF(J)+HL*TINF*(2.*X(J)+X(M))/6.
       EF(M)=EF(M)+HL*(TINF/6.)*(X(J)+2.*X(M))
       ESM(J,J)=ESM(J,J)+(3.*X(J)+X(M))*HL/12.
       ESM(J,M)=ESM(J,M)+(X(J)+X(M))*HL/12.
       ESM(M,J)=ESM(J,M)
    10 ESM(M,M)=ESM(M,M)+(X(J)+3.*X(M))*HL/12.
CCC
C   INSERTION OF ELEMENT PROPERTIES INTO THE GLOBAL STIFFNESS MATRIX
CCC
     8 DO 7 I=1,3
       II=NS(I)
       J5=2*NP+II
       A(J5)=A(J5)+EF(I)
       DO17 J=1,3
       JJ=NS(J)
       JJ=JJ-II+1
       IF(JJ) 17,17,16
    16 J5=J5SM+(JJ-1)*NP+II
       J6=J6CM+(JJ-1)*NP+II
CCC
C      AJ5=A MATRIX
C      AJ6=P MATRIX
C      A*T(NEW)=P*T(OLD)-2*F
CCC
       A(J5)=A(J5)+ECM(I,J)+(DT/2.)*ESM(I,J)
       A(J5)=A(J6)+ECM(I,J)-(DT/2.)*ESM(I,J)
    17 CONTINUE
     7 CONTINUE
CCC
C   CALCULATION AND OUTPUT OF AREA
C   AVERAGE ENTHALPY
CCC
       IF (KK-135) 711,712,712
   712 AEH=SH1/SA
       PRINT 4111,AEH
  4111 FORMAT (' ','AREA AVERAGE ENTHALPY',F10.3)
   711 CONTINUE
CCC
C      DCMPBD DECOMPOSES A INTO UPPER TRIANGLE MATRIX
CCC
       CALL DCMPBD(A(J5SM+1),NP,NBW)
       RETURN
       END
```

```
      SUBROUTINE TRANSNT(GCM,GHM,P,TR,XI,NP,NBW,NCL,DT,NIT,INTR,NN,CRHO,
     1KXX,KYY,H,TINF,JGSM,JGCM,NE,JEND,A)
     1H,W)
      COMMON/TLE/TITLE(20)
      COMMON/PROP/BI,RI,HS,DW,DI,TD,KI,KW,CPW,TF,IWC,UFWC,DS,KS,MS,CFS,
     $IK,ICP,LFD
      COMMON/VV1/VV(12)
      DIMENSION GCM(NP,NBW),GHM(NP,NBW),P(NP,1),TR(NP,1)
      DIMENSION A(JEND),BDYPHI(23),IB(23),IPBV(23)
      DIMENSION XV(4,2),ND(4,2)
      DIMENSION XI(NP,1)
      DIMENSION XF(27)
      REAL KXX,KYY
      IL=1
      SDT=0.0
      DO 6001 I=1,NP
      XF(I)=10.
 6001 XI(I,1)=64.
      WRITE(61,6) TITLE
    6 FORMAT(1H1,//,1X,18HTRANSIENT ANALYSIS//1X,20A4)
      WRITE(61,7) SDT,(I,XF(I),I=1,NP)
    7 FORMAT(//1X,6HTIME =,F9.4/(1 X,I3,3X,E17.6,5X,I3,3X,E17.6,5X,I3,3X
     1,E17.6,5X,I3,3X,E17.6))
      LCOUNT=NP/3+4
      DO90 N=1,23
   90 IB(N)=0
      KN=0
CCC
C CALCULATION OF PHI(I+1) FROM PHI(I)
CCC
      DO 13 KK=1,NIT
      IF(KN.EQ.0) GO TO 22
      DO 16 JJ=1,KN
 16   IPBV(JJ)=IB(JJ)
CCC
C SAVING OF PRESCRIBED BOUNDARY VALUES IN BDYPHI
CCC
   22 IF(KN.EQ.0) GOTO15
      DO14I=1,KN
      J=IPBV(I)
   14 BDYPHI(I)=XI(J,1)
   15 CONTINUE
      SDT=SDT+DT
      CALL MULTBL(GHM,XI,TR,NP,NBW,NCL)
      DO9I=1,NP
    9 TR(I,1)=TR(I,1)+DT*P(I,1)
CCC
C DECOMPOSES F AND SOLVES FOR TEMPERATURE
CCC
      CALL SLVBD(GCM,TR,XI,NP,NBW,NCL,ID)
CCC
C RESETTING OF THE PRESCRIBED BOUNDARY VALUES
CCC
      IF(KN.EQ.0) GOTO21
      DO20I=1,KN
      J=IPBV(I)
   20 XI(J,1)=BDYPHI(I)
   21 CONTINUE
CCC
C CALCULATION OF SURFACE PRODUCT TEMPERATURE
C AND INSERTION INTO THE MATRIX
CCC
      CALL TVAR (SDT,XI,NP)
      REWIND 2
      DO 510 IK=1,NP
      WRITE (2,1005) XI(IOK,1)
 1005 FORMAT(E17.5)
  510 CONTINUE
CCC
C OUTPUT OF THE RESULTS
CCC
      IF (((KK/INTR)*INTR).NE.KK) GO TO 6011
      DO 555 I=1,NP
  555 XF(I)=(XI(I,1)-32.)*5./9.
      WRITE (61,7) SDT,(I,XF(I),I=1,NP)
      LCOUNT=LCOUNT+NP/3+3
 6011 CONTINUE
      KLOUNT=3*NP+2*NP*NBW
      DO 501 I=1,KLOUNT
      A(I)=0.0
  501 CONTINUE
CCC
C SET THE NEW ELEMENT MATRICES FOR
C THE NEXT TIME STEP
CCC
      CALL SLTMAI(A,CRHO,KXX,KYY,H,TINF,NP,JGSM,JGCM,DT,NE,NN,NBW,JEND,
     1NCL,NIT,INTR,KK)
      DO 430 IXM=1,NP
      XI(IXM,1)=A(IXM)
      TR(IXM,1)=0.0
      NEKO=IXM+NP*2
      P(IXM,1)=A(NEKO)
  430 CONTINUE
      LC1=3*NP+1
      LC2=3*NP+NBW*NP+1
      DO 431 I5=1,NBW
      DO 432 I6=1,NP
      GHM(I6,I5)=A(LC2)
      GCM(I6,I5)=A(LC1)
      LC2=LC2+1
      LC1=LC1+1
  432 CONTINUE
  431 CONTINUE
   13 CONTINUE
      RETURN
      END
```

```
      SUBROUTINE TVAR (SDT,XI,NP)
      COMMON/VV1/VV(12)
      DIMENSION XI(NP,1),TV(13)
      TV(13)=-20.
      IF (SDT-1.5)4001,4201,4201
4201  IF(SDT-3.5)4301,4401,4401
4301  DO 511 II=1,12
511   TV(II)=-SDT-16.5
      GO TO 4002
4401  DO 611 II=1,12
611   TV(II)=-20.
      GO TO 4002
4001  DO 410 II=1,12
      IF (II-4) 421,422,422
421   TV(II)=2.9*VV(II)*(SDT**2)-1.47*VV(II)*SDT-24.40*SDT+6.61
      GO TO 441
422   IF (II-10) 423,423,424
423   IF (VV(II).GT.11.0)  GO TO 425
      TV(II)=1.76*VV(II)*(SDT**2)-0.36*VV(II)*SDT-26.16*SDT-3.19
      GO TO 441
425   TV(II)=1.51*VV(II)*(SDT**2)-2.76*VV(II)*SDT-0.20*SDT+6.04
      GO TO 441
424   TV(II)=3.95*VV(II)*(SDT**2)-4.96*VV(II)*SDT-5.97*SDT-8.95
441   TVV=-TV(II)
      IF (TVV-20.0)410,410,442
442   TV(II)=-20.0
410   CONTINUE
4002  MM=6
      IMM=1
      DO 431 II=1,NP
      IF (II.GT.3)  GO TO 433
      XI(II,1)=(TV(IMM)*9./5.)+32.
      IMM=IMM+1
      GO TO 431
433   IF (II-25) 434,435,435
434   IF (II.LT.MM)  GO TO 431
      XI(II,1)=(TV(IMM)*9./5.)+32.
      IMM=IMM+1
      MM=MM+3
      GO TO 431
435   XI(II,1)=(TV(IMM)*9./5.)+32.
      IMM=IMM+1
431   CONTINUE
      RETURN
      END
```

```
CCC
C   SUBROUTINES DCMPBD, MULTBD AND SLVBD
C   WERE DEVELOPED BY SEGERLIND, 1976
CCC
      SUBROUTINE DCMPBD(GSM,NP,NBW)
      DIMENSION GSM(NP,NBW)
      IO=61
      NP1=NP-1
      DO226I=1,NP1
      MJ=I+NBW-1
      IF(MJ.GT.NP) MJ=NP
      NJ=I+1
      MK=NBW
      IF((NP-I+1).LT.NBW) MK=NP-I+1
      ND=0
      DO225J=NJ,MJ
      MK=MK-1
      ND=ND+1
      NL=ND+1
      DO225K=1,MK
      NK=ND+K
  225 GSM(J,K)=GSM(J,K)-GSM(I,NL)*GSM(I,NK)/GSM(I,1)
  226 CONTINUE
      RETURN
      END


      SUBROUTINE MULTBD(GSM,GF,RF,NP,NBW,NCL)
      DIMENSION GSM(NP,NBW),GF(NP,NCL),RF(NP,NCL)
      DO278KK=1,NCL
      DO277I=1,NP
      SUM=0.0
      K=I-1
      DO276J=2,NBW
      M=J+I-1
      IF(M.GT.NP) GOTO275
      SUM=SUM+GSM(I,J)*GF(M,KK)
  275 IF(K.LE.0) GOTO276
      SUM=SUM+GSM(K,J)*GF(K,KK)
      K=K-1
  276 CONTINUE
  277 RF(I,KK )=SUM+GSM(I,1)*GF(I,KK)
  278 CONTINUE
      RETURN
      END

      SUBROUTINE SLVBD(GSM,GF,X,NP,NBW,NCL,ID)
      DIMENSION GSM(NP,NBW),GF(NP,NCL),X(NP,NCL)
      COMMON/TLE/TITLE(20)
      IO=61
      NP1=NP-1
      DO265KK=1,NCL
      JM=KK
      DO250I=1,NP1
      MJ=I+NBW-1
      IF(MJ.GT.NP) MJ=NP
      NJ=I+1
      L=1
CCC
C   DECOMPOSITION OF THE COLUMN VECTOR GF( )
CCC
      DO250J=NJ,MJ
      L=L+1
  250 GF(J,KK)=GF(J,KK)-GSM(I,L)*GF(I,KK)/GSM(I,1)
CCC
C   BACKWARD SUBSTITUTION FOR DETERMINATION OF X( )
CCC
      X(NP,KK)=GF(NP,KK)/GSM(NP,1)
      DO252K=1,NP1
      I=NP-K
      MJ=NBW
      IF((I+NBW-1).GT.NP) MJ=NP-I+1
      SUM=0.0
      DO251J=2,MJ
      N=I+J-1
  251 SUM=SUM+GSM(I,J)*X(N,KK)
  252 X(I,KK)=(GF(I,KK)-SUM)/GSM(I,1)
CCC
C   OUTPUT OF THE CALCULATED NODAL VALUES
CCC
      IF(ID.EQ.1) GOTO265
      WRITE(IO,260) TITLE,KK
  260 FORMAT(1H1///1X,20A4//1X,26HNODAL VALUES, LOADING CASE,I2)
      WRITE(IO,264) (I,X(I,KK),I=1,NP)
  264 FORMAT(1X,I3,E14.5,3X,I3,E14.5,3X,I3,E14.5,3X,I3,E14.5,3X,I3,E14.5
     1)
  265 CONTINUE
      RETURN
      END
```

```
CCC
C   SUBROUTINES READ1, PROP1 AND ALL OTHER SUBROUTINES
C   RELATED TO THEM WERE DEVELOPED BY HELDMAN AND GORBY, 1974
CCC
      SUBROUTINE READ1
      COMMON/PROP/BI,RI,HS,DW,DI,TO,KI,KW,CPW,TF,IWC,UFWC,DS,KS,MS,CPS,
     $IK,ICP,IPD
      REAL IWC,IPD,ICP,MS,KI,KW,KS,IK
CCC
C   READ    B,RI,HS,DW,DI,TO,KI,KW,CPW
CCC
      BI=460. $ RI=1.987 $ HS=144. $ DW=62.4 $ DI=57.2
      TO=32. $ KI=1.34 $ KW=.32 $ CPW=1.
      PRINT 1000,BI,RI,HS,DW,DI,TO,KI,KW,CPW
      READ 2000,TF,IWC,UFWC,IPD,ICP,IK
      PRINT 1001,TF,IWC,UFWC,IPD,ICP,IK
      CALL PARAM1
 1000 FORMAT(*1*,*THE RANDOM MODEL FOR THERMAL CONDUCTIVITY HAS BEEN *
     1   *SPECIFIED*/*0*,*THE FOLLOWING PHYSICAL CONSTANTS HAVE BEEN *
     2  *READ IN*,*0*,*CONVERSION TO DEGREES ABSOLUTE = *,E12.5/
     3  *0*,*GAS CONSTANT = *,E12.5/
     4  *0*,*HEAT OF FUSION FOR WATER = *,E12.5/
     5  *0*,*DENSITY OF WATER = *,E12.5/
     6  *0*,*DENSITY OF ICE = *,E12.5/
     7  *0*,*FREEZING POINT FOR PURE WATER = *,E12.5/
     8  *0*,*THERMAL CONDUCTIVITY OF ICE = *,E12.5/
     9  *0*,*THERMAL CONDUCTIVITY OF WATER = *,E12.5/
     1  *0*,*SPECIFIC HEAT OF WATER = *,E12.5///)
 1001 FORMAT(*0*,*THE FOLLOWING PRODUCT DATA HAS BEEN READ IN*/
     1  *0*,*FREEZING POINT OF PRODUCT = *,E12.5/
     2  *0*,*INITIAL WATER CONTENT = *,E12.5/
     3  *0*,*UNFREEZABLE WATER CONTENT = *,E12.5/
     4  *0*,*INITIAL PRODUCT DENSITY = *,E12.5/
     5  *0*,*INITIAL SPECIFIC HEAT OF PRODUCT = *,E12.5/
     6  *0*,*INITIAL THERMAL CONDUCTIVITY OF PRODUCT = *,E12.5///)
 2000 FORMAT(6F10.0)
      RETURN
      END

      SUBROUTINE PROP1 (T,CPA,K,PD,H1)
CCC
      THIS SUBROUTINE CALCULATES PROPERTY VALUES AT A GIVEN TEMPERATURE
CCC
      COMMON/PROF/BI,RI,HS,DW,DI,TO,KI,KW,CPW,TF,IWC,UFWC,DS,KS,MS,CPS,
     $IK,ICP,IPD
      REAL MS,KS,IWC,K,KW,KI,KC,MI
      IF(T.LE.TF) GO TO 1
      MI=0.0
      WC=IWC
      CALL DENSE(IWC,DW,MI,DI,IWC,DS,PD)
      CALL VOLD(PD,IWC,DS,MI,DI,VFS,VFI,VFW)
      CALL THREED(VFS,KS,KW,K)
      CPA=IWC*CPW+(1.0-IWC)*CPS
      GO TO 2
    1 CALL DEPREL(RI,BI,HS,TO,MS,UFWC,IWC,T,WC,MI)
      CALL DENSE(WC,DW,MI,DI,IWC,DS,PD)
      CALL VOLD(PD,IWC,DS,MI,DI,VFS,VFI,VFW)
      VFC=VFI/(VFI+VFW)
      CALL THREED(VFC,KI,KW,KC)
      CALL THREED(VFS,KS,KC,K)
      CALL ENTHAL(CPS,CPW,HS,IWC,MI,WC,UFWC,T,H1)
      T2=T-.005
      CALL DEPREL(RI,BI,HS,TO,MS,UFWC,IWC,T2,WC,MI)
      CALL ENTHAL(CPS,CPW,HS,IWC,MI,WC,UFWC,T2,H2)
      CPA=(H1-H2)/0.005
    2 CONTINUE
      RETURN
      END

      SUBROUTINE PARAM1
      COMMON/PROF/BI,RI,HS,DW,DI,TO,KI,KW,CPW,TF,IWC,UFWC,DS,KS,MS,CPS,
     $IK,ICP,IPD
      REAL IK,ICP,IPD,IWC,KS,CPW,KW,MS,MI
      MI=0.0
      CALL DENSOL(IPD,IWC,DW,DS)
      CALL VOLD(IPD,IWC,DS,MI,DI,VFS,VFI,VFW)
      CALL CON1(VFS,KW,IK,KS)
      CALL AMW(RI,BI,HS,IWC,UFWC,TO,TF,MS)
      EMS=1.0-IWC
      CPS=(ICP-IWC*CPW)/EMS
      PRINT 1000,DS,KS,MS,CPS
 1000 FORMAT(*0*,*THE FOLLOWING PARAMETERS HAVE BEEN CALCULATED*
     1  /*0*,*THE RANDOM MODEL FOR THERMAL CONDUCTIVITY HAS BEEN *
     2   *SPECIFIED*/*0*,*DENSITY OF SOLIDS = *,E12.5/*0*,
     3   *THERMAL CONDUCTIVITY OF SOLIDS = *,E12.5/
     4   *0*, *APPARENT MOLECULAR WEIGHT OF SOLUTE = *,E12.5.
     5   *0*,*SPECIFIC HEAT OF SOLIDS = *,E12.5///)
      RETURN
      END
```

```
      SUBROUTINE DENSOL(IPD,IWC,DW,DS)
      REAL IPD,IWC
      DS=1.0/((1.0/IPD-IWC/DW)/(1.0-IWC))
      RETURN
      END

      SUBROUTINE VOID(PD,IWC,DS,MI,DI,VFS,VFI,VFW)
      REAL MI,IWC
      EMS=1.0-IWC
      VFS=EMS*PD/DS
      VFI=MI*PD/DI
      VFW=1.0-(VFI+VFS)
      RETURN
      END

      SUBROUTINE CON1(VF,KC,IK,KS)
      REAL IK,KS,KC,M,MSQ
      ROOT1=2.0/3.0
      ROOT2=1.0/3.0
      MSQ=VF**ROOT1
      M=VF**ROOT2
      Q=(KC-IK)/(IK*M+KC-IK)
      KS=(MSQ-Q)*KC/MSQ
      IF (KS.LLE.0.2) KS=0.2
      RETURN
      END

      SUBROUTINE AMW(RI,BI,MS,IWC,UFWC,TO,TF,MS)
      REAL IWC,MS,MW
      MW=18.01534
      XS=EXP(HS*MW/RI*(1./(TO+BI)-1./(TF+BI)))
      EMW=IWC-UFWC
      EMS=1.0-IWC
      MS=XS*MW*EMS/(EMW*(1.0-XS))
      RETURN
      END

      SUBROUTINE THREED(VF,KD,KC,K)
      REAL M,KD,KC,K,MSQ
      ROOT1=2.0/3.0
      ROOT2=1.0/3.0
      MSQ=VF**ROOT1
      M=VF**ROOT2
      Q=MSQ*(1.0-KD/KC)
       K =  KC*(1.-Q)/(1.-Q*(1.-M))
      RETURN
      END

      SUBROUTINE DENSE(WC,DW,MI,DI,IWC,DS,PD)
      REAL MI,IWC
      EMS=1.0-IWC
      PD=1.0/(WC/DW+MI/DI+EMS/DS)
      RETURN
      END

      SUBROUTINE ENTHAL(CPS,CPW,HS,IWC,MI,WC,UFWC,T,H)
      REAL IWC,MI
      EMS=1.0-IWC
      A=.4662E103
      B=.00000713
      CPI=A+B*T
      H=EMS*CPS*(T+40.0)+WC*(HS+CPW*(T+40.0))+MI*CPI*(T+40.0)-UFWC*HS
      RETURN
      END

      SUBROUTINE DEPRESS(RI,BI,HS,TO,MS,UFWC,IWC,T,WC,MI)
      REAL MS,IWC,MI,MW
      MW=18.01534
      XS=EXP(HS*MW/RI*(1./(TO+BI)-1./(T+BI)))
      EMS=1.0-IWC
      EMW=MW*XS*EMS/(MS*(1.0-XS))
      WC=EMW+UFWC
      IF (WC.GT.IWC) WC=IWC
      MI=1.0-(WC+EMS)
      RETURN
      END
```

APPENDIX B

PHYSICAL PROPERTIES OF GROUND BEEF, COMPUTER INPUT PARAMETERS AND VARIABLES, AND EXPERIMENTAL DATA

TABLE B.1.--Moisture Content and Density of Ground Beef at Various Experimental Treatments[a]

Treatment	Air Velocity m/s	Air Tempera-ture, °C	Moisture Content, %	Meat Weight, g		Density[b] g/cm^3	
				Unfrozen	Frozen	Unfrozen	Frozen
Elliptical							
EV1	7.4	-20.0 ± 2.0	70.30	2963.5	2853.4	1.048	1.008
EV2	11.3	-20.0 ± 2.0	69.55	2865.2	2782.1	1.014	0.984
EV3	15.2	-20.0 ± 1.5	69.28	3008.9	2925.7	1.064	1.030
Trapezoidal							
TV1	7.4	-20.0 ± 1.5	70.71	1179.7	1160.5	1.074	1.057
TV2	11.3	-20.0 ± 1.0	69.09	1172.5	1152.9	1.067	1.050
TV3	15.2	-20.0 ± 0.8	70.90	1198.3	1186.9	1.092	1.081

[a]Average from three replications per each treatment.

[b]Density was obtained from weight divided by volume.

Volume of elliptical model $= 1/2\ (\pi a.b.l)$
$= 2827.43\ cm^3$

Volume of trapezoidal model $= 1/6\ (\pi h(a^2+ab+b^2))$
$= 1097.59\ cm^3$

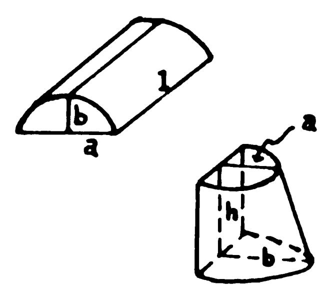

TABLE B.2.--Physical Properties of Ground Beef

Thermal Conductivity,[a] W/m K	Specific Heat[b] J/Kg K	Density,[b] kg/m^3	Initial Freezing Point,[a] °C
0.4	3430	1060	-1.5

[a]Values obtained from literature for mince meat (Sörenfors, 1974).

[b]Values determined by experiment.

TABLE B.3.--Input Parameters for Computer Program

1.	Product Properties (ground beef)	Parameters	IWC[a] UFWC = 0.01 IPD = 1060 kg/m^3 ICP = 3430 J/kg K IK = 0.4 W/m K TIF = -1.5°C
2.	Physical Properties of Ice, Water, and Gas	Parameters	DI = 920 kg/m^3 DW = 1000 kg/m^3 KPI = 2.32 W/m K KPW = 0.55 W/m K LW = 335.10^3 J/kg CPW = 4180 J/kg k T_{WF} = 0°C R_1 = 8314 J/kg-mole K
3.	Freezing Medium Properties	Variables	v, m/s — $\bar{h}$, W/m^2K 7.4 — 61.7 11.3 — 70.6 15.2 — 142.5 T = -14°C, -18°C, -22°C
4.	Finite Element Properties	Parameters[b]	NP:number of nodal temperature NE:number of element NBW:number of bandwith NIT:number of iterations
		Variable	DT:time step = 1 minute and 3 minutes

[a]See Table B.1.

[b]Supplied by the GRID program.

TABLE B.4.--Recorded Temperature Data (°C) at One-Hour Time Increments During Freezing Process[a]

Product Geometry	Treatment v, m/s	Nodal Number[b]	Time, Hr[c]																	
			1		2		3		4		5		6		7		8		9	
Elliptical	7.4	3	16.1	1.7	7.8	2.2	0.3	2.5	- 1.2	2.7	- 4.0	3.1	-11.5	1.8	-16.3	0.6	-19.7	0.1	-19.8	0.0
		18	3.6	2.2	- 2.0	2.4	- 7.2	2.5	-11.5	2.5	-14.8	1.7	-16.0	0.2	-19.2	0.0	-19.6	0.0	-19.9	0.0
		23	-15.0	2.6	-17.4	1.6	-18.3	0.1	-19.0	0.0	-19.3	0.0	-19.5	0.0	-19.7	0.0	-19.9	0.0	-20.0	0.0
	11.3	3	13.8	2.4	4.0	2.4	- 0.8	2.5	- 1.5	3.1	-10.0	2.7	-13.6	2.0	-16.8	1.1	-19.9	0.1		
		18	2.0	2.5	- 5.4	2.4	- 9.2	1.9	-12.1	2.0	-15.3	0.8	-18.5	0.2	-19.6	0.0	-19.9	0.0		
		23	-13.4	2.1	-17.9	2.0	-19.1	2.5	-19.6	0.3	-19.8	0.0	-19.9	0.0	-19.9	0.0	-20.0	0.0		
	15.2	3	13.6	1.0	3.9	1.5	- 1.3	2.1	- 2.4	3.1	- 9.1	2.6	-15.5	1.6	-18.7	0.0	-19.8	0.0		
		18	1.5	2.5	- 5.3	2.5	-10.0	2.4	-13.7	2.6	-17.6	0.6	-18.7	0.0	-19.2	0.0	-19.8	0.0		
		23	-16.0	2.6	-17.5	2.4	-18.9	1.2	-19.2	0.5	-19.6	0.0	-19.8	0.0	-19.9	0.0	-19.9	0.0		
Trapezoidal	7.4	4	14.2	1.6	1.8	2.4	- 1.0	2.8	-14.0	1.5	-18.9	0.1	-19.8	0.0						
		19	- 2.8	1.6	-11.4	1.8	-15.8	1.2	-18.9	0.8	-19.9	0.0	-20.0	0.0						
		15	-19.2	1.4	-19.9	0.7	-20.0	0.0	-20.0	0.0	-20.0	0.0	-20.0	0.0						
	11.3	4	13.9	1.5	2.0	2.4	- 1.1	3.0	-14.2	1.3	-19.9	0.0								
		19	- 0.8	1.6	- 9.4	2.7	-15.7	1.3	-19.0	1.1	-20.0	0.0								
		15	-18.6	1.2	-19.8	0.5	-20.0	0.0	-20.0	0.0	-20.0	0.0								
	15.2	4	13.5	2.1	1.2	2.5	- 1.5	3.1	-14.6	1.2	-20.0	0.0								
		14	- 1.3	2.3	-11.5	1.6	-16.9	1.6	-18.9	0.9	-20.0	0.0								
		15	-19.8	0.8	-20.0	0.0	-20.0	0.0	-20.0	0.0	-20.0	0.0								
			M	S	M	S	M	S	M	S	M	S	M	S	M	S	M	S	M	S

[a]Average from three replications per each treatment.

[b]Refer to Figure 4.3 for elliptical and Figure 4.5 for trapezoidal.

[c]Initial product temperature 18°C.

[d]M: Average value of temperature; S: Standard Deviation (°).

APPENDIX C

THE TRANSFORMATION OF LOCAL SURFACE HEAT TRANSFER COEFFICIENT FROM THE CIRCULAR CYLINDER TO THE ELLIPTICAL CYLINDER

APPENDIX C

THE TRANSFORMATION OF LOCAL SURFACE HEAT TRANSFER COEFFICIENT FROM THE CIRCULAR CYLINDER TO THE ELLIPTICAL CYLINDER

The local surface heat transfer coefficient was shown to be a function of location as investigated by Katinas et al. (1976) and Zdanavichyus et al. (1977) on a circular cylinder and by Chavarria (1978) on a flat plate. The computer simulation used to predict the freezing rate of a food product with elliptical geometry in this research incorporated the varying surface heat transfer coefficient. Since there has been no publication of variations in local surface heat transfer coefficient for an elliptical cylinder, the transformation from Zdanavichyus' data for a circular cylinder to an elliptical cylinder was obtained by implementing conformal mapping to the air flow around the obstacle geometries (Spiegel, 1964).

The relationship between the ratio of local heat transfer coefficient to average heat transfer coefficient, $h/\overline{h}$, and angle θ for an air flow with $Re = 1.1 \times 10^5$ is illustrated in Figure C.3 (Zdanavichyus et al., 1976). Using these data, mathematical equations were computed by least square method for n-order regression utilizing a Wang 2200 computer.

$0° \leq \theta \leq 90°$

$$\begin{aligned} h/\bar{h} &= 1.129 - 1.148\text{x}10^{-2}\ \theta + 1.589\text{x}10^{-3}\ \theta^2 \\ &\quad - 8.861\text{x}10^{-5}\ \theta^3 + 2.222\text{x}10^{-6}\ \theta^4 \\ &\quad - 2.572\text{x}10^{-8}\ \theta^5 + 1.098\text{x}10^{-10}\ \theta^6 \end{aligned} \tag{C.1}$$

$90° < \theta \leq 180°$

$$\begin{aligned} h/\bar{h} &= -47.42 + 1.48\ \theta - 1.523\text{x}10^{-2}\ \theta^2 \\ &\quad + 3.441\text{x}10^{-5}\ \theta^3 + 4.13\text{x}10^{-7}\ \theta^4 \\ &\quad - 2.838\text{x}10^{-9}\ \theta^5 + 5.226\text{x}10^{-12}\ \theta^6 \end{aligned} \tag{C.2}$$

The coefficient of correlations were 0.992 and 0.999 respectively for equations (C.1) and (C.2), and the standard error of estimate were $3.14\text{x}10^{-2}$ and $8.662\text{x}10^{-3}$.

The magnitude of complex velocity of the circular surface which is placed as an obstacle in an air flow (Figure C.1) is a function of θ and laminar velocity V_o (Spiegel, 1964)

$$V_c = V_o \sqrt{2 - 2 \cos \theta} \tag{C.3}$$

Thus, θ in equations (C.1) and (C.2) can be replaced as a function of V_c and V_o by modification of equation (C.3)

$$\theta = 0.5 \text{ arc cos } (1 - V_c^2/2V_o^2) \tag{C.4}$$

The complex potential of fluid flow for an elliptic obstacle (Figure C.2) using conformal mapping by solving Dirichlet's problem was given as follows (Spiegel, 1964)

$$\Omega(z) = V_o \, [\zeta + (a + b)^2/4\zeta]$$

where

$$\zeta = 0.5 \, (z + \sqrt{z^2 - a^2 + b^2}) \qquad (C.5)$$

By algebraic manipulation, equation (C.5) can be rewritten into

$$\Omega(z) = \frac{V_o}{(a - b)} \, (az - b \sqrt{z^2 - a^2 + b^2}) \qquad (C.6)$$

The complex velocity is a derivative of $\overline{\Omega}(z)$

$$v = d\overline{\Omega}(z)/dz = \overline{\Omega}'(z) \qquad (C.7)$$

Taking the derivative of equation (C.6)

$$\Omega'(z) = \frac{V_o}{(a - b)} \, [a - (bz/\sqrt{z^2 - a^2 + b^2})] \qquad (C.8)$$

Let $z = r\,e^{i\theta}$, or expressed in trigonometric function as $z = r \cos \theta + r\,i \sin \theta$, where r is the distance of a given point on the stream line to the center of the ellips and θ is the slope. For the point on the surface of the ellips, r becomes

$$r = \sqrt{a^2b^2/(a^2 \sin^2\theta + b^2 \cos^2\theta)} \tag{C.9}$$

Then, the complex expression in equation (C.8) can be solved as

$$\frac{z}{\sqrt{z^2 - a^2 + b^2}} = X + Yi \tag{C.10}$$

By substituting equation (C.10) back into equation (C.8), it can be further formulated as follows

$$\Omega'(a) = \frac{(a - bX)\ V_o}{(a - b)} - i\ \frac{bY\ V_o}{(a - b)} \tag{C.11}$$

Thus, the complex velocity is

$$v = \overline{\Omega}'(z) = \frac{(a - bX)\ V_o}{(a - b)} + i\ \frac{bY\ V_o}{(a - b)} \tag{C.12}$$

And the magnitude of the velocity on the elliptical surface is

$$V_e = \frac{V_o}{(a-b)} \sqrt{(a - bX)^2 + b^2Y^2} \tag{C.13}$$

Replacing V_c in equation (C.4) by V_e and substituting θ back into equations (C.1) and (C.2) will provide a new value of $h/\overline{h}$ for a given location on the elliptical surface. The calculation was carried out in subroutine HVAR which was incorporated into the main program. The result of subroutine HVAR was presented in Figure C.3.

Zdanavichyus' data was obtained for a degree of stream turbulence Tu = 1.2%. It showed a lower heat transfer coefficient at the upstream compared to downstream. This contradicted the experimental results which indicated higher heat transfer coefficient at the upstream. Katinas et al. (1976) investigated the effect of degree of turbulence on the surface heat transfer coefficient for circular cylinder, and found out that higher coefficient occurred at the upstream when the degree of turbulence Tu = 7.8%. Using Katinas' data, equations (C.1) and (C.2) were modified into

$0° \leq \theta \leq 90°$

$$\begin{aligned} h/\bar{h} = {} & 1.34 + 4.84 \times 10^{-3}\ \theta - 5.21 \times 10^{-4}\ \theta^2 \\ & + 1.58 \times 10^{-5} \times \theta^3 - 2.60 \times 10^{-7}\ \theta^4 \\ & + 1.91 \times 10^{-9}\ \theta^5 - 4.86 \times 10^{-12}\ \theta^6 \end{aligned} \tag{C.14}$$

$90° \leq \theta \leq 180°$

$$\begin{aligned} h/\bar{h} = {} & 20.21 - 0.59\ \theta + 5.23 \times 10^{-3}\ \theta^2 \\ & + 8.60 \times 10^{-6}\ \theta^3 - 3.89 \times 10^{-7}\ \theta^4 \\ & + 2.15 \times 10^{-9}\ \theta^5 - 3.83 \times 10^{-12}\ \theta^6 \end{aligned} \tag{C.15}$$

The computed values for elliptical cylinder using Katinas' data by subroutine HVAR were also presented in Figure C.3. The latter result was used for further investigation in this study.

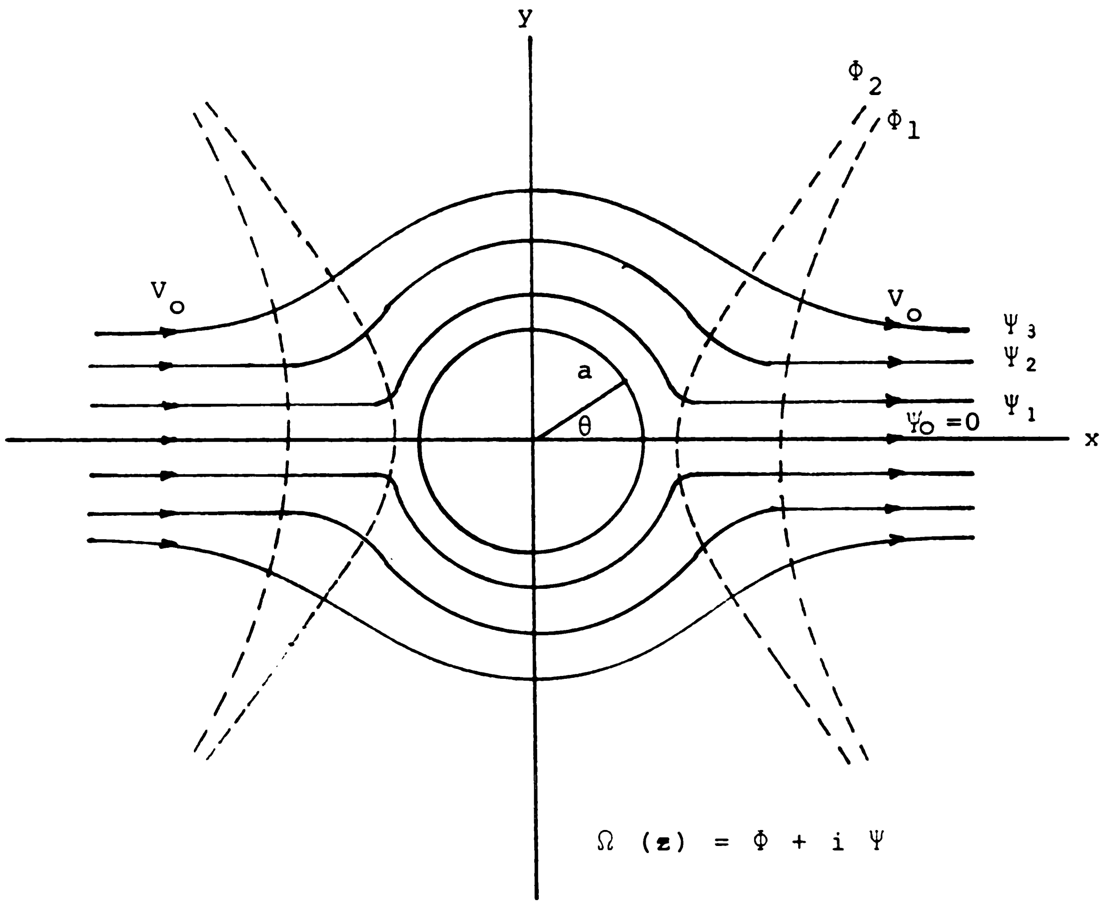

Figure C.1. The air flow pattern around a circular obstacle.

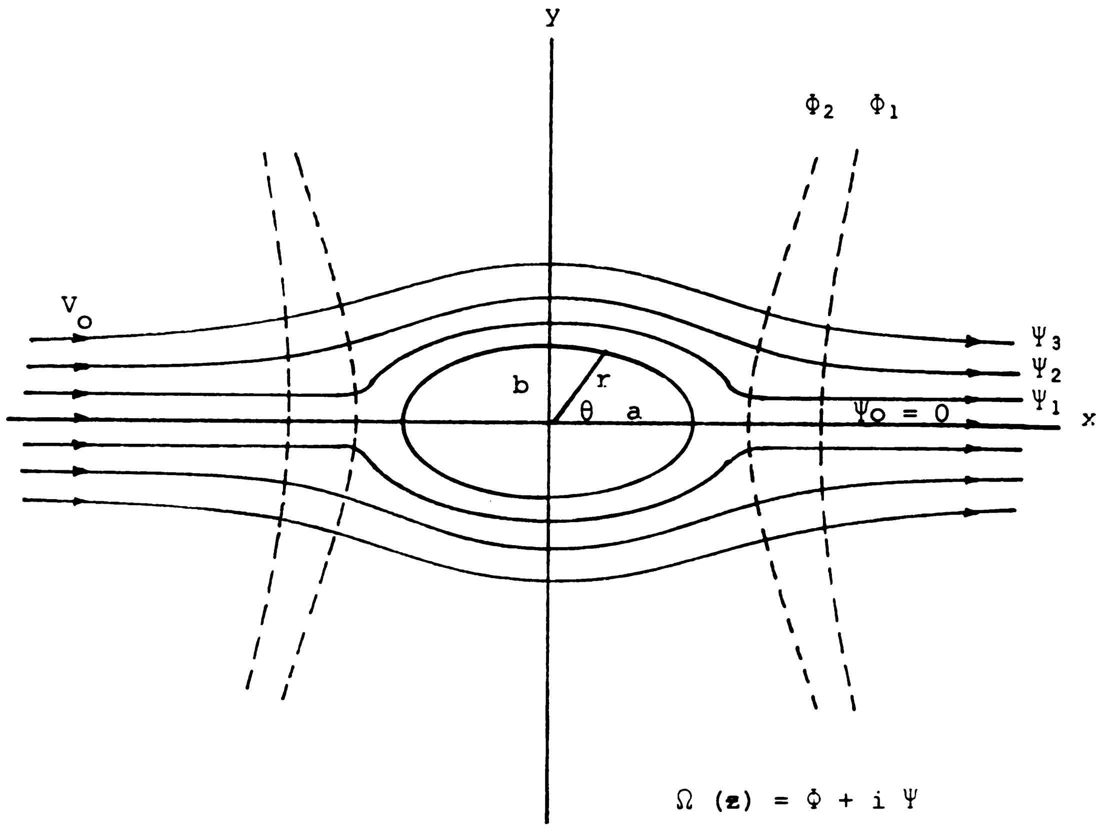

Figure C.2. The air flow pattern around an elliptical obstacle.

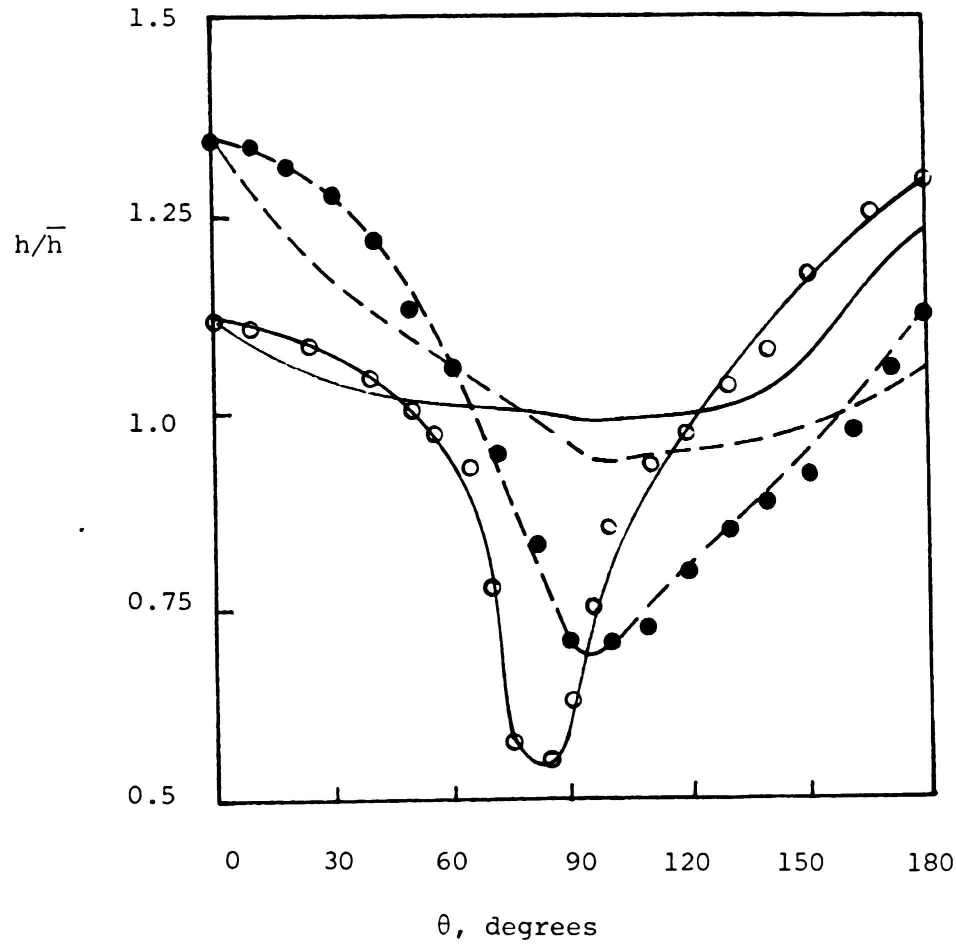

Katinas' data for circular cylinder
Zdanavichyus' data for a circule surface

——— Transformation result using conformal mapping for an elliptical surface
----- Transformation result from Katinas' data

Figure C.3. Local surface heat transfer coefficient for circular cylinder and elliptical cylinder.

APPENDIX D

THE DATA FITTING OF LOCAL SURFACE TEMPERATURE AT TRAPEZOIDAL PRODUCT GEOMETRY USING LEAST SQUARE REGRESSION

APPENDIX D

THE DATA FITTING OF LOCAL SURFACE TEMPERATURE AT TRAPEZOIDAL PRODUCT GEOMETRY USING LEATS SQUARE REGRESSION

Since the local surface heat transfer coefficient for trapezoidal geometry cannot be solved with conformal mapping as in the elliptical case, another method was applied to describe the influence of surface heat transfer coefficient. Surface temperature of the trapezoidal product was measured during freezing at nodal locations illustrated in Figure D.1. for every time step. Mathematical model to describe the local surface temperature as a function of location, x, and time, t, was as follows

$$T = A\, x\, t^2 + B\, x\, t + C\, t + D \qquad (D.1)$$

The mathematical model was applied to all sides of trapezoidal product except the bottom side which was insulated (Figure D.1). Two different equations were used to describe the local surface temperature on side 2, one was for 0 cm $\leq$ x $\leq$ 11 cm and the other for 11 cm $\leq$ x $\leq$ 15.5 cm.

Figure D.1 shows the temperature curves as functions of x at t = 0.5 hours and 1.0 hour for all three sides of the trapezoid at v = 7.9 m/s. The temperature data were substituted into the model at various x and t applying the least square method. The result of mathematical model for each side was presented at Table D.1. These polynomial functions were supplied to subroutine TVAR which computed the temperature at each time step and substituted back to subroutine SETMAT as surface temperature.

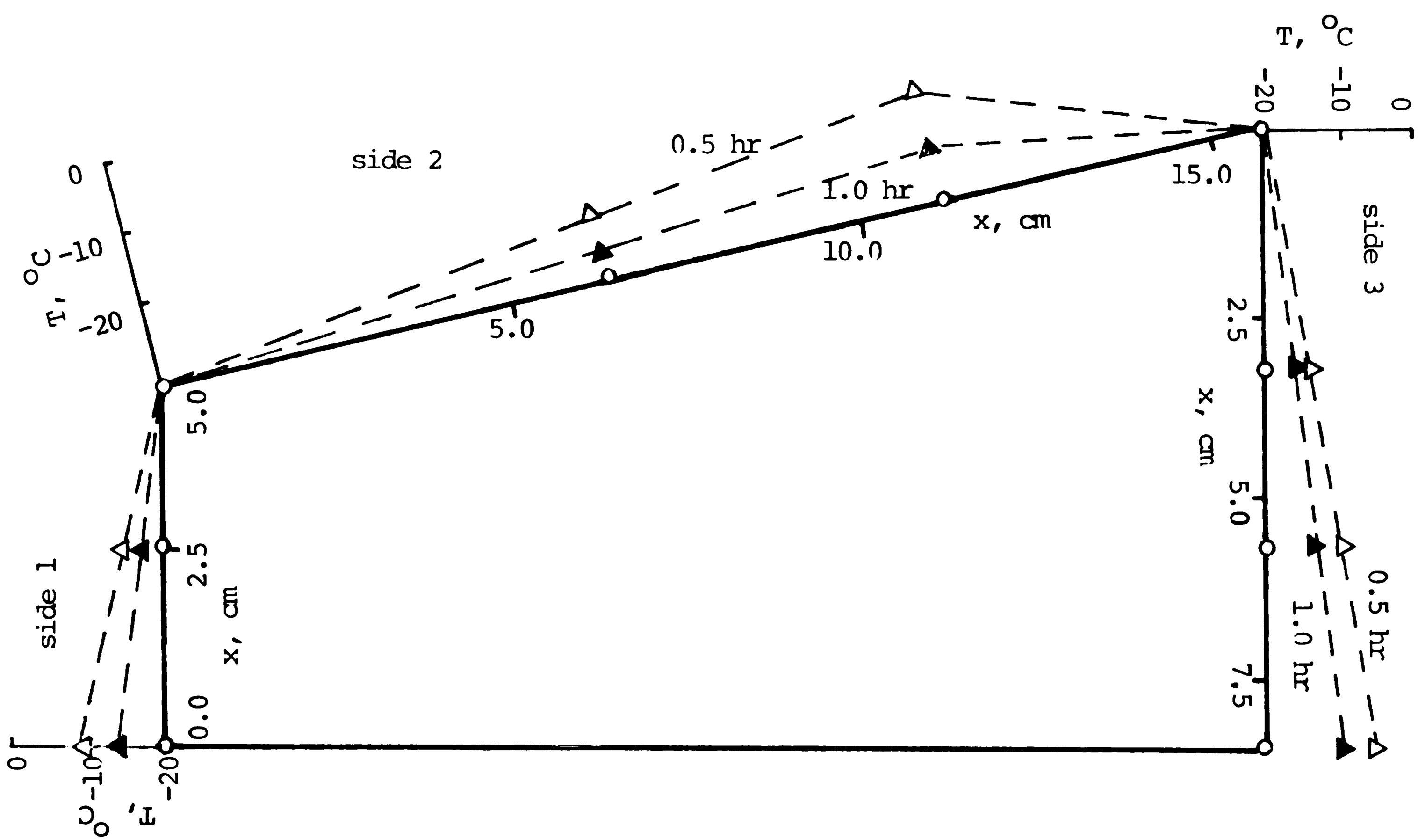

Figure D.1. The surface temperature on trapezoidal ground beef during air-blast freezing at v = 7.9 m/s.

TABLE D.1.--Mathematical Models Describing Surface Temperature as a Function of Time and Location at $v = 7.9$ m/s

Time, hr	x, cm	Temperature, °C
$t = 0$	For all sides and x	$T = 18$
$t > 0$	For nodal 15	$T_{15} = -20$
$0 < t < 1.5$	Side 1	$T = 3.95 \times t^2 - 4.98 \times t - 5.97t - 8.95$
	Side 2: $0 < x < 11$	$T = 1.76 \times t^2 - 0.38 \times t - 26.16t - 3.19$
	$11 < x < 15.5$	$T = 1.51 \times t^2 - 2.76 \times t + 0.20t + 0.04$
	Side 3	$T = 2.90 \times t^2 - 1.47 \times t - 24.4t + 0.61$
$t > 1.5$	For all sides and x	$T = -t - 16.5$
$t \geq 3.5$	For all sides and x	$T = -20$

BIBLIOGRAPHY

BIBLIOGRAPHY

AOAC. 1965. Official Methods of Analysis of the Association of Official Agricultural Chemists. Tenth Edition. Assoc. Offic. Chem., Washington, D.C.

Bakal, A. and K. Hayakawa. 1973. Heat transfer during freezing and thawing of foods. Advances in Food Res. 20: 217.

Bonacina, C. and G. Comini. 1973a. On a numerical method for the solution of the unsteady state heat conduction equation with temperature dependent parameters. Proceedings of the XIII Int. Congress of Refr. 2: 329.

Bonacina, C. and G. Comini. 1973b. On the solution of the non-linear heat conduction equations by numerical methods. Int. J. Heat Mass Transfer 16: 581.

Bonacina, C., G. Comini, A. Fasano, and M. Primicerio. 1973. Numerical solution of phase change problems. Int. J. Heat Mass Transfer, 16: 1825.

Bonacina, C., G. Comini, A. Fasano, and M. Primicerio. 1974. On the estimation of thermophysical properties in non-linear heat-conduction problems. Int. J. Heat Mass Transfer, 17: 861.

Bonnerot, R. and P. Jamet. 1974. A second order finite element method for the one-dimensional Stefan problem. Int. J. Numerical Methods in Engr., 8: 811.

Bruch Jr., J. C. and G. Zyvoloski. 1974. Transient two-dimensional heat conduction problems solved by the finite element method. Int. J. Numerical Methods in Engr., 8: 481.

Carslaw, H. S. and J. C. Jaeger. 1959. Conduction of Heat in Solids. Claredon Press, Oxford, England.

Charm, S. E. 1971. The Fundamentals of Food Engineering. 2nd edition. The AVI Pub. Co., Inc., Westport, CT.

Charm, S. E., D. H. Brand, and D. W. Baker. 1972. A simple method for estimating freezing and thawing times of cylinders and slabs. ASHRAE J. 14 (11): 39.

Charm, S. E. and J. Slavin. 1962. A method for calculating freezing time of rectangular packages of food. Int. Institute of Refr. Meeting Commissions 2, 3, 4, and 6A, Washington, D.C. Bulletin, Annexe: 567.

Chavarria, V. M. 1978. Experimental determination of the surface heat transfer coefficient under food freezing conditions. M.S. Thesis. Department of Agricultural Engineering. Michigan State University, East Lansing, MI.

Cho, S. H. and J. E. Sunderland. 1974. Phase change problems with temperature-dependent thermal conductivity. J. Heat Transfer 95: 214.

Cleland, A. C. and R. L. Earle. 1977a. A comparison of analytical and numerical methods of predicting the freezing times of foods. J. Food Science, 42: 1390.

Cleland, A. C. and R. L. Earle. 1977b. The third kind of boundary condition in numerical freezing calculations. Int. J. Heat Mass Transfer, 20: 1029.

Comini, G. and C. Bonacina. 1974. Application of computer codes to phase-change problems in food engineering. Int. Institute of Refr. Meeting of Commissions B1, C1, and C2, Bressanone, Italy. Bulletin, Annexe: 15.

Comini, G., C. Bonacina and S. Barina. 1974. Thermal properties of foodstuffs. Int. Institute of Refr. Meeting of Commissions B1, C1, and C2. Bressanone, Italy. Bulletin Annexe: 163.

Comini, G. and R. W. Lewis. 1976. A numerical solution of two-dimensional problems involving heat and mass transfer. Int. J. Heat Mass Transfer, 19: 1387.

Comini, G., S. Del Giudice, M. Strada and L. Rebellato. 1978. The finite element method in refrigeration engineering. Int. J. Refr., 1: 113.

De Baerdemaeker, J., R. P. Singh, and L. J. Segerlind. 1977. Modelling heat transfer in foods using the finite element method. J. Food Process Engr., 1: 37.

Desai, C. S. and J. F. Abel. 1972. Introduction to the Finite Element Method. Van Nostrand, Reinhold, New York, N.Y.

Dickerson Jr., R. W. 1969. Thermal properties of food. In: D. K. Tressler. 1969. The Freezing Preservation of Foods. 4th ed. Vol. II. The AVI Pub. Co., Inc., Westport, Ct.

Emery, A. F. and W. W. Carson. 1971. An evaluation of the use of the finite element method in the computation of temperature. J. Heat Transfer, 92: 136.

Fleming, A. K. 1973. The numerical calculation of freezing processes. Proceedings of the XIII Int. Congress of Refr., 2: 303.

Golovkin, N. A., R. G. Geinz, G. V. Maslova, and I. R. Nozdrunkova. 1973. Studies on meat subfreezing process and its application for cold storage of animal products. Proceedings of the XIII Int. Congress of Refr., 4: 221.

Goodrich, L. E. 1978. Efficient numerical technique for one-dimensional thermal problems with phase change. Int. J. Heat Mass Transfer, 21: 615.

Hayakawa, K. and A. Bakal. 1974. Formulas for predicting transient temperatures in food during freezing or thawing. AICHE Symposium Series, 69 (132): 14.

Hashemi, H. T. and C. M. Sliepcevich. 1967. A numerical method for solving two-dimensional problems of heat conduction with change of phase. AICHE Symposium Series, 63 (79): 34.

Heldman, D. R. 1974a. Predicting the relationship between unfrozen water fraction and temperature during food freezing using freezing point depression. Trans. ASAE, 17: 63.

Heldman, D. R. 1974b. Computer simulation of food freezing processes. Proceedings of the VI Int. Congress of Food Science and Technology, IV: 397.

Heldman, D. R. 1975. Food Process Engineering. The AVI Pub. Co., Inc., Westport, CT.

Heldman, D. R. and D. P. Gorby. 1974a. Predictions of thermal conductivity in frozen food. ASAE Paper No. 74-6017.

Heldman, D. R. and D. P. Gorby. 1974b. Computer simulation of ice cream freezing. Int. Institute of Refr. Meeting of Commissions Bl, Cl, and C2., Bressanone, Italy. Bulletin Annexe: 29.

Heldman, D. R. and D. P. Gorby. 1975. Computer simulation of individual-quick-freezing of foods. ASAE Paper No. 75-6016.

Hsieh, R. C., L. E. Lerew, and D. R. Heldman. 1977. Prediction of freezing times for foods as influenced by product properties. J. Food Proc. Engr., 1: 183.

Joshi, C. and L. C. Tao. 1974. A numerical method of simulating the axisymmetrical freezing of food systems. J. Food Science, 39: 623.

Katinas, V. I., I. I. Zhyugzhda, A. A. Zhukauskas, and S. A. Shvegzhda. 1976. The effect of the turbulence of an approaching stream of viscous fluid on local heat transfer from a circular cylinder. Int. Chem. Engr., 16: 283.

Kopelman, I. J. 1966. Transient heat transfer and thermal properties in food systems. Ph.D. Thesis. Department of Food Science and Human Nutrition. Michigan State University, East Lansing, MI.

Krutz, G. W. 1976. A Thermo-metallurgical model predicting the strength of welded joints using the finite element method. Ph.D. Thesis. Deparment of Agricultural Engineering. Michigan State University, East Lansing, MI.

Langford, D. 1973. The heat balance integral method. Int. J. Heat Mass Transfer, 15: 2424.

Lees, M. 1966. A linear three-level difference scheme for quasilinear parabolic equations. Math. Comput. 20: 516.

Lescano, C. E. and D. R. Heldman. 1973. Freezing rates in codfish muscle. ASAE Paper No. 73-367.

Luikov, A. V. 1968. Analytical Heat Diffusion Theory. Academic Press Book, New York, N. Y.

Mikhailov, M. D. 1976. Exact solution for freezing of humid porous half-space. Int. J. Heat Mass Transfer, 19: 651.

Neter, J. and W. Wasserman. 1974. Applied Linear Statistical Models. Richard D. Irwin, Inc., Homewood, Ill.

Rebellato, L., S. Del Giudice, and G. Comini. 1978. Finite element analysis of freezing processes in foodstuffs. J. Food Science, 43: 239.

Richardson, P. D. and Y. M. Shum. 1969. Use of finite element methods in solution of transient heat conduction problems. ASME Winter Annual Meeting. Paper No. WA/HT-36.

Riley, D. S. and P. W. Duck. 1977. Application of the heat-balance integral method to the freezing of a cuboid. Int. J. Heat Mass Transfer, 20: 294.

Segerlind, L. J. 1976. Applied Finite Element Analysis. John Wiley and Sons, Inc., New York, N. Y.

Shamsundar, N. and E. M. Sparrow. 1975. Analysis of multidimensional conduction phase change via the enthalpy model. J. Heat Transfer, 96: 333.

Singh, R. P. and L. J. Segerlind. 1974. The finite element method in food engineering. ASAE Paper No. 74-6015.

Slavin, J. W. 1964. Freezing seafood--now and in the future. ASHRAE J. 6 (5): 43.

Sörenfors, P. 1974. Determination of the thermal conductivity of minced meat. Cited from: V. M. Chavarria. 1978. Experimental determination of the surface heat transfer coefficient under food freezing conditions. M.S. Thesis. Department of Agricultural Engineering. Michigan State University, East Lansing, MI.

Spiegel, M. R. 1964. Complex Variables. Schaum's Outline Series. McGraw-Hill Book Co., New York, N. Y.

Tarnawski, W. 1976. Mathematical model of frozen consumption products. Int. J. Heat Mass Transfer, 19: 15.

Tressler, D. K., W. B. Van Arsdel, M. J. Copley, and W. R. Woolrich. Editors. 1968. The Freezing Preservation of Foods. The AVI Pub. Co., Inc., Westport, CT.

Visser, W. 1965. A finite element method for the determination of non-stationary temperature distribution and thermal deformations. Proceedings Conference on Matrix Methods in Structural Mechanics. Cited from: L. J. Segerlind. 1976. Applied Finite Element Analysis. John Wiley and Sons, Inc., New York, N.Y.

Wellford Jr., L. C. and R. M. Ayer. 1977. A finite element free boundary formulation for the problem of multiphase heat conduction. Int. J. Numerical Methods in Engr., 11: 933.

Wilson, E. L. and R. E. Nickell. 1966. Application of the finite element method to heat conduction analysis. Nuclear Engr. and Design, 4: 276.

Yalamanchili, R. V. S. and S. C. Chu. 1973. Stability and oscillation characteristics of finite element, finite difference, and weighted-residuals methods for transient two-dimensional heat conduction in solids. J. Heat Transfer, 94: 235.

Zdanavichyus, G. B., V. Y. Survila, and A. A. Zhukauskas. 1977. Influence of the degree of turbulence of an inflowing air stream on local heat transfer on a circular cylinder in the critical flow regime. Int. Chem. Engr., 17: 115.

Zienkiewicz, O.C. 1971. The Finite Element Method in Engineering Science. McGraw-Hill Book Co., London, Great Britain.

Zienkiewicz, O. C. and Y. K. Cheung. 1965. Finite elements in the solution of field problems. The Engineer, 220: 507.